Effect of Dopamine on Synchronous Neuronal Oscillations in the Globus Pallidus-Subthalamic Nucleus Network

ALEXANDRE LOUCIF

Doctor of Philosophy

ASTON UNIVERSITY

June 2006

Aston University

Effect of Dopamine on Synchronous Neuronal Oscillations in the Globus Pallidus-Subthalamic Nucleus Network

Thesis submitted for the degree of Doctor of Philosophy, by Alexandre Julien Chau Loucif, June 2006.

Changes in the pattern of activity of neurones within the basal ganglia are relevant in the pathophysiology and symptoms of Parkinson's disease. The globus pallidus (GP) - subthalamic nucleus (STN) network has been proposed to form a pacemaker driving regenerative synchronous bursting activity. In order to test whether this activity can be sustained *in vitro* a 20° parasagittal slice of mouse midbrain was developed which preserved functional connectivity between the STN and GP.

Mouse STN and GP cells were characterised electrophysiologically by the presence or absence of a voltage sag in response to hyperpolarising current steps indicative of I_h and the presence of rebound depolarisations. The presence of evoked and spontaneous post-synaptic GABA and glutamatergic currents indicated functional connectivity between the STN and GP. In control slices, STN cells fired action potentials at a regular rate, activity which was unaffected by bath application of the $GABA_A$ receptor antagonist picrotoxin (50 μM) or the glutamate receptor antagonist CNQX (10 μM). Paired extracellular recordings of STN cells showed uncorrelated firing. Oscillatory burst activity was induced pharmacologically using the glutamate receptor agonist, NMDA (20 μM), in combination with the potassium channel blocker apamin (50 -100 nM). The burst activity was unaffected by bath application of picrotoxin or CNQX while paired STN recordings showed uncorrelated activity indicating that the activity is not produced by the neuronal network. Thus, no regenerative activity is evident in this mouse brain preparation, either in control slices or when bursting is pharmacologically induced, suggesting the requirement of other afferent inputs that are not present in the slice.

Using single-unit extracellular recording, dopamine (30 μM) produced an excitation of STN cells. This excitation was independent of synaptic transmission and was mimicked by both the D1-like receptor agonist SKF38393 (10 μM) and the D2-like receptor agonist quinpirole (10 μM). However, the excitation was partially reduced by the D1-like antagonist SCH23390 (2 μM) but not by the D2-like antagonists sulpiride (10 μM) and eticlopride (10 μM).

Using whole-recordings, dopamine was shown to induce membrane depolarisation. This depolarisation was caused either by a D1-like receptor mediated increase in a conductance which reversed at -34 mV, consistent with a non-specific cation conductance, or a D2-like receptor mediated decrease in conductance which reversed around -100 mV, consistent with a potassium conductance. Bath application of dopamine altered the pattern of the burst-firing produced by NMDA an apamin towards a more regular pattern. This effect was associated with a decrease in amplitude and increase in frequency of TTX-resistant plateau potentials which underlie the burst activity.

Keywords: basal ganglia, non-specific cation current, I_h current, 5-HT.

Acknowledgements

I would like to thank my supervisor Dr Ian Stanford for his excellent supervision and his constant support. I would also like to thank Dr Gavin Woodhall and Prof Ian Martin for their permanent guidance and encouragement throughout this project.

I would like to acknowledge other members of the laboratory who provided a pleasant working environment, as well as social interaction: Drs Claire Wilson and Rhein Parri, Nicola Morgan, Tina Pittimaki and Naoki Yamawaki.

I would like to thank all members of the laboratory of Michel Hamon.

Finally, I would like to thank my family.

Contents

List of figures

List of tables

Abbreviations

aCSF	artificial cerebrospinal fluid
ACPD	1S-3R-1-aminocyclopentane-1,3-dicarboxylate
AHP	after-hyperpolarisation
AMPA	α-amino-3-hydroxy-5-methyl-4 isoxasole propionic acid
ATP	adenosine 5'-triphosphate
BAPTA	1,2-bis(2-aminophenoxy)-ethane-N, N, N', N'-tetraacetic acid
BG	basal ganglia
BK channels	large conductance calcium-activated potassium channels
cAMP	cyclic adenosine monophosphate
CNQX	6-cyano-7-nitroquinoxaline-2,3-dione
DA	dopamine hydrochloride
DL-AP5	DL-2-amino-5-phosphopentanoic acid
DMSO	dimethylsulfoxide
EGTA	ethylene glycol-bis-(β-aminoethyl ether) N, N, N', N'-tetraacetic acid
EP	entopeduncular nucleus
EPSC	excitatory postsynaptic current
EPSP	excitatory postsynaptic potential
GABA	gamma-amino-butyric acid
GP	globus pallidus
GPe	globus pallidus (external segment)
GPi	globus pallidus (internal segment)
GR113808	1-[2-(methylsulphonyl]-4-piperidinyl]methyl 1-methyl-1H-indole-3-carboxylate
GTP	guanosine 5'-triphosphate
5-HT	5-hydroxytryptamine
IPSC	inhibitory postsynaptic current
IPSP	inhibitory postsynaptic potential
mGluR	metabotropic glutamate receptors
mOsm	milliosmols

MPP^+	1-methyl-4-phenylpyridium
MPTP	1-methyl-4-phenyl-1, 2, 3, 6-tetrahydropyridine
MSN	medium spiny neurone
NaOH	sodium hydroxide
NMDA	N-methyl-D-aspartate
6-OHDA	6-hydroxydopamine
PD	Parkinson's disease
PPN	pedunculopontine nucleus
RT-PCR	reverse transcription polymerase chain reaction
RS102221	8-[5-(2,4-dimethoxy-5-(4-trifluoromethylphenylsulfonamido)phenyl-5-oxopentyl)] -1,3,8-triazaspiro[4.5]decane-2,4-dione hydrochloride
SEM	standard error of the mean
SK channels	small conductance calcium-activated potassium channels
SCH23390	(*R*)-(+)-7-chloro-8-hydroxy-3-methyl-phenyl-2,3,4,5-tetrahydro-1H-3-benzazepine
SKF383393	(±)-1-phenyl-2,3,4,5-tetrahydro-(1 H)-3-benzazepine7,8-diol hydrochloride
SNc	substantia nigra *pars compacta*
SNr	substantia nigra *pars reticulata*
STN	subthalamic nucleus
TANs	tonically active neurones
TEA	tetraethylammonuim chloride
TTX	tetrodotoxin
VTA	ventral tegmental area
WAY100135	(S)-N-tert-Butyl-3(4-(2-methoxyphenyl)-piperazin-1-yl)-2-phenylpropanamide

Chapter 1. Introduction

1.1. Parkinson's disease

1.1.1. Incidence and history

Parkinson's disease (PD) is a progressive neurodegenerative disorder involving dysfunction of a group of brain nuclei called the basal ganglia (BG). It is observed in 1% of the population over 65 years of age (Gross *et al.*, 1999). The symptoms of the disease were initially described in 1817 in an essay entitled 'The shaking palsy' written by the clinician James Parkinson (Parkinson, 1817). However, it took another one hundred and forty nine years to show that the degeneration of dopaminergic neurones within the brain and specifically of the substantia nigra *pars compacta* (SNc) was the primary cause of the disease (Hornykiewicz, 1966). Later, a correlation between the deficiency of the neurotransmitter dopamine within the caudate putamen (striatum) and the clinical symptoms of PD was shown, implicating the nigro-striatal pathway (Bernheimer *et al.*, 1973). The treatment with the dopamine precursor levodopa was then established (Hornykiewicz, 1973) and it is still the most effective treatment to date.

1.1.2. Symptoms of Parkinson's disease

PD is characterised by paucity of voluntary movement and resting tremor. The typical features of PD are akinesia (poverty of movement), bradykinesia (slowness in movement execution), muscle rigidity and a 4-6 Hz resting tremor (which is present in approximately 30% of all the patients). Upon progression of the disease many patients show cognitive deficits and dementia, with the mean survival time following diagnosis being 10 years. These symptoms become evident when striatal dopamine loss reaches 60-70 % (Delong, 1990; Magnin *et al.*, 2000).

1.1.3. Causes of Parkinson's disease

In many cases the causes of PD are unknown (idiopathic), although up to 10% are said to have a genetic basis implicating the proteins α-synuclein and parkin (Le & Appel, 2004). Idiopathic PD is a sporadic disease the incidence of which increases with age. Many theories have been put forward as to the cause of PD including a theory involving environmental factors which was developed in the 1980's following the story of the frozen addict (Langston *et al.*, 1983). In the 1982, a small group of heroin addicts were found to present the symptoms of akinesia, rigidity and tremor. The investigations that followed determined that these patients had injected themselves with drugs contaminated containing the toxic by product called 1-methyl-4-phenyl-1, 2, 3, 6-tetrahydropyridine (MPTP) (Langston *et al.*, 1983). In the brain, MPTP is oxidised to 1-methyl-4-phenylpyridium (MPP^+) by the enzyme monoamine oxidase B. MPP^+ is then selectively captured by dopaminergic neurones via the dopamine transporter. MPP^+ toxicity leads directly to disruption of mitochondrial respiration, oxidative stress, possible glutamate toxicity and cell death (Blandini *et al.*, 2000).

1.1.4. Pharmacological interventions in Parkinson's disease

One important pharmaco-therapeutic strategy in PD is the replacement of lost dopamine. This is achieved by chronic treatment with the dopaminergic precursor, levodopa, which is able to cross the blood-brain barrier (Hornykiewicz, 1973). Studies in human and monkey indicate that administration of levodopa reduces most of the symptoms of PD (Nutt *et al.*, 2000). However, a major limitation of levodopa therapy is the development of motor complications such as motor fluctuations and involuntary movements (dyskinesia). Indeed, patients can cycle between "on" responses, in which they benefit from levodopa but experience dykinesia, and "off" responses ("wearing off" and "on-off"), in which levodopa is not effective and patients experience parkinsonian symptoms. These dramatic side effects are not present at the initiation of the therapy, but gradually emerge after years of levodopa treatment (Graybiel *et al.*, 2000).

Due to the dramatic side effects of prolonged levodopa treatment, various levodopa sparing adjunct therapies have been developed. These include dopa-decarboxylase inhibitors which block the peripheral metabolism of levodopa, dopamine receptor agonists which mimic the action of dopamine such as bromocriptine, pergolide, ropinirole and pramipexole and inhibitors of dopamine metabolism such as catechol-O-methyltranferase inhibitor (entacopone) and monoamine oxidase B inhibitors (selegiline).

Acetylcholine antagonists such as benztropine have also been used to block the hyperactivity of cholinergic interneurones which enhances the symptoms of the disease (Pisani *et al.*, 2003). Furthermore, non competitive glutamate receptor antagonists such as amantadine have been used for the treatment of advanced PD (Blanchet *et al.*, 2003). Currently, glutamate antagonist candidates such as the non-competitive NMDA receptor antagonist MK-801 and the AMPA receptor antagonist LY293558 are under investigations in animal models of the disease (Allers *et al.*, 2005; Vila *et al.*, 1999).

1.2. Animal models of Parkinson's disease

1.2.1. MPTP-treated non-human primates

Following the discovery that MPTP triggered the symptoms of PD in heroin addicts (Langston *et al.*, 1983), the action of this neurotoxin was investigated in non-human primates. Systemic injection of the MPTP in non-human primates selectively destroyed dopaminergic neurones of the SNc and was accompanied by the development of parkinsonian symptoms indistinguishable from those of sporadic PD (Jenner *et al.*, 1986; Shimohama *et al.*, 2003). The MPTP-treated monkey became a useful animal model that has helped to understand the mechanisms by which the disease arises and led to better understanding of BG function in the normal and the pathological state. This model is the closest one to human idiopathic disease.

1.2.2. MPTP-treated mice

Due to the ethical issues surrounding the use of non-human primates other models of PD were sought. MPTP-treated mice constitute a rodent model of the disease. This model also involves systemic injections and shows comparable dopamine depletion in the striatum. However, this model does not show reliable motor deficits and behavioural changes (Sedelis *et al.,* 2001).

1.2.3. 6-Hydroxydopamine-lesioned rats

Interestingly, rats are not sensitive to systemic injections of MPTP due to differences in catabolism of MPTP by the enzyme monoamine oxidase B (Giovanni *et al.,* 1994). A valuable rat model of PD is the 6-hydroxydopamine (6-OHDA)-lesioned rat. A selective lesion of the nigro-striatal pathway is achieved by injection of the neurotoxin 6-OHDA into the SNc unilaterally where it selectively destroys SNc neurones. Alternatively, the toxin may be injected into the medial forebrain bundle, where it causes a degeneration of dopamine cells of the SNc and ventral tegmental nucleus (VTA) following retrograde transport.

In intact rats, unilateral electrical stimulation of the dopamine containing nigro-striatal pathway elicits contralateral turning behaviour (away from the activated side) (Arbuthnott & Crow, 1971; Ungerstedt & Arbuthnott, 1971). In unilateral 6-OHDA-lesioned rats, systemic administration of the dopamine releasing agent, amphetamine, elicits ipsilateral turning behaviour (toward the lesioned side) through its action on the intact side (Ungerstedt & Arbuthnott, 1970) while the non selective dopaminergic agonist, apomorphine, elicits ipsilateral turning behaviour via its action on the lesioned side (Ungerstedt *et al.,* 1971). The turning behaviour is due to the existence of an imbalance between the activities of the BG output nuclei of each brain hemisphere in favour of the intact side (Arbuthnott & Ungerstedt, 1975; Garcia-Munoz *et al.,* 1983).

1.3. Basal ganglia structure and function

The BG comprise a set of six nuclei that is involved in the planning and execution of voluntary movement and in a variety of other behavioural functions such as oculomotor, cognitive and limbic processes (Albin *et al.,* 1989; Alexander *et al.*, 1990; Delong, 1990). These nuclei include the caudate putamen (striatum in rodents), the pallidum comprising the external globus pallidus (GPe) (GP in rodents, this abbreviation will be used throughout this study) and the internal globus pallidus (GPi) (entopeduncular nucleus; EP in rodents), the subthalamic nucleus (STN) the substantia nigra *pars reticulata* (SNr) and substantia nigra *pars compacta* (SNc).

1.3.1. The striatum

The striatum is the largest nucleus in BG with 2.79 million neurones in each hemisphere of the rat brain (Oorschot, 1996). It receives major excitatory glutamatergic monosynaptic afferent projections from different areas of the cortex in a topographical manner (Parent & Hazrati, 1995a) and glutamatergic projections from the thalamus (Smith *et al.,* 1994b). In addition, the striatum receives an extensive dopaminergic projection from the SNc (Moore *et al.,* 1971) and a 5-HT (5-hydoxytryptamine) projection from the raphe nuclei (Lavoie & Parent, 1990). 95% of the cells within the striatum are medium spiny projection neurones (MSNs). These cells express either GABA/enkephalin or GABA/substance P which appears to correlate with their target nuclei (see later section 1.4.1). Electrophysiologically, MSNs are characterised by resting membrane potential around -80 to -90 mV, pronounced inward rectification in response to hyperpolarising current injection and depolarising ramps prior to spike threshold and low input resistance (Kawaguchi *et al,* 1989).

In vivo, due to the excitatory cortical influence, MSNs oscillate between an up-state, in which they fire action potentials, and a down-state in which they are silent (Wilson & Kawaguchi, 1996). Up-state transitions are not seen *in vitro* since excitatory cortical input is interrupted (Kawaguchi *et al,* 1989). MSNs exert a powerful control of both intra-striatal and extra-striatal activities through an extensive axon

collateralisation. Within the striatum, MSNs contact each other via chemical (Tepper *et al.*, 2004) and electrical synapses (Venance *et al.*, 2004). Furthermore, dye coupling (indicative of the presence of gap junctions) between MSNs is increased in 6-OHDA-leioned rats (Cepeda *et al.*, 1989; Onn & Grace, 1994).

In addition to MSNs, there are four classes of local interneurones which constitute the remaining 5% of the population. These include large cholinergic interneurones (identifiable by the presence of choline-acetyltransferase), GABA /parvalbumin-containing interneurones, GABA/calretinin-containing interneurones and GABA/somatostatin/nitric oxide synthase/ neuropeptide Y-containing interneurones (Kawaguchi *et al.*, 1995; Koos & Tepper, 1999; Tepper & Bolam, 2004). *In vivo*, cholinergic interneurones (sometimes referred to as tonically active neurones, TANs) fire in an irregular pattern with a firing rate of 2-10 Hz. They display a prolonged after-hyperpolarisation and a pronounced anomalous inward rectifier due to the channel I_h (hyperpolarisation-activated cation current) (Kawaguchi *et al.*, 1995). Parvalbumin-containing interneurones are fast-firing cells with action potentials of short duration and short after-hyperpolarisations. Somatostatin/ nitric oxide synthase / neuropeptide Y-containing interneurones can generate plateau potentials, calcium-dependent low-threshold spikes and fast spiking (Kawaguchi *et al.*, 1995). The electrophysiology of calretinin-containing interneurones remains to be characterised.

1.3.2. The globus pallidus (external segment)

The GP contains 46,000 neurones in each hemisphere of the rat brain (Oorschot, 1996). The GP receives widespread projections including a GABA projection from the striatum (Chang *et al.*, 1981), excitatory glutamate projections from the STN (Nauta & Cole, 1978; Shink *et al.*, 1996) and reticular thalamus (Deschenes *et al.*, 1996), a cholinergic projection from pedunculopontine nucleus (PPN) (Lavoie & Parent, 1994), 5-HT projection from the dorsal raphe nucleus (Lavoie & Parent 1990), and a dopamine projection from the SNc (Lindvall & Bjorklund, 1979). In return, the GP sends GABA projections to the striatum (Nambu *et al.*, 1997; Bevan *et al.*, 1998), the STN (Carpenter *et al.*, 1968; Shink *et al.*, 1996), the SNr (Smith & Bolam, 1989; Smith & Bolam, 1990)

and the GPi (Shink *et al.,* 1996; Smith *et al.,* 1994b; Hazrati *et al,* 1990). In fact, a single GP cell can project to 1) the GPi, STN and SNr, 2) the GPi and STN, 3) the STN and SNr, or 4) the striatum (Sato *et al.,* 2000a) where they form symmetrical synapses and innervate proximal regions of neurones in a basket-like fashion (Smith *et al.,* 1998). In addition, projections to the thalamus have been reported (Cornwall *et al.,* 1990).

Early extracellular studies *in vivo,* in primates, revealed two types of firing pattern indicative of two populations of GPe cell (Delong, 1971). 1) Neurones with high frequency discharge periods separated by periods of silence (high frequency discharge with pause) which represented 85 % of the population and 2) neurones with low frequency discharge separated by intermittent high frequency bursts (low-frequency discharge with burst) accounted for 15 % of the population.

Neuronal heterogeneity in the rat GP was further described in the anatomical studies of Millhouse, (1986) and Kita & Kitai, (1994) which both revealed the existence of two subtypes of GP neurones. Similarly two populations of GP neurone can be distinguished on the basis of calcium binding protein expression: parvalbumin-immunoreactive neurones (66 %) projecting to downstream nuclei, STN and GPi, and non-parvalbumin immunoreactive neurones which projecting to the striatum (Kita, 1994).

Electrophysiological studies have also indicated that the GP is composed of heterogeneous population of cells. However, the classification differs according to the animal species, the nature of the preparation (*in vivo* or *in vitro*) and the (recording) techniques. The intrinsic electrophysiological properties of GP cells will be reviewed in chapter 3.

1.3.3. The subthalamic nucleus

The STN contains approximately 13,600 neurones in each hemisphere of the rat brain (Oorschot, 1996). These cells form a homogenous population of glutamatergic projection neurones (Hamond & Yelnik, 1983). The STN receives glutamatergic projection from the cortex (Kitai & Deniau, 1981), thalamus (Sugimoto *et al.,* 1983; Sugimoto & Hattori, 1983) and PPN (Canteras *et al.,* 1990) whilst sending

glutamatergic projections to different BG nuclei, including the SNr (Nauta & Cole, 1978; Van Der Kooy & Hattori, 1980; Kita & Kitai, 1987), GPi (Nauta & Cole, 1978; Kita & Kitai, 1987; Shink & Smith, 1995), GPe (Nauta & Cole, 1978; Kita & Kitai, 1987; Van Der Kooy & Hattori, 1980; Shink *et al.,* 1996) and the thalamus (Nauta & Cole, 1978).

The glutamatergic projection from the cortex (Canteras *et al.,* 1990; Bevan *et al.,* 1995; Parent & Hazrati, 1995a; Maurice *et al.,* 1998; Smith *et al.,* 1998; Maurice *et al.,* 1999; Nambu *et al.,* 2002; Orieux *et al.,* 2002) is the fastest way that cortical information reaches the BG. Indeed, electrical stimulation of the cortex elicits early excitation followed by inhibition and late excitation in the STN (Ryan & Clark, 1991; Fujimoto & Kita, 1993; Maurice *et al.,* 1998; Nambu *et al.,* 2002). The first excitatory response is due to the action of the direct cortico-subthalamic projection while the delayed inhibitory component is due to the reciprocal connectivity with GP and delayed excitation due to cortico-striatal projection releasing the spontaneous inhibitory drive of GP onto the STN.

In addition to the afferent projections from the cortex, STN receives glutamatergic projections from the parafascicular nucleus of the thalamus (Sugimoto & Hattori, 1983; Canteras *et al.,* 1990; Mouroux *et al.,* 1995; Sadikot *et al.,* 1992) and glutamatergic/cholinergic input from the PPN (Nomura *et al.,* 1980). The effect of the cholinergic input is excitatory and is mediated through muscarinic receptors (Flores *et al.,* 1996).

The STN also receives a direct dopaminergic input from the SNc (Hassani *et al.,* 1997; Cossette *et al.,* 1999; Gauthier *et al.,* 1999; Prensa *et al.,* 2000; Smith & Kieval, 2000) and a direct 5-HT input from the dorsal raphe (Mori *et al.,* 1985; Lavoie & Parent, 1990). Indeed, there is increasing evidence for a functional role for this direct nigro-subthalamic projection (Kreiss *et al.,* 1997; Hassani & Feger, 1999; Ni *et al.,* 2001a) and raphe-subthalamic projection (Eberle-Wang *et al.,* 1996; Barwick *et al.,* 2000) (see chapter 5).

1.3.4. The globus pallidus (internal segment)

The GPi is the smallest nucleus in the BG containing approximately 3,200 neurones per hemisphere of the rat brain (Oorschot, 1996). It is one of two output nuclei of BG (along with the SNr) sending inhibitory GABAergic projections to thalamus (Parent & Parent, 2004). The GPi receives GABAergic input primarily from the striatum (Bolam *et al.,* 1993) and also from the GPe (Smith *et al.,* 1994b; Shink *et al.,* 1996) and receives a glutamatergic input from the STN (Nauta & Cole, 1978; Smith *et al.,* 1994a).

Two cell subtypes called types II and I have been found in GPi in rat (Nakanishi *et al.,* 1990). Most of neurones (73 %) belong to the type I, which is characterised by the presence of I_h, and rebound excitation with low-threshold calcium spikes. The remaining neurones (type II) display strong spike adaptation and an A-like potassium current.

1.3.5. The substantia nigra *pars reticulata*

The SNr represents one of two output nuclei of BG (along with the GPi) sending GABAergic projections to the thalamus (Bentivoglio *et al.,* 1979). The SNr receives GABAergic projections from the striatum (Bolam & Smith, 1990), GPe (Smith & Bolam 1990) and GPi and glutamatergic inputs from the STN (Nauta & Cole, 1978; Nakanishi *et al.,* 1987b).

The SNr is a sparsely populated nucleus composed of 26,300 GABA neurones per hemisphere of the rat brain (Oorshot, 1996). Electrophysiological studies *in vitro* have shown two types of SNr neurones (Richards *et al.,* 1997). Type I neurones (Stanford & Lacey, 1996) are GABAergic projection neurones and account for 95 % of the population whereas type II neurones are (displaced) dopaminergic neurones electrophysiologically identical to those of SNc (see next 1.3.6). Among GABAergic neurones, parvalbumin containing neurones are located medially (McRitchie *et al.,* 1996) whilst calbindin neurones are observed dorsally and medially (Hontanilla *et al.,* 1998).

1.3.6. The substantia nigra *pars compacta*

With 7,200 neurones in each hemisphere of the rat brain (Oorschot, 1996), the SNc receives GABAergic projections from the striatum (Bolam & Smith, 1990), GPe (Smith & Bolam, 1990) and SNr (Grofova *et al.,* 1982). The SNc receives also glutamatergic projections from the cortex (Kornhuber *et al.,* 1984), STN (Nakanishi *et al.,* 1987a), cholinergic projections from PPN (Lavoie & Parent, 1994) and 5-HT projections from the raphe nuclei (Lavoie & Parent, 1990). The SNc sends dopaminergic projections primarily to the striatum (Bentivoglio *et al.,* 1979) but also to the GPe, GPi and STN (Lindvall & Björklund, 1979; Lavoie *et al.,* 1989; Smith *et al.,* 1989; Hassani *et al.,* 1997; Cossette *et al.,* 1999; Prensa *et al.,* 2000) and SNr (Smith & Kieval, 2000). Calbindin- and calretinin-containing neurones have been found in the caudo-medial region of SNc but there was no evidence of parvalbumin-containing neurones (McRitchie *et al.,* 1996).

The SNc is composed mainly (95 %) of dopaminergic neurones. Remaining neurones are GABAergic neurones similar to those of the SNr (Lacey *et al.,* 1989). *In vitro*, dopamine neurones of the SNc are characterised by a regular firing pattern that is in contrast with the irregular/bursting discharge observed *in vivo*. Whole-cell recordings from dopaminergic neurones have revealed that they are quiescent or fire action potentials at 1-8 Hz, display a pronounced I_h and are inhibited by dopamine (Grace & Bunney 1983; Lacey *et al.,* 1989).

Studies of the modulation of the firing pattern of dopamine neurones have focused on excitatory inputs arising from the cortex and the STN and the cholinergic action from the PPN (Kitai *et al.,* 1999). It has emerged that glutamate release from cortical (Murase *et al.,* 1993), subthalamic (Chergui *et al.,* 1994) or peduculopontine (Lokwan *et al.,* 1999) afferents *in vivo* may be able to promote or facilitate burst firing in dopamine neurones. Indeed, local glutamate infusion has been shown to increase bursting activity *in vivo* (Overton & Clark, 1992). However, the mechanisms of such burst activity are still controversial. In slices, burst discharge can be promoted in

dopamine neurones using NMDA and this is potentiated by apamin, the blocker of small conductance calcium-activated potassium (SK) channels (Seutin *et al.,* 1993).

1.4. The classical model of basal ganglia function

1.4.1. Definition of the classical model

Information processing through BG is thought to take place through series of anatomically and functionally segregated cortico-BG-thalamocortical loops. Each of these circuits projects to discrete regions of BG and cortex and subserves distinct functions including motor, occulomotor and limbic functions (Albin *et al.,* 1989; Alexander & Crutcher, 1990; Delong, 1990).

Based on neuro-anatomical, electrophysiological and lesion experiments a simple model of BG function emerged. For simplicity, I will only describe the motor circuit due to its implication in movement disorders such as PD (figure 1.1).

The striatum receives cortical information and is considered to be the main input station of the BG. Cortical information flows via two parallel, but essentially opposing pathways, to the output nuclei of the BG from where it is sent back to the cortex via the thalamus. The two pathways termed 'direct' and 'indirect' exert opposing effects on the activity of output nuclei, the GPi and SNr. These two pathways are assumed to arise from separate populations of GABAergic striatal neurones. The direct pathway originates from striatal neurones containing substance P and dynorphin and provides a monosynaptic projection to the output nuclei while the indirect pathway arises from striatal neurones containing enkephalin and projects to the GPi/SNr via relays in GPe and STN (Albin *et al.,* 1989). Thus, the direct pathway produces inhibition of the GPi/SNr while the indirect pathway produces excitation.

The action of dopamine was thought to occur only at the level of the striatum facilitating the activity of the direct pathway via excitatory D1 receptors and inhibiting transmission along the indirect pathway via inhibitory D2 receptors (Gerfen *et al.,* 1990; Smith & Kieval, 2000).

1.4.2. Parkinson's disease according to the classical model

The classical model of 1990 served as a basis for understanding not only of PD but other disorders of movement such as Huntington's disease and ballism which are associated with pathology and dysfunction of BG. In the case of PD, the symptoms of akinesia and rigidity were proposed to result from an increased GABAergic inhibition of thalamo-cortical activity. Normally, dopamine controls the activity of the direct and indirect pathways via striatal excitatory D1 and inhibitory D2 dopamine receptors respectively. However, in PD, there is a loss of dopamine in the striatum, which leads both to a reduced activity of the direct pathway and an enhanced activity of the indirect pathway. The increased activity of GABAergic striatopallidal neurones (in the indirect pathway) induces a hypo-activity of the GABAergic GP cells. This relieves the tonic inhibition of the STN inducing hyperactivity of this excitatory nucleus. The activity of the output nuclei is therefore increased and as these projections are inhibitory this leads to enhanced inhibition of thalamo-cortical neurones resulting in the inhibition of movement.

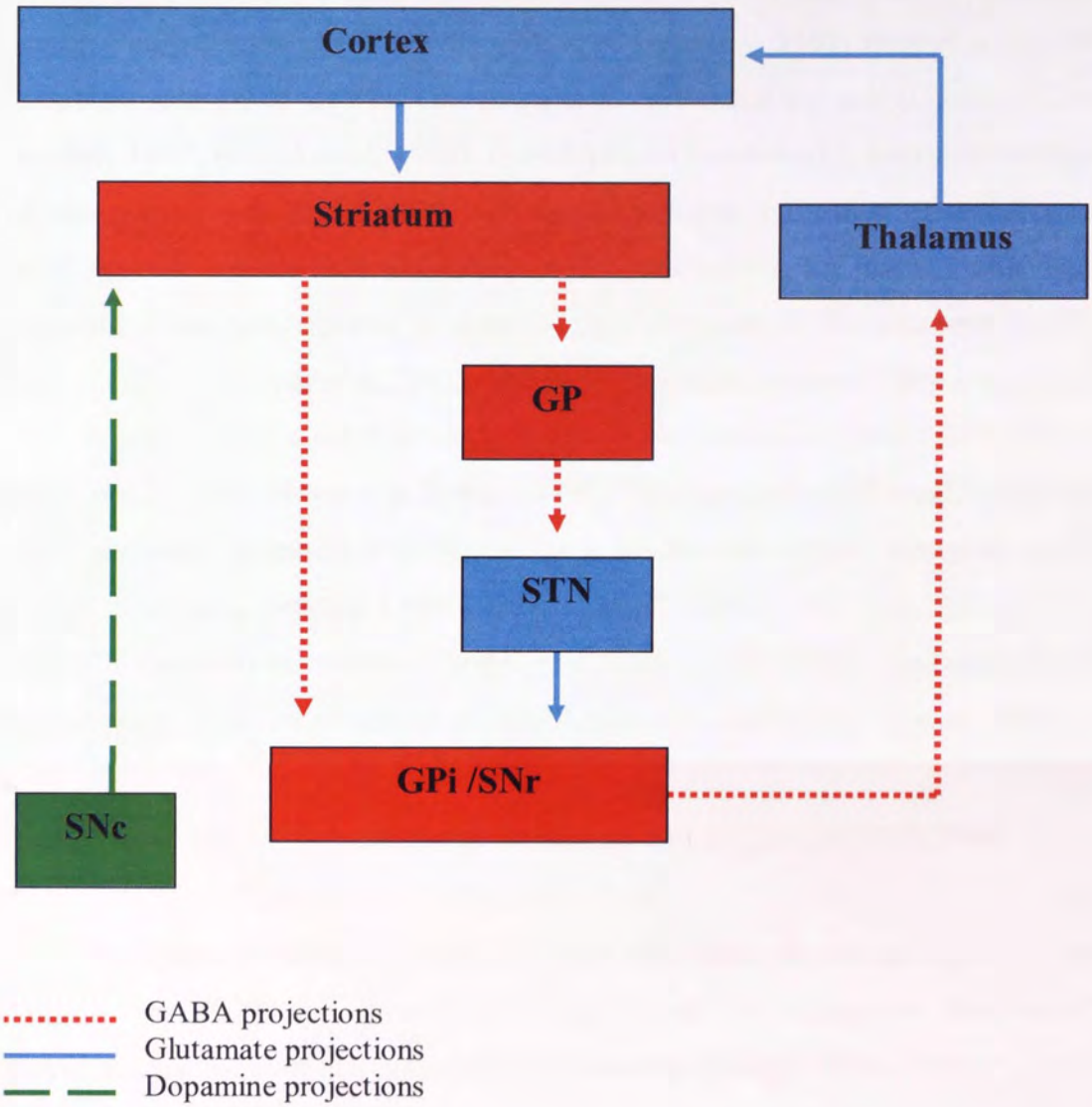

Figure 1.1: BG organisation in the classical model. STN: subthalamic nucleus, GP: globus pallidus (external segment), GPi: globus pallidus (internal segment), SNr: substantia nigra *pars reticulata*, SNc: substantia nigra *pars compacta*.

1.4.3. Support for the classical model from Parkinson's disease patients and animal models of the disease

Studies in the MPTP-treated monkey have shown that loss of dopamine is associated with decreased GP activity (Filion & Tremblay, 1991; Boraud *et al.*, 1998), an increased activity of the STN (Bergman *et al.*, 1994) and the output nuclei (Filion & Tremblay, 1991; Boraud *et al.*, 1998). In addition, an increase of 2-deoxyglucose uptake was observed in the GPi of the MPTP-treated monkey, indicative of an increase in overall synaptic activity (Mitchell *et al.*, 1989). Furthermore, the mixed D1/D2 agonist apomorphine has been reported to decrease the firing rate of GPi neurones in MPTP-treated monkeys (Heimer *et al.*, 2002) and in parkinsonian patients (Levy *et al.*, 2001).

In vivo studies in 6-OHDA-lesioned rats have revealed increased STN firing rate (Kreiss *et al.*, 1997; Hassani & Feger, 1999). This has been confirmed by metabolic studies showing increased STN levels of a marker of overall metabolic activity, cytochrome oxidase (subunit I mRNA) (Vila *et al.*, 1999; Vila *et al.*, 2000; Orieux *et al.*, 2002). Furthermore, increased levels of mRNA for the GABA synthetic precursor GAD_{67} have been reported (Vila *et al.*, 1999; Vila *et al.*, 2000; Orieux *et al.*, 2002).

1.5. Limitations of the classical model of basal ganglia function

The classical model provided a coherent explanation for the emergence of motor disorders such as PD, but recent research has shown that many new features of BG function are not incorporated in the model (Chesselet & Delfs, 1996).

1.5.1. Integration of direct and indirect pathways

The classical model is based on a strict anatomical segregation between the direct and indirect pathways. Neurones of the direct pathway project exclusively to the output nuclei while the neurones of the indirect pathway exclusively innervate the GP (Alexander *et al.*, 1991). However, in addition to the existence of extensive collateralisation within the striatum (Tepper *et al.*, 2004), it has emerged that there is a significant degree of overlap between the direct and indirect pathways as striatal

neurones of the so-called direct pathway send collaterals to the GPe (Parent *et al.*, 1995; Parent *et al.*, 2000; Wu *et al.*, 2000) and substance P immunoreactivity was found in the GP (Sadek, 2005).

The classical model also states that that there is segregation of dopamine D1 and D2 receptors in the striatum with neurones of the direct pathway expressing excitatory D1 receptors while neurones of the indirect pathway expressing inhibitory D2 receptors (Gerfen *et al.*, 1990; Dragunow *et al.*, 1990; Robertson *et al.*, 1990; Gerfen *et al.*, 1995). This view was initially contested (Surmeier *et al.*, 1992) and then accepted following *in situ* hybridisation (Le Moine *et al.*, 1990) and immunocytochemical studies (Hersch *et al.*, 1995; Sadek, 2005).

1.5.2. Lack of GP hypoactivity

An important limitation of the classical model is the lack of consensus on whether there is a hypoactivity of the GP following nigrostriatal dopamine lesions. Functional studies *in vivo* in monkey (Bezard *et al.*, 1999) and PD patients (Goldberg *et al.*, 2002) have revealed that nigrostriatal dopamine lesion does not result in a decrease of GP activity. Indeed, chronic administration of levodopa in MPTP-treated monkey decreases GPi firing rate but does not affect the GP activity (Boraud *et al.*, 1998) while administration of apomorphine in patients failed to change the firing rate of the GP but did reduce STN activity (Stefani *et al.*, 2002). Furthermore, the overall metabolic activity in the GP as measured by mitochondrial cytochrome oxidase expression does not change in 6-OHDA-lesioned rats (Vila *et al.*, 2000) and MPTP-treated monkey (Vila *et al.*, 1996; Vila *et al.*, 1997). Furthermore, post-mortem level of glutamic acid decarboxylase GAD_{67}, the rate-limiting enzyme of GABA synthesis, in the MPTP-treated monkey and PD patients appears to be normal suggesting normal GABAergic transmission (Levy *et al.*, 1997).

1.5.3. The GP: an important integrative centre

According to the classical model, the GP is a simple relay which funnels information though the indirect pathway (Alexander *et al.*, 1990). However, this simple view is no longer tenable. There is extensive axon collateralisation of the GP neurones not only within the GP itself (Milhouse, 1986; Kita & Kitai, 1994; Nambu & Llinas, 1997; Stanford, 2003) and the STN (Smith *et al.*, 1990; Parent & Hazrati, 1995b) but also to the striatum (Bevan *et al.*, 1998), GPi, (Kincaid *et al.*, 1991; Bolam & Smith, 1992), SNr (Smith & Bolam, 1989) and reticular nucleus of the thalamus (Cornwall *et al.*, 1990; Hazrati & Parent, 1991; Gandia *et al.*, 1993). The reciprocal STN-GP connectivity is of particular importance (Carpenter *et al*, 1981; Shink *et al.*, 1996; Smith *et al*, 1998) and this will be discussed later in this chapter.

1.5.4. Dopaminergic nigro-pallidal and nigro-subthalamic projections

Although dopaminergic innervation of the GP is sparse (Lindvall & Björklund, 1979; Lavoie *et al.*, 1989; Parent & Smith, 1987), local application of dopamine or dopamine agonists in the GP reduces the effectiveness of applied GABA (Bergstrom & Walters, 1984). In addition, locally applied dopamine increases GP cell firing by the attenuation of the inhibitory effect of iontophoretically applied GABA or striatal stimulation *in vitro* (Nakanishi *et al.*, 1985). Systemic apomorophine administration also mimics direct dopamine GP application by increasing the activity of GP neurones (Bergstrom *et al.*, 1982; Carlson *et al.*, 1990), although in these studies, actions of dopamine in other nuclei cannot be discounted.

Anatomical studies have shown that the STN receives a direct dopaminergic projection from the SNc (Hassani *et al.*, 1997; Cossette *et al.*, 1999; Gauthier *et al.*, 1999; Prensa *et al.*, 2000; Smith & Kieval, 2000) suggesting an action of dopamine at extrastriatal sites in BG. However, due to low fibre density, the nigrosubthalamic projection has been assumed to play a minor role (Hassani *et al.*, 1997; Hedreen, 1999; Francois *et al.*, 2000).

1.5.5. The hyperdirect cortico-subthalamic projection

A key limitation of the classical model concerns the input stages of cortical afferents of BG. In the classical model, the cortex influences the BG via a unique innervation of the striatum. However, it is now known that the STN also receives an extensive glutamatergic excitatory functional projection directly from the cortex (the so-called hyperdirect pathway) (Fujimoto & Kita, 1993; Maurice *et al.,* 1998; Nambu *et al.,* 2002). The STN also receives glutamatergic projections from the thalamus and the PPN (Bevan *et al.,* 2003). Therefore, cortical information may exert a powerful influence on the whole BG network through direct action on the STN.

1.5.6. The pattern versus the rate of activity

The original model of BG function explains movement disorders only in terms of changes in the rate of neuronal firing. However, upon loss of dopamine in idiopathic and experimental models of PD, neurones of the GP and STN show increases in burst firing and synchronisation of activity (Bergman *et al.,* 1994).

Many studies subsequently have confirmed this observation. In the MPTP-treated monkey, experiments revealed changes of firing pattern through different BG nuclei (Wichmann & DeLong, 2003). Indeed, changes in pattern have been observed in the striatum (Raz *et al.,* 1996; Raz *et al.,* 2001), the pallidum (Filion & Tremblay, 1991; Nini *et al.,* 1995; Heimer *et al.,* 2002; Raz *et al.,* 2000; Raz *et al.,* 2001), the STN (Bergman *et al,* 1994) and the SNr (Wichmann *et al.,* 1999). Studies in 6-OHDA-lesioned rats have supported these observations with the emergence of oscillatory burst firing observed in the striatum (Tseng *et al.,* 2001a), the GPe (Ni *et al.,* 2000), STN (Hassani *et al.,* 1996; Vila *et al.,* 2000; Ni *et al.,* 2001a; Ni *et al.,* 2001b; Zhu *et al.,* 2002a), SNr (Murer *et al.,* 1997; Tseng *et al.,* 2001b).

In each of these studies there are changes in the pattern of activity which invariably shifts from uncorrelated, asynchronous and irregular in normal conditions to correlated, synchronous and periodic (oscillatory) bursting activity in animal models.

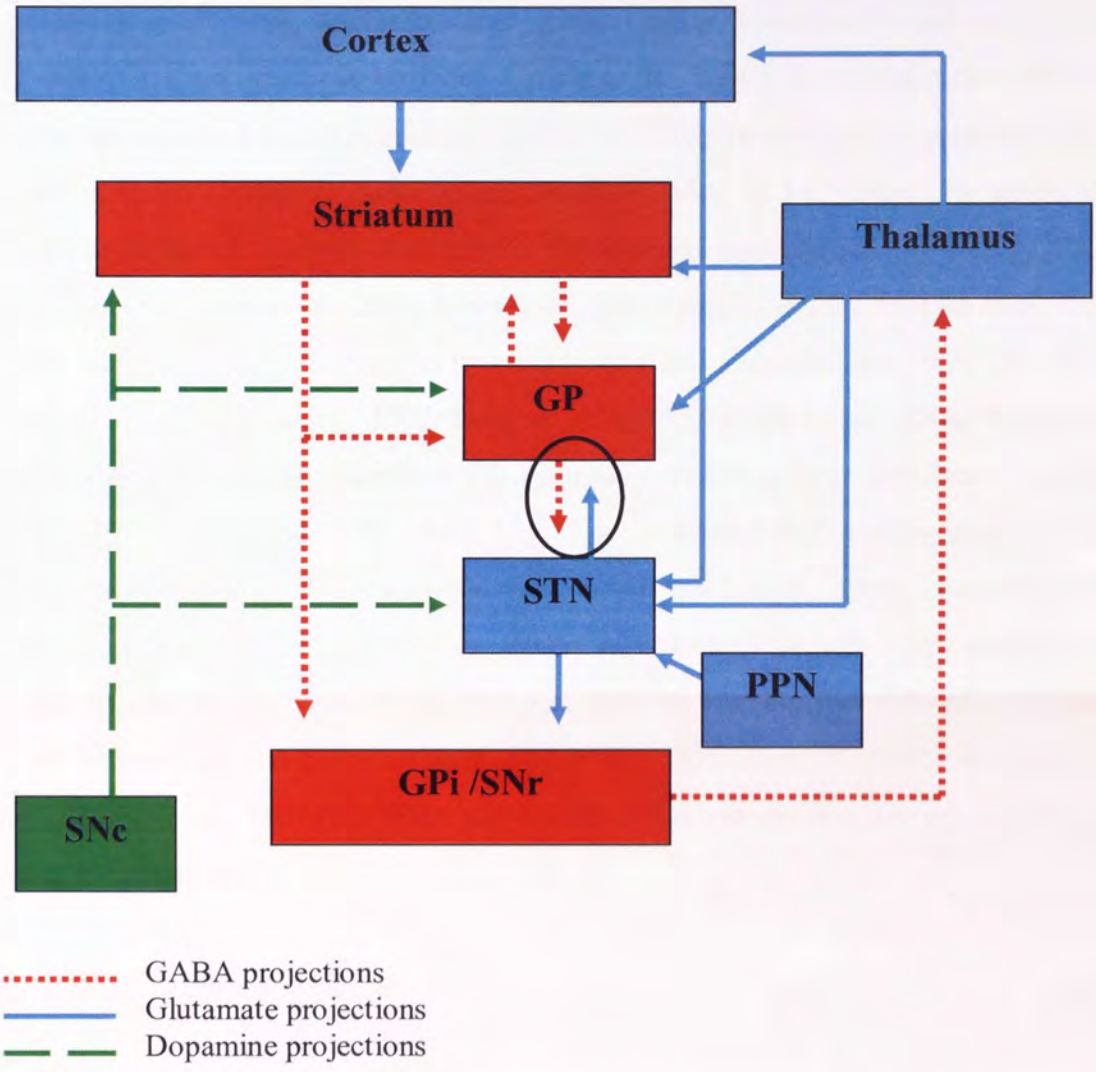

Figure 1.2: BG organisation when the limitations of the classical model are taken into account. Note the presence of reciprocal connectivity between the STN and the GP (indicated by a circle). STN: subthalamic nucleus, GP: globus pallidus (external segment), GPi: globus pallidus (internal segment), SNr: substantia nigra *pars reticulata*, SNc: substantia nigra *pars compacta*.

1.6. Physiological and pathological oscillatory frequencies

1.6.1. Delta, beta and gamma oscillations

Studies in non-human primates during quiet wakefulness (Delong *et al.*, 1985; Matsumura *et al.*, 1992; Wichmann *et al.*, 1994a) and in anaesthetised rodents (Kreiss *et al.*, 1996; Hassani et *al.*, 1996, 1997; Urbain *et al.*, 2000) have shown that STN cells exhibit spontaneous activity ranging between 18-25 Hz in non-human primates and 13-18 Hz in rodents, with irregular and uncorrelated firing in each case. However, upon dopamine depletion, periods of correlated synchronous bursting activity emerge, both in the pallidum (Brown *et al.*, 2001; Levy *et al.*, 2002b) and the STN (Brown *et al.*, 2001). These oscillations are expressed in two forms: 1) a beta frequency (at 10-30 Hz) (Brown *et al.*, 2001; Cassidy *et al.*, 2002; Levy *et al.*, 2002b; Kuhn *et al.*, 2004; Priori *et al.*, 2004) which appears to exacerbate PD symptoms and 2) a delta oscillatory frequency (at 4-7 Hz) in GPi and STN which has been correlated with resting muscle tremor (Filion & Tremblay, 1991; Bergman *et al.*, 1994; Nini *et al.*, 1995; Hutchison *et al.*, 1997; Levy *et al.*, 2000; Magnin *et al.*, 2000). Following dopamine replacement therapy or during voluntary movement, the power of the beta frequency is reduced and replaced by an increase in gamma frequency (30-70 Hz) (Brown *et al.*, 2001; Heimer *et al.*, 2002; Levy *et al.*, 2002a), a frequency which is thought to be a carrier frequency for motor information (Brown & Marsden, 1998).

1.6.2. Deep brain stimulation

As the classical model of BG function suggests, the STN has become a key target in the treatment of PD, not only as the site of irreversible subthalamic lesions, but also as the site for deep brain stimulation (DBS) (Limousin *et al.*, 1995; Krack *et al.*, 1998; Benabid *et al.*, 2000) to relieve the symptoms of PD. As lesions reduce STN and BG output activity, DBS in both PD patients (Benabid *et al.*, 2005; Dostrovsky *et al.*, 2002) and animal models of the disease (Benazzouz *et al.*, 1993; Benazzouz *et al.*, 1996; Boraud *et al.*, 1996) was thought to produce a reversible lesion inhibiting activity possibly through a depolarising block (Benazzouz *et al.*, 1993). However, more recent

studies suggest that this is not the case and alternative views including STN excitation and inhibition have been put forward (Dostrovsky & Lozano, 2002; Garcia *et al.*, 2005). Irrespective of the precise mechanism of action, the observation of the beneficial therapeutic improvements of the symptoms of PD following lesions or DBS of the nucleus (Bergman *et al.*, 1990; Wichmann *et al.*, 1994) suggests that the STN could play a role in the generation or the control of the pathological rhythmic activity observed in PD.

1.7. Possible origin of oscillatory activity in the STN

1.7.1. Cortico-subthalamic interactions

In vivo, single-unit extracellular recordings in normal rats have revealed low-frequency oscillatory activity (~1Hz) of the GP and the STN correlated between the two nuclei and between the two nuclei and slow-wave activity in the cortex (Magill *et al.*, 2000). Interestingly, this correlation appears more pronounced in 6-OHDA-lesioned rats (Magill *et al.*, 2001). Furthermore, modification of cortical activity (by cortical activation or depression) suppresses the low-frequency oscillatory activity, suggesting that the oscillatory activity within BG nuclei could be driven by the pattern of cortical input. However, a small percentage of neurones in 6-OHDA-lesioned rats still oscillate (GP~ 15%, STN ~20%), indicating that STN and GP neurones may be able to oscillate without the influence of extrinsic input when dopamine is depleted. Either the local STN-GP network and/or intrinsic membrane properties may sustain the activity of these neurones.

Recently, DBS of primary cortex in the MPTP-treated monkey has been found to normalise the firing rate of STN (and thus GPi) and reduce the symptoms of akinesia and bradykinesia (Drouot *et al.*, 2004). Thus, direct stimulation of the cortex appears to be a potential new target for the treatment of PD.

1.7.2. The STN-GP network

Using organotypic co-culture of GP, STN, striatum and cortex, synchronised oscillatory bursting at slow frequency (0.4, 0.8 and 1.8 Hz) was observed in both STN and GP neurones (Plenz & Kitai, 1999; Wichmann & Delong, 1999). This synchronised activity was maintained when cortical or striatal inputs were removed suggesting that the synchronised bursting does not require cortical influences. Interestingly, the bursting activity reverts to single-spike firing when GP is disconnected from the STN. Thus, intact connectivity between the STN and the GP seems to be crucial to the generation of synchronised oscillatory bursting. This led Plenz and Kitai to propose that recurrent inhibitory and excitatory connections between the GP and the STN may provide sufficient conditions for maintaining synchronised oscillatory activity. The recurrent oscillatory activity also appears dependent on the intrinsic properties of the STN cells themselves such that GABA transmission from GP is able to elicit rebound burst firing in STN neurones which will drive the GP cells once more.

1.8. Aims and Objectives

The bursting activity observed by Plenz & Kitai, (1999) in organotypic co-culture is dependent on the existence of an intact STN-GP network. The model proposed, if reproduced *in vitro* would allow the study the mechanisms of synchronous oscillatory bursting and also the action of dopamine upon his activity. The STN-GP connectivity in the rat slice preparation did not appear robust and no synchronous oscillatory activity was observed (Wilson *et al.*, 2004). However, in the mouse slice preparation, the distance between the STN and the GP may be reduced sufficiently to preserve the two nuclei. Once present, the role of the STN-GP network in maintaining synchronous oscillatory activity can be assessed as well as the role of dopamine.

Thus, the specific questions to be addressed include:

1) Can connectivity between the GP and STN be maintained in the slice preparation?

2) Does the maintained STN-GP network sustain oscillatory activity?

3) If not, can oscillatory activity be induced pharmacologically?

4) What is the effect of the network on oscillatory activity?

5) What role does dopamine play in mediating oscillatory activity?

Chapter 2. Materials and methods

2.1. The brain slice preparation

2.1.1. Separation of the brain hemispheres

CB57BL/6JCrL male mice and MPTP-treated mice, aged between 21-50 days, were used throughout the study. These animals were anaesthetised with fluorothane 4 % in O_2/N_2O and were humanely killed in accordance with the Animals (Scientific Procedures) Act (1986), U.K. The brain was quickly removed and placed in an ice-cold sucrose modified artificial cerebrospinal fluid (aCSF) solution previously saturated with $95\%O_2/5\%CO_2$.

The brain was placed on its ventral surface on a filter paper (Whatmann, UK) soaked in an ice-cold aCSF solution. Using a razor blade (Wilkinson Sword, UK), which had been cleaned with ethanol, two coronal cuts were carried out, one caudally to remove the cerebellum and one rostrally to remove the frontal part of the brain. Then, a sagittal cut was performed in the midline allowing the separation of the two brain hemispheres (figure 2.1) which were positioned on their medial side on filter paper.

2.1.2. Slicing of the brain

Previous work by Wilson, (2004) had determined (by biocytin labelling) that a sagittal slice preparation cut at 20° to the midline maintained robust STN-GP connectivity. In order to reproduce this orientation, a 20° agarose support, made of agarose (3 %, Sigma, UK) and NaCl (0.6 %), was used (figure 2.2). The two brain hemispheres were adhered to the agarose support (Ultrafast cyanoacrylate adhesive, RS, UK), attached to a metal tray and held in place on a DTK1000 microslicer (Dosaka, Japan). The tray was then filled with the ice-cold aCSF solution and continuously bubbled with $95\%O_2/5\%CO_2$. Up to 2 slices of 300 μm thickness per hemisphere containing both the STN and the GP were obtained (figure 2.3). These slices were kept on a mesh in a holding chamber filled with aCSF solution saturated with $95\%O_2/5\%CO_2$ at room temperature (21-23 °C) until required.

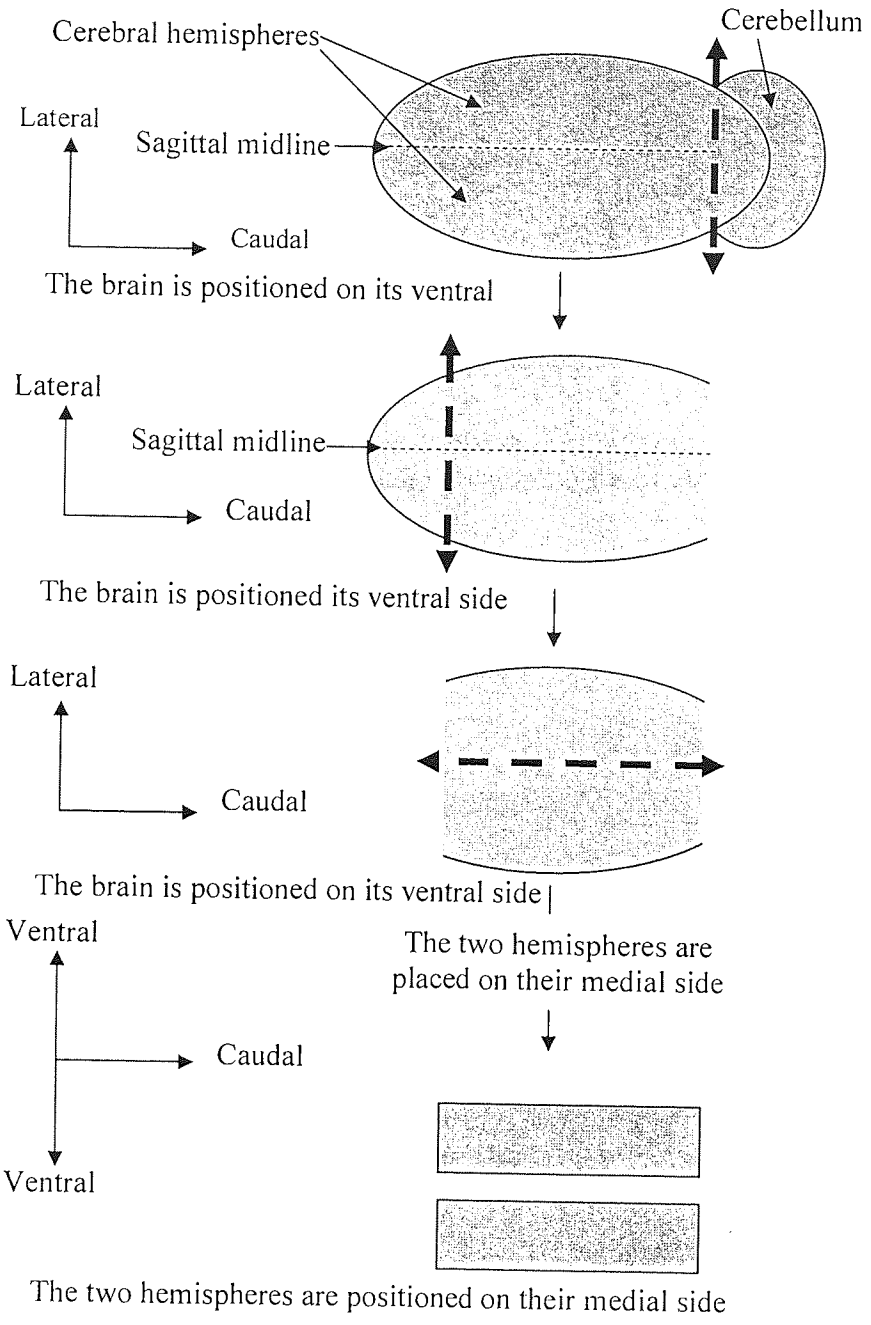

Figure 2.1: Separation of the mouse brain hemispheres. The cuts are indicated by a thick broken line with double-headed arrows.

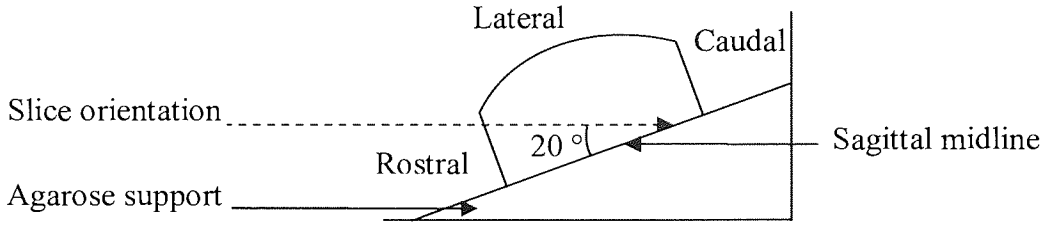

Figure 2.2: Position of one brain hemisphere on the agarose support. Note that the brain hemisphere is placed on its medial side with the caudal side facing the top of the support.

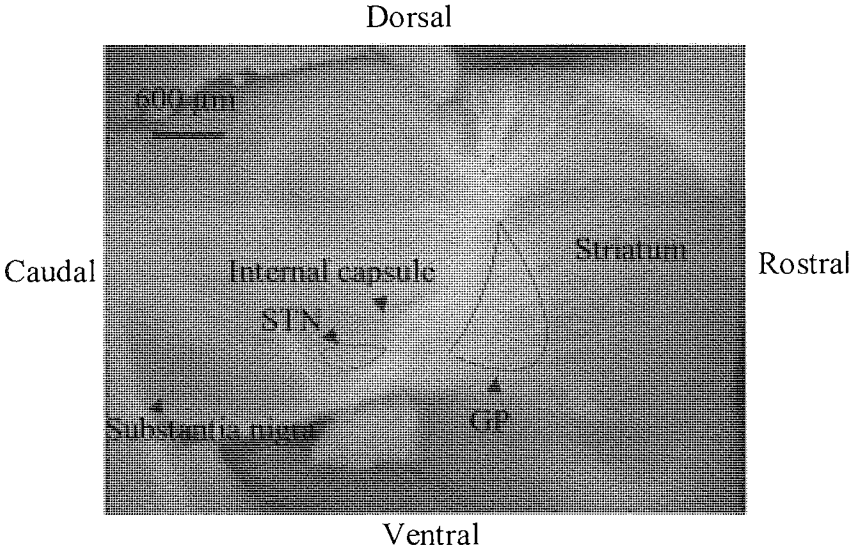

Figure 2.3: Photography of the mouse 20° parasagittal slice showing both the STN and the GP. (Obtained with the permission of Dr Claire Wilson).

2.2. MPTP-treated mice

The work described in this paragraph was carried out by Cash D (Neuroimaging Research Group, Institute of Psychiatry, London, SE5 8AF). Male adult C57BL/6J mice (Harlan, UK) were treated with 4 intra-peritoneal injections at hourly intervals of either 10 mg/kg MPTP-HCl (Sigma-Aldrich; dose adjusted for free base) in 10 ml/kg sterile saline (23 animals), or an equivalent volume of saline (n=5), using the method originally described by Araki *et al,* 2001. 20 MPTP-lesioned mice survived for more than 48 hours, with no apparent signs of ill-health, of which 15 were used subsequently for electrophysiological experiments. 5 additional MPTP-treated mice and 5 saline-treated mice were killed by an overdose of barbiturate anaesthetic 15-16 days after MPTP treatment. Their brains were removed immediately and hemisected: one hemisphere (left or right, randomly chosen) was used for high performance liquid chromatography analysis of striatal catecholamines and the other hemisphere was used for tyrosine hydroxylase immunohistochemistry. Indeed, lower concentration of striatal dopamine compared to those from control mice and reduced tyrosine hydroxylase immunostaining in the striatum and SNc were observed. Electrophysiological recordings were made, 10-21 days following the treatment with MPTP, from STN neurones in 20 ° parasagittal slices from MPTP-treated mice and age-matched normal animals.

2.3. The solutions

2.3.1. The aCSF solution

The aCSF solution contained (in mM) NaCl 126, KCl 2.5 (in some experiments KCl was raised to 4.5), NaH_2PO_4 1.2, $MgCl_2$ 1.3, $CaCl_2$ 2.4, glucose 10 and $NaHCO_3$ 26 at pH 7.7. The osmolarity of the aCSF solution, measured by a Model 3300 osmometeter (Advanced Instruments, USA), was 300-310 mOsm/litre. The compounds used to prepare the aCSF solution were from Fisher Scientific, UK with the exception of $CaCl_2$ which was from BDH, UK.

2.3.2. Preparation of the aCSF solution

The aCSF solution was initially made as 10-fold stock solution (without glucose and $NaHCO_3$) in distilled water and diluted 10-fold on the morning of use before the addition of glucose and $NaHCO_3$. Before setting up the perfusion system, the aCSF solution was saturated with 95%O_2/5%CO_2 at 40°C in a water bath (Grant Instruments, UK) for at least 25 minutes.

2.3.3. The sucrose aCSF solution

The sucrose aCSF contained (in mM) sucrose 206, KCl 2.5, $CaCl_2$ 2, $NaHCO_3$ 26, NaH_2PO_4 1.25, $MgCl_2$ 1, Glucose 10. NaCl was substituted for sucrose to improve cell viability during the dissection. To further improve viability, a cyclooxygenase inhibitor, indomethacin, was added to the sucrose aCSF solution at final concentration of 45 μM (Aghajanian & Rasmussen, 1989). A stock of indomethacin, at a concentration of 45 mM, was prepared weekly in dimethylsulfoxide (DMSO) and kept at 4-6 °C. The indomethacin and the DMSO were from Sigma, UK.

2.4. Whole-cell recordings

2.4.1. The recording chamber

The slices containing the STN and the GP were transferred to a recording chamber (volume: ~1.5 ml) and held in position using four platinum wires (length: 4-5 mm; diameter: 0.5 mm; PT 005146/65, Goodfellow Cambridge Limited, UK). The bottom of the recording chamber was made of microscope glass cover slip (diameter: 22 mm; Chance Propper Ltd, UK). The recording chamber was continuously perfused with the aCSF solution previously saturated with 95%O_2/5%CO_2 at around 40 °C (figure 2.4).

2.4.2. The perfusion system

A closed perfusion system was used in order to maintain constant saturation with 95%O_2/5%CO_2, constant flow rate (2-3 ml/min) and pH (7.7) (figure 2.5). The

aCSF solution flowed from the bottom of a reservoir (a bottle of ~1.2 litres) to the recording chamber. To ensure constant saturation with 95%O_2/5%CO_2, constant flow rate and pH, a 3 litres intravenous bag (Baxter, CLINTEC) filled with 95%O_2/5%CO_2 was tightly connected to the top of the reservoir. Between the reservoir and the recording chamber, a series of four 3-way taps were connected to allow bath application of drugs. Large syringes (50 ml) were used as drug bottles that were attached to taps for drug applications with a dead time of 30 sec. The height of the drug bottles was adjusted so that the flow rate from the drug bottles was the same as of the flow rate from the reservoir. The aCSF solution was siphoned off to waste. The aCSF solution was heated (32-34 °C) using a heat exchanger jacket supplied with water from a Circulator C-85A heater (Techne, UK).

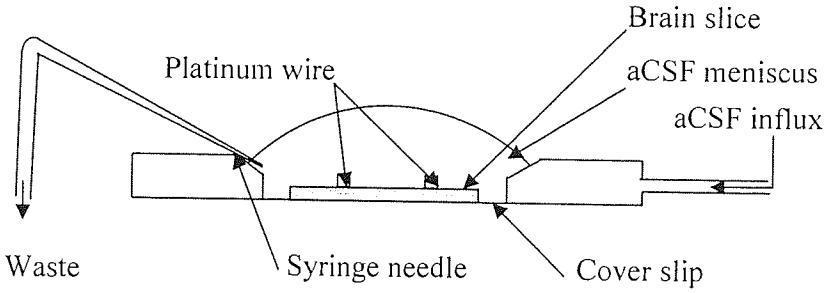

Figure 2.4: The recording chamber configuration used in whole-cell.

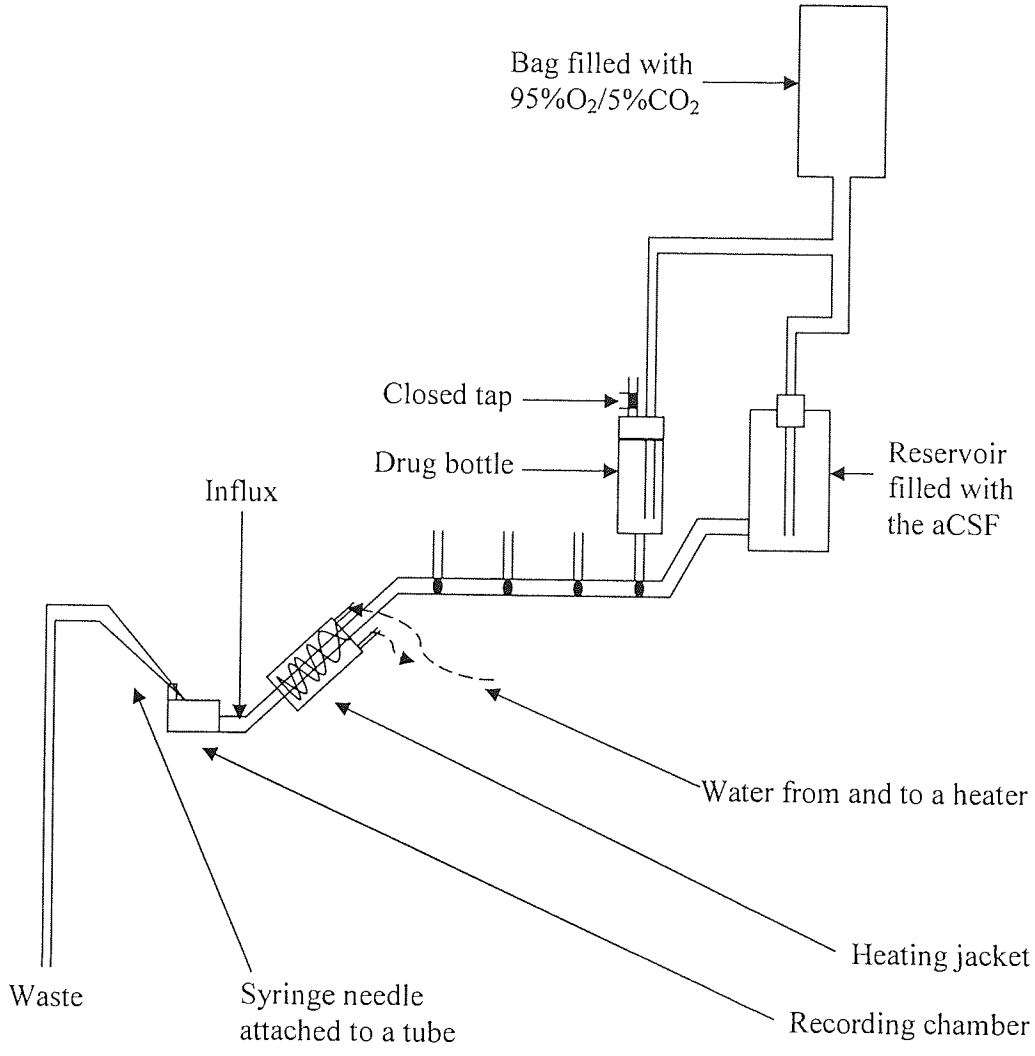

Figure 2.5: The closed perfusion system.

2.4.3. The recording electrodes

Recording electrodes were pulled from borosilicate glass tubes (GC120F-10, Harvard Apparatus, UK) on a Model P-97 micropipette puller (Sutter Instruments, USA). The electrodes were filled with an internal solution containing (in mM) K gluconate 125, NaCl 10, $CaCl_2$ 1, $MgCl_2$ 2, EGTA 0.5 (or BAPTA 10), HEPES 10, GTP 0.3, Na_2ATP_2. The internal solution was adjusted to pH 7.3 with KOH and 280 mOsmol/litre with double processed tissue-culture water (Sigma, UK). The resistance of the electrodes was 3-5 MΩ when filled with the internal solution. The recording electrode was mounted in a holder which contained a Ag/AgCl coated silver wire (length: 4-5 cm; diameter: 0.25 mm; AG 005140/3, Goodfellow Cambridge Limited, UK) attached to a headstage (CV 203 BU, Axon Instruments, USA) whose movement was controlled by a TS-5000-150 micromanipulator (Burleigh, USA). The Ag/AgCl coat allowed electrical continuity between the internal solution and the wire.

2.4.4. Whole-cell recordings

Single cells were visualised with a differential interference infra-red upright microscope (BX 50WI, Olympus, Japan). The microscope was fitted with an infrared video camera (KP-M1, Hitachi, Japan), an image enhancer system (ADV-2, Brian Reece Scientific Ltd, Newbury, UK) connected to a monochrome video monitor (WV-BM 1400, Panasonic). Under visual guidance (with 10x objective and 40x water immersion objective) and with continuous positive pressure and 2 mV hyperpolarising steps (duration: 200 ms; frequency: 2 Hz) in voltage-clamp configuration, the recording electrode was advanced towards the soma. When a small depression was observed on the soma, positive pressure was released in order to form a tight seal between the electrode and the somatic membrane (cell-attached configuration). A tight seal corresponds to a resistance in excess of one GΩ and is visualised by a decrease in the amplitude of the current elicited in response to the 2 mV hyperpolarising steps. Once, the tight seal was formed, a slight negative pressure (by gentle suction) was applied to break through the membrane (whole-cell configuration) and the cell was immediately clamped at -60 mV in voltage-clamp configuration.

2.4.5. Recording the neuronal activity

Electrophysiological signals were monitored using an Axopatch 200B amplifier (Axon Instruments, Foster City, CA, USA). Membrane potentials were recorded in fast current-clamp mode and were corrected with respect to the null potential measured at the end of the recording. The fast mode was used instead of the normal mode to improve the accuracy of the recordings. Signals were low-pass filtered at 2 KHz and digitized at 10 KHz. Data was monitored on a HM305 oscilloscope (Hameg Instruments, Germany) and acquired and analysed with a micro-1401 interface (Cambridge Electronic Design, UK) and Signal 2.10 software (Cambridge Electronic Design, UK). The microscope, the headstage and the micromanipulator were on an anti-vibrating table (model VH3036-OPT, Newport, USA).

The offset was set to zero on entry into the bath and again prior to patching the cells. Liquid junction potentials estimated to be +8 mV were not corrected. Series resistance which include pipette resistance and any other resistance between the cell and the electrode was not compensated unless otherwise stated. Series resistance compensation allows the actual membrane potential to reach the voltage command within the time of the applied voltage step. Series resistance was routinely compensated to 60-80 %, and ranged from 5.6 to 22 MΩ. During the course of an experiment, if series resistance changed by more than 20 % the cell was discarded. To determine the input resistance of the cell, the current evoked in response to a 5 mV hyperpolarising step from a holding potential of -60 mV was measured and the corresponding resistance calculated using the Ohm's law. Cells with an input resistance less than 100 MΩ, action potential amplitude less than 50 mV (from the action potential threshold to the peak) and a resting membrane potential above -40 mV were discarded. Resting membrane potential was obtained in voltage- clamp configuration when the holding current is null.

Action potential (AP) parameters were quantified as indicated below in the figure 2.6.

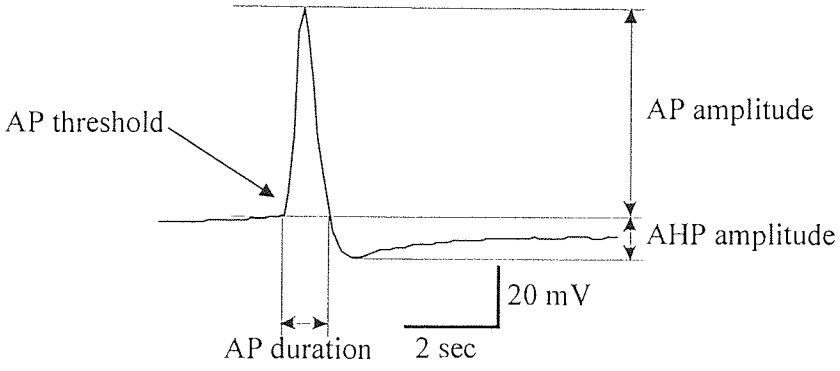

Figure 2.6: Quantification of action potential parameters. Note the criteria used to quantify the parameters of action potentials. AP: action potential. AHP: after-hyperpolarisation.

2.5. Extracellular recordings

2.5.1. The recording chamber and the perfusion system

The recording chamber used in extracellular experiments is shown in figure 2.7. Slices were placed on a mesh and held by four platinum wires (length: 4-5 mm; diameter: 0.5 mm; PT 005146/65, Goodfellow Cambridge Limited, UK). The temperature of the recording chamber was maintained at 32-34 °C as in whole-cell recordings. The perfusion system used was the same as for whole-cell recordings (figure 2.5).

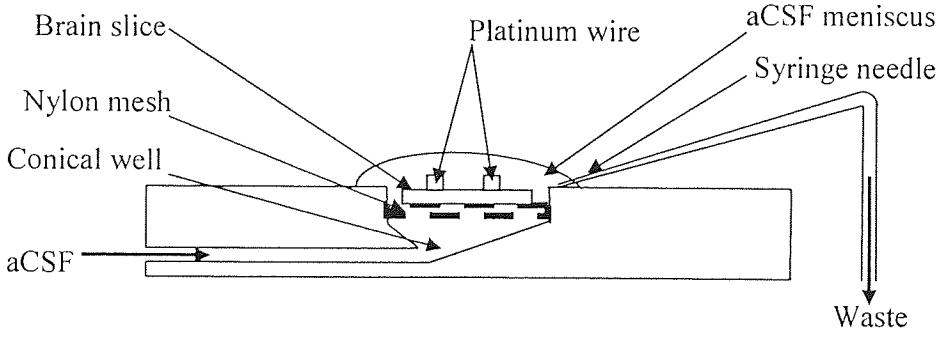

Figure 2.7: The recording chamber configuration used in extracellular recordings.

2.5.2. The recording electrodes

Recording electrodes were pulled from borosilicate glass tubes (GC100FS-10, Harvard Apparatus, UK) using a p-97 micropipette puller (Sutter Instruments, USA). Recording electrodes were filled with a 2 M NaCl solution and then slightly broken back by a gentle shock on the platinum wire in order to obtain a resistance of around 10 MΩ. The recording electrodes were held on a micromanipulator (Kanatec, Japan) and contained a silver wire (length: 4-5 cm; diameter: 0.25 mm; AG 005140/3, Goodfellow Cambridge Limited, UK) attached to an AI 402 x50 ultra-low noise amplifier headstage (Axon Instruments, USA) which was connected to an eight channel CyberAmp 380 amplifier (Axon Instruments, USA). The slices could be observed under a 16x objective of a dissecting microscope (Jena, Carl Zeiss, Germany).

2.5.3. The recording of neuronal activity

Single "unit" (single cell) waveforms were detected and amplified 50 times with the AI 402 x50 ultra-low noise amplifier headstage and 200 times with the CyberAmp 380 amplifier and monitored on a HM407 oscilloscope (Hameg Instruments, Germany). Data were acquired and analysed with a micro-1401 mk II interface (Cambridge Electronic Design, UK) and Spike2 5.00/5.11 software (Cambridge Electronic Design, UK). Single-units were discriminated from noise and sorted off-line. In some recordings, two units were recorded in the same time using two headstages connected to the same CyberAmp 380 amplifier.

2.6. Electrical stimulation of the GP and the STN

To show connectivity between the GP and the STN, synaptic neurotransmitter release was evoked using single focal bipolar shock stimulation in the GP and the STN. A constant current DS2A stimulation unit (Digitimer Ltd, UK) connected to a Master-8 eight-channel programmable pulse generator (Intracel, UK) was used. The stimulating electrode consisted of two insulated 80% nickel / 20% chromium wires of 0.05 mm diameter (Gi718, Advent, UK) twisted around each other. The stimulating parameters used were 0.02-0.2 ms, 1-30 mA.

2.7. Drugs used in this study

Drugs were applied to the superfusate by exchanging the aCSF solution to the recording chamber with a dead time of 30 s. The concentrations used, suppliers and solvents in which the drugs were prepared are indicated in the table 2.1. The drugs are indicated by their abbreviation as used in the text. All the drugs were kept frozen except for 1S-3R-ACPD, 5-HT and sulpiride, which were stored at 4-6 °C. Dopamine was prepared daily and continuously bubbled in N_2 at room temperature to prevent its oxidation.

Drugs	Suppliers	Concentrations used (μM)	Stock concentrations (mM); solvent
1S-3R-ACPD	Tocris, UK	1, 3, 10, 30, 100	100; H_2O
Apamin	Tocris, UK	0.05, 0.1	0.1 ; methanol
Bicuculline methiodide	Tocris, UK	10	10 ; H_2O
CNQX	Sigma, UK	10	2 ; NaOH
DL-AP5	Tocris, UK	50	50 ; NaOH
Dopamine	Sigma, UK	30	30 , H_2O
Eticlopride	Sigma, UK	10	10 ; H_2O
GR113808	Tocris, UK	0.100	0.5 ; 25 mM HCl
5-HT	Sigma, UK	1, 3, 10, 30, 100	10; H_2O
NMDA	Tocris, UK	20	20 ; H_2O
Quinpirole	Tocris, UK	100	10 ; H_2O
Picrotoxin	Tocris, UK	50	50 ; H_2O
RS102221	Tocris, UK	0.5	1 ; DMSO
SKF38393	Sigma, UK	10	10 ; H_2O
SCH23390	Tocris, UK	2	2 ; H_2O
Sulpiride	Tocris, UK	10	10 ; ethanol
TTX	Sigma, UK	1	1 ; H_2O
WAY100135	Tocris, UK	1	1 ; H_2O

Table 2.1: The drugs used in this study. The suppliers, the concentrations of perfusing and stock solutions, the solvents used for stock solutions are indicated.

2.8. Statistical analysis

Statistical analysis was performed with Prism 2.01 software (Graphpad, San Diego, USA). Paired Student or Wilcoxon matched paired tests were used to compare the effect of two drugs applied on the same cells. Unpaired Student or Mann-Whitney tests were used when two drugs were applied on different cells. The normality of distributions was tested using the Kolmorgorov-Smirnov two sample test. Correlation between control firing rate and responses to drug was assessed by the Pearson test. The level of significance accepted was $P<0.05$. Data were expressed as mean ± standard error of the mean unless otherwise stated.

The control firing rate of cells was calculated from the reciprocal of the mean interspike interval over a 2-minute period before the application of the first drug. Changes in the firing rate following drug application were measured at the steady state of the drug response. Rate-meters were represented with a bin size of 1 s.

When an attempt was made to pharmacologically promote burst firing activity, the firing pattern was assessed using the burst and oscillation detection algorithm of Kaneoke & Vitek, 1996. In this program, the algorithm detects a discharge density (number of spikes in a given train) which differs significantly from a Poisson (irregular) distribution of mean 2, giving thus a burst index > 0.5. Neurones were thus considered burst-firing when the burst index was above 0.5 and fired three or more bursts, consisting of more than 3 spikes, in the 2 min analysis in question. The burst parameters quantified were the interburst frequency, the number of spikes and the interspike interval (ISI) within the burst; autocorrelograms of the discharge were constructed with a bin size of 10 ms and a lag time of 5 s. Lomb periodograms were used to assess the statistical significance of any oscillation. The frequency spectra were displayed and the relative power of any peak was indicated by the significance level (represented by a dashed line).

To determine whether the firing of two cells is synchronous, cross-correlograms of action potentials were calculated for a 2 min period using Spike2 version 5.11 (Cambridge Electronic Design, UK) based on a bin size of 0.2 ms and a lag time of 100 ms.

Chapter 3. Intrinsic properties of mouse GP and STN cells

3.1. Introduction

This chapter examines the intrinsic electrophysiological properties of neurones of the GP and the STN in the mouse slice preparation using single-unit extracellular and whole-cell recordings. As the whole-cell recording technique was used to classify GP cells of the rat *in vitro* (Cooper & Stanford, 2000), similar criteria were adopted for the separation of different neuronal subtypes in this study.

3.1.1. Intrinsic properties of GP cells

Many studies using intracellular recordings have attempted to classify GP neurones on the basis of their electrophysiological properties. However, no consensus has emerged (Table 3.1).

In vivo, in rat, Kita & Kitai, (1991) have reported three cell types. The most common cell type (73 % of the population) was characterised by repetitive firing activity at 2-40 Hz, with little spike accommodation (the reduction in action potential amplitude during a sustained depolarising current step) and frequency adaptation (the reduction in the frequency of AP firing during a sustained depolarising current step). The second subtype accounted for 18 % of the population and was characterised by periodic burst-firing in response to depolarising currents and rebound burst depolarisations on termination of hyperpolarising current steps. The last subtype account for 9 % of the population and was silent at rest.

Sharp microelectrode recordings *in vitro* have revealed three cell types in the guinea-pig (Nambu & Llinás, 1994, 1997). In these studies, Type I cells (18 % of the population) expressed calcium-dependent subthreshold membrane oscillations and burst-firing with strong accommodation upon membrane depolarisation. Type II cells represented the most abundant cell type (73 % of the population). These cells displayed sodium subthreshold membrane oscillations, rebound depolarisations but no I_h. Type III cells show properties similar to those of rat striatal cells. Similarly, a whole-cell patch clamp study in the rat (Cooper & Stanford, 2000) provided evidence for three subtypes of GP cell. In this study, type A cells represent 63 % of all classified cells. In response to hyperpolarising current injection, type A cells

show a sag in membrane voltage indicative of I_h current and rebound depolarisation accompanied by action potential firing at the end of the hyperpolarising current injection. In comparing type A cells with type II cells of Nambu & Llinas, (1994), the proportions appear comparable (A: 63 %, II: 73 %), and both display sodium subthreshold membrane oscillations and rebound depolarisations, although I_h was not described in type II cells.

Type B cells constitute 32 % of the total population (Cooper & Stanford, 2000) These cells respond with regular firing upon depolarising current injection and do not express I_h or the transient low threshold calcium current I_t. These cells may correspond with type I cells of Nambu & Llinas, (1994).

Type C cells have wide action potentials, high input resistance and no evidence of I_h or I_t (Cooper & Stanford, 2000). However these cells do not correspond with the type III cells described by Nambu & Llinas, (1994, 1997), which show similar properties to striatal MSNs. Type C cells may well be cholinergic neurones, perhaps displaced from the basal nucleus of Meynert (Cooper & Stanford, 2000), although this hypothesis has never been directly tested.

Authors Animal species *In vivo* or *in vitro*	Kita & Kitai, 1991 Rat *In vivo*			Nambu & Llinas, 1994 Guinea pig *In vitro*			Cooper & Stanford, 2000 Rat *In vitro*		
Recording techniques	Sharp intracellular			Sharp intracellular			Whole-cell		
Name of the cell types	Repetitive firing cells	Periodic burst firing cells	Silent cells	I	II	III	A	B	C
Proportions of each cell type (%)	73	18	9	18	73	9	63	32	5
Activity at rest (tonic, silent or burst)	Tonic 2-40 Hz	Periodic burst	Silent	Silent	Tonic Silent	Silent	Tonic Silent	Tonic	Silent
Presence of I_h (voltage sag)	No	No	N.A	N.A	No	N.A	Yes	No	No
Presence of rebound firing	No	Yes	N.A	Yes	Yes	N.A	Yes	Yes	N.A
Responses to depolarising current injection (Tonic or burst)	Tonic	Burst	Tonic	Burst	Tonic	Tonic	Tonic	Tonic	Tonic
Membrane oscillations are dependent on	N.A	N.A	N.A	Calcium	Sodium	N.A	Sodium	N.A	N.A

Table 3.1: Summary of intrinsic membrane properties of GP subtypes in rat and guinea pig. These data are taken from the papers of Kita & Kitai, (1991), Nambu & Llinas, (1994), Cooper & Stanford, (2000) and Stanford IM, (2003). NA: non available.

3.1.2. Intrinsic properties of STN cells

In slices, extracellular recordings of STN cells have reported spontaneous firing with a regular or pacemaker-like pattern ranging between 6 and 30 Hz (Flores *et al.*, 1995; Abbott *et al.*, 1997; Zhu *et al.*, 2002a; Tofighy *et al.*, 2003; Wilson *et al.*, 2004). This spontaneous, regularly firing pattern was also described in perforated patch recordings (Bevan & Wilson, 1999; Bevan *et al.*, 2000; Bevan *et al.*, 2002a; Bevan *et al.*, 2002b; Hallworth *et al.*, 2003) and whole-cell recordings (Beurrier *et al.*, 1999; Wigmore & Lacey, 2000; Baufreton *et al.*, 2001; Zhu *et al.*, 2002b) and is largely dependent on a TTX-sensitive persistent sodium current which contributes to the depolarising phase of membrane oscillations (Bevan & Wilson, 1999; Beurrier *et al.*, 2000) and SK currents which contribute to the hyperpolarising phases (Bevan & Wilson, 1999).

Early intracellular recordings by Nakanishi *et al.*, (1987a) and more recent studies by Beurrier *et al.*, (1999) and Otsuka *et al.*, (2001) have revealed that STN cells can also produce slow depolarising plateau potentials which outlast brief duration depolarising current injections elicited from hyperpolarised potentials. The level of membrane hyperpolarisation is critical to the generation of these plateaus since reducing the level of hyperpolarisation eliminates the plateaus. Depolarising excitatory glutamatergic synaptic input can also elicit plateau potentials when the STN cells are hyperpolarised (Otsuka *et al.*, 2001). STN cells have also been reported to generate rhythmic bursting with low (<1 Hz) frequency following continuous hyperpolarising current injection (Beurrier *et al.*, 1999), although this was not confirmed by other authors (Wilson *et al.*, 2005).

STN cells also display time- and voltage-dependent anomalous inward rectification in response to hyperpolarising voltage steps indicative of I_h (Nakanishi *et al.*, 1987a; Bevan & Wilson, 1999; Wigmore & Lacey, 2000) and pronounced rebound depolarisation accompanied by action potential firing indicative of the transient low-threshold calcium current (I_t) (Nakanishi *et al.*, 1987a; Bevan & Wilson, 1999; Wigmore & Lacey, 2000). The extent of this rebound can be either short (<100 ms in 76 % of the STN cells) or long (>100 ms with an average of 367.7 ± 286.5 ms) and has led

some authors to question whether there is neuronal heterogeneity in the STN with respect to the rebound duration (Bevan & Wilson, 1999; Bevan *et al.*, 2002).

SK channels are responsible not only for the slow phase of the after-hyperpolarisation following an action potential, but also play an important role in the determination of firing pattern of STN cells. Block of the SK channel with apamin not only extends the duration of rebound burst (Hallworth *et al.*, 2003) but is also able to enhance burst activity (Beurrier *et al.*, 1999; Hallworth *et al.*, 2003).

3.2. Results

3.2.1. Mouse GP cells

In order to examine whether there is a heterogeneous population of GP cells whole-cell recordings of 66 GP neuones were performed. Distribution histograms of the resting membrane potential (RMP), input resistance (IR) and action potential (AP) duration were plotted (figure 3.1). The distribution did not follow a normal distribution for the three parameters indicative of the existence of more than one population of GP cells. Following this, GP cells were classified into two populations depending on whether the recorded cell expressed I_h and rebound depolarisation.

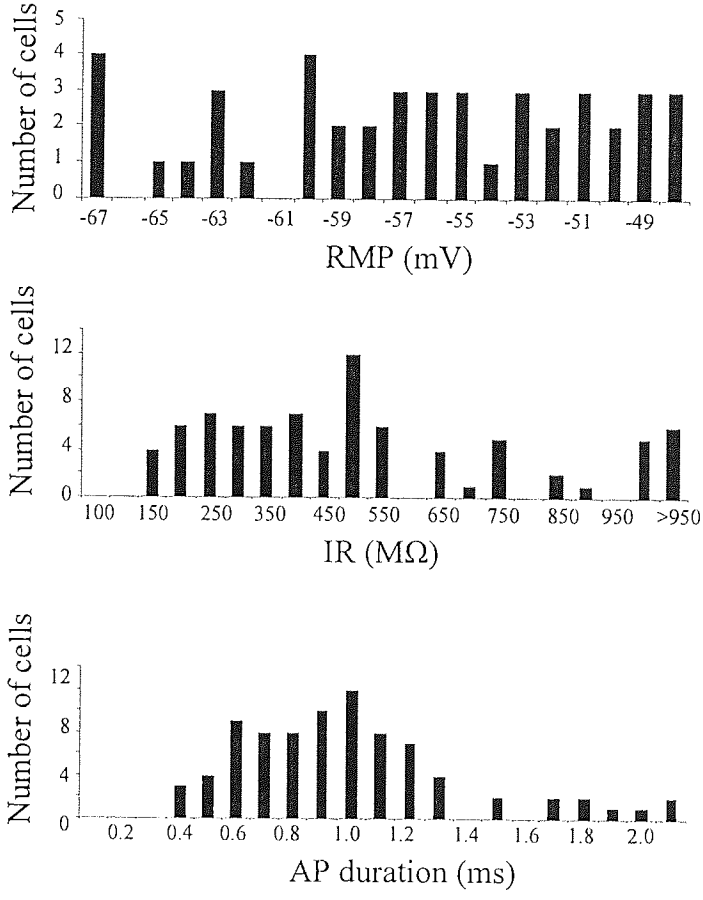

Figure 3.1: The distribution of RMP, IR and AP duration suggests a heterogeneous population of GP neurones. Distribution histograms of RMP (**A**), IR (**B**) and AP duration (**C**). These parameters did not display a normal distribution indicative of a heterogeneous population of GP neurones.

3.2.2. Type A GP cells

Most mouse GP neurones (n=66 of 83, 79 %) showed evidence of both I_h and rebound depolarisations. In voltage- clamp, I_h was observed as a time- and voltage-dependent inward current in response to 5 mV hyperpolarising steps (figure 3.2A). In current clamp this current was seen as a depolarising 'sag' in the membrane voltage in response to hyperpolarising current steps (Harris & Constanti, 1995). In addition, rebound depolarisations accompanied by action potential firing were observed following repolarisation of the membrane (figure 3.2B). Little adaptation and accommodation was observed in response to depolarising current injection (figure 3.2C).

31 of 66 (47 %) of type A GP cells were quiescent, with a mean resting membrane potential of -58.2 ± 0.9 mV. The remaining fired action potentials at an average frequency of 20.0 ± 3.7 Hz (n=35 of 66, 53 %). There was no significant difference between these two sets of cells with respect to the IR (P=0.40), AP amplitude (P=0.28), AP duration (P=0.16), AP threshold (P=0.86) and AHP amplitude (P=0.65) and therefore the data were pooled. The mean IR of these cells was 600.3 ± 44.5 MΩ (n=66), AP amplitude 75.8 ± 1.3 mV (n=66), and AP duration 0.98 ± 0.06 ms (n=66). The amplitude of the AHP following the AP was 21.6 ± 0.8 mV (n=66) (figure 3.2D, table 3.1).

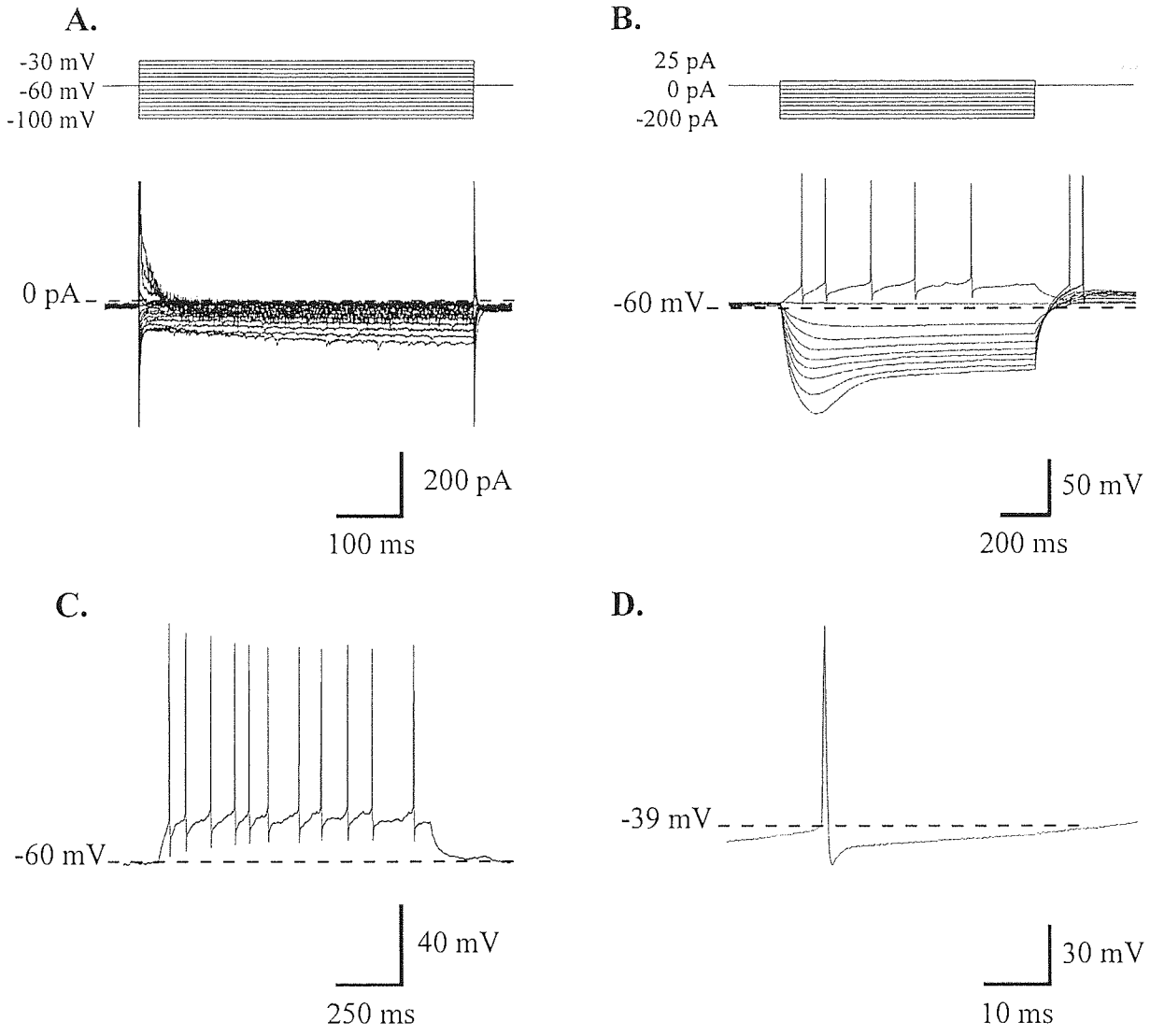

Figure 3.2: Example of type A GP cell. A. Currents recorded in response to 5 mV hyperpolarising steps of 300 ms duration from a holding potential of -60 mV. Note the time- and voltage-dependent inward currents at hyperpolarised potentials indicative of the presence of I_h. **B.** Membrane potentials recorded in response to 25 pA current steps. Note the sag at hyperpolarised potential indicative of I_h. **C.** Membrane potential recorded in response to 50 pA showing spike frequency adaptation. **D.** A single AP from the same cell showing a prominent AHP.

An after-depolarisation potential (ADP) was observed at the end of depolarising current steps in 5 of 66 type A cells, (9 %) (figure 3.3). The minimum currents injected which elicited the ADP varied from cell to cell, ranging between +25 and +300 pA. In two cells, the ADP consisted of depolarisation without action potential firing. In 3 cells, the ADP consisted of depolarisation accompanied by action potential firing. A pronounced accommodation was observed in cells expressing an ADP.

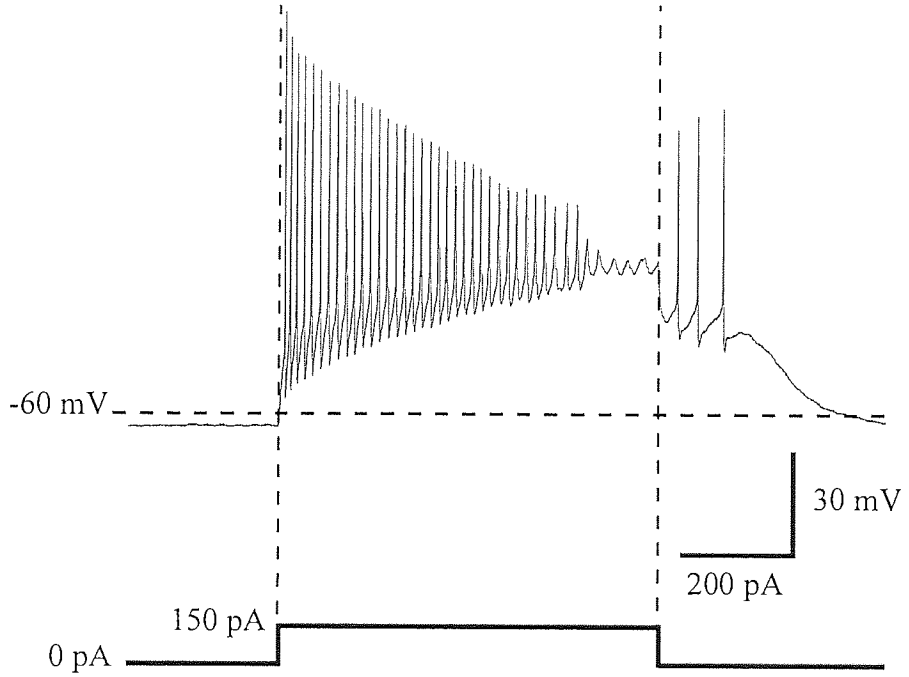

Figure 3.3: Some GP cells showed an ADP. Current-clamp whole-cell recording of a type A GP cell in response to a 150 pA depolarising current step from the RMP. At the end the depolarising current injection, note subsequent action potential firing. Note the pronounced accommodation preceding the ADP.

3.2.3. Type B GP cells

In voltage clamp mode, 17 of 83 GP cells (21 %) showed no evidence of I_h or rebound depolarisations and were therefore classified as type B GP neurones (figure 3.4AB). No adaptation or accommodation was observed in response to depolarising current injection (figure 3.4C). The mean input resistance of this population was 344.3 ± 58.9 MΩ (n=17) which is significantly different from type A cells (P=0.007).

11 of 17 (65 %) type B GP cells were quiescent, with a mean resting membrane potential of -55.6 ± 3.2 mV. The remaining cells (6 of 17, 35 %) fired action potentials at a frequency of 5.0 ± 3.0 Hz. Their AP amplitude was 68.8 ± 2.6 mV (n=13) and AP duration 1.12 ± 0.11 ms (n=13) and were followed by an AHP with a mean amplitude of 20.4 ± 1.8 mV (n=13).

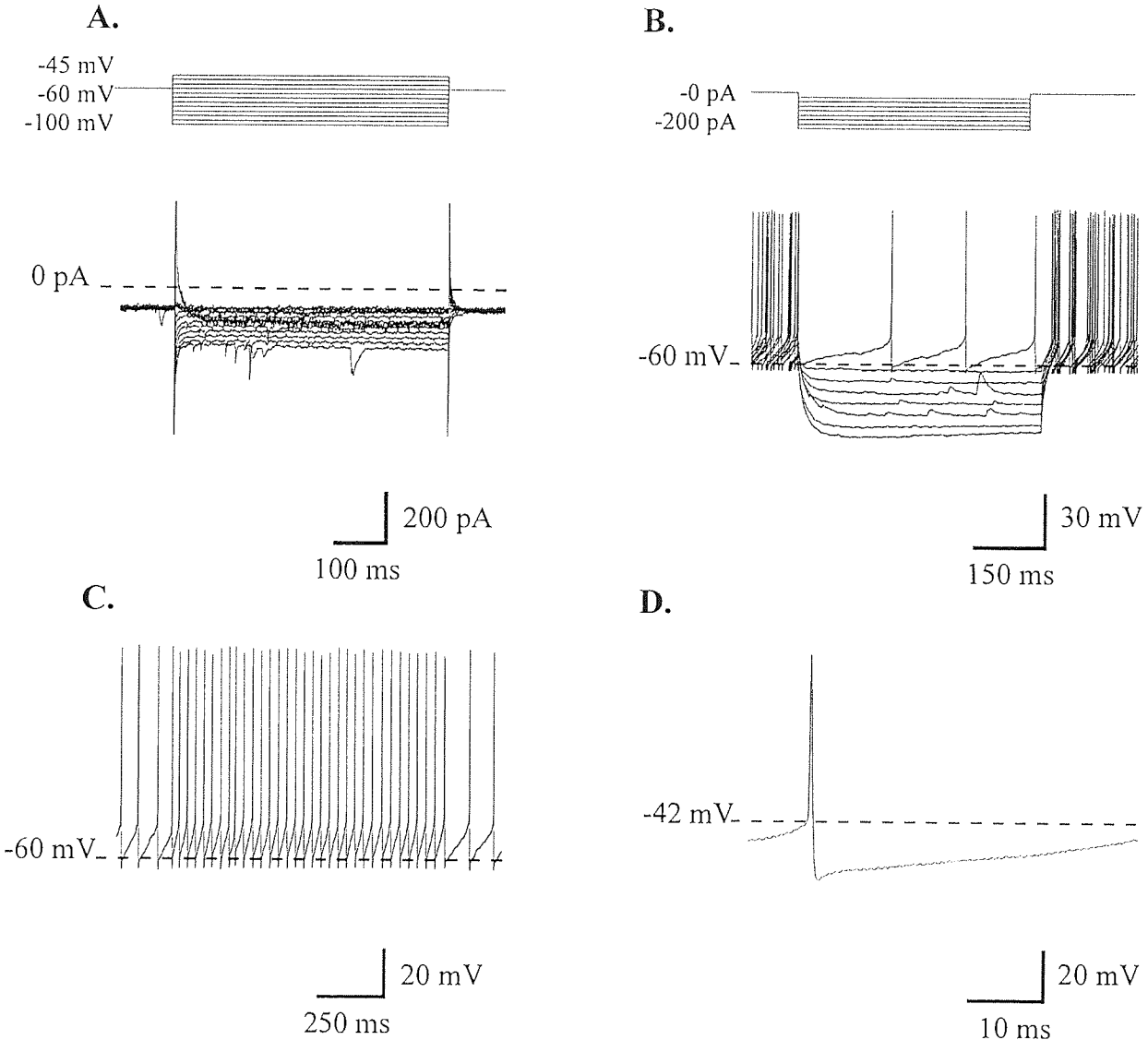

Figure 3.4: Example of a type B GP cell. A. Currents recorded in response to 5 mV hyperpolarising steps from a holding potential of -60 mV. Note absence of I_h **B.** Membrane potentials recorded in response to 25 pA current steps. Note the absence of voltage 'sag' **C.** Membrane potential recorded in response to 50 pA showing no adaptation or accommodation. **D.** A single action potential from the same cell.

	Type A GP cell	Type B GP cell
RMP (mV)	53.0 ± 1.8	56.5 ± 1.6
IR (MΩ)	**600.3 ± 44.5**	**344.3 ± 58.9 (*P*=0.007)**
AP threshold (mV)	37.4 ± 0.5	37.1 ± 1.0
AP amplitude (mV)	**75.8 ± 1.3**	**68.8 ± 2.6 (*P*=0.01)**
AP duration (ms)	0.98 ± 0.06	1.12 ± 0.11
AHP amplitude (mV)	21.6 ± 0.8	20.4 ± 1.8

Table 3.2: Pooled data showing RMP, IR and AP parameters of GP cells. Significant differences are indicated in bold.

3.2.4. Extracellular recordings of STN cells

Using single-unit extracellular recordings the firing pattern of STN cells was shown to be regular with a mean firing rate of 7.16 ± 0.29 Hz (n= 280 cells). The firing rate followed a Gaussian distribution indicating the presence of a single population of STN cells (figure 3.5). In order to excite the network and maybe to initiate oscillatory activity, the external potassium concentration was raised from 2.5 mM to 4.5 mM. The mean firing rate in 4.5 mM external potassium concentration was 9.96 ± 0.65 Hz (n=85). This manipulation did not change the pattern of activity of STN cells.

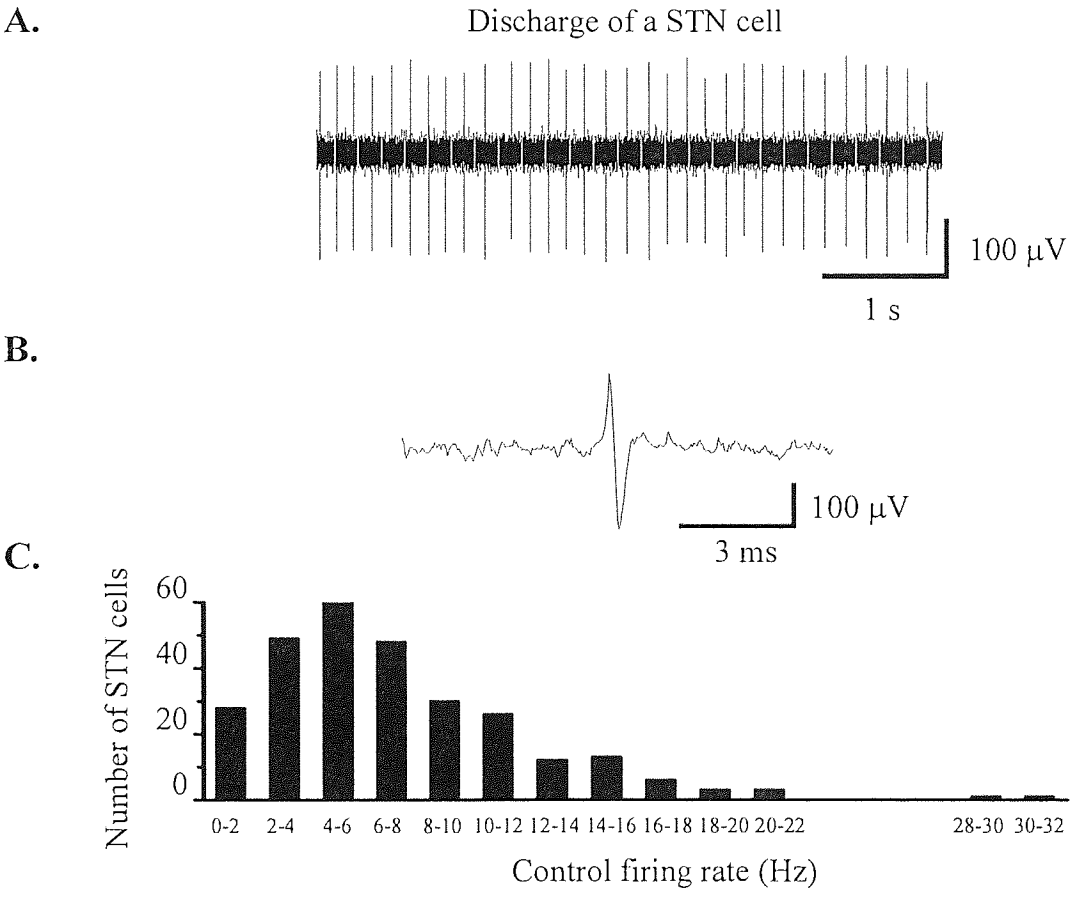

Figure 3.5: Extracellular recording of regular firing STN cells. A. Raw data showing single-unit activity. Note the regular discharge. **B.** Expanded time scale (A) showing a voltage deflections corresponding to single AP. **C.** Histogram of firing rate of STN cells showing a normal distribution, indicative of the presence of one population of STN cells.

3.3.5. Whole-cell recordings of STN cells

All whole-cell STN recordings were made with intracellular solutions containing EGTA (0.5 mM). Following the voltage clamp protocol (~1 min after breakthrough) 205 of 300 (68 %) of the cells were quiescent with a mean resting membrane potential of -56.7 ± 0.3 mV. The remaining fired action potentials at an average frequency of 13.1 ± 1.8 Hz (n=95 of 300, 32 %). The mean input resistance of these cells was 271.3 ± 6.9 MΩ (n=300), the AP amplitude 82.6 ± 0.5 mV, AP duration 0.61 ± 0.01 ms, AP threshold -39.1 ± 0.2 mV and APs were followed by an AHP of amplitude 27.1 ± 0.3 mV. However, following breakthrough and the onset of whole-cell dialysis most STN cells showed evidence of membrane hyperpolarisation in the order of a few mV leading to a cessation in action potential firing. There was no evidence of spontaneous burst-firing in STN cells while hyperpolarising current injection simply produced hyperpolarisation without change in the pattern of activity.

All STN neurones showed the same electrophysiological characteristics. Hyperpolarising voltage steps from a holding potential of -60 mV evoked a time- and voltage- dependent inward current, indicative of the presence of I_h. This was followed by a rebound depolarisation accompanied by action potential firing on repolarisation of the membrane (figure 3.6).

3.2.6. Whole-cell recordings of STN cells from MPTP-treated mice

Extracellular recordings of STN neurones from dopamine-depleted, MPTP-treated mice showed a lower firing rate and more irregular firing pattern than of those observed in STN neurones from normal mice (Stanford IM, unpublished observations). This may be explained by a change in intrinsic membrane properties of STN cells. To examine this question, STN cells were recorded in MPTP-treated mice using whole-cell patch-clamp technique in current- and voltage-clamp modes.

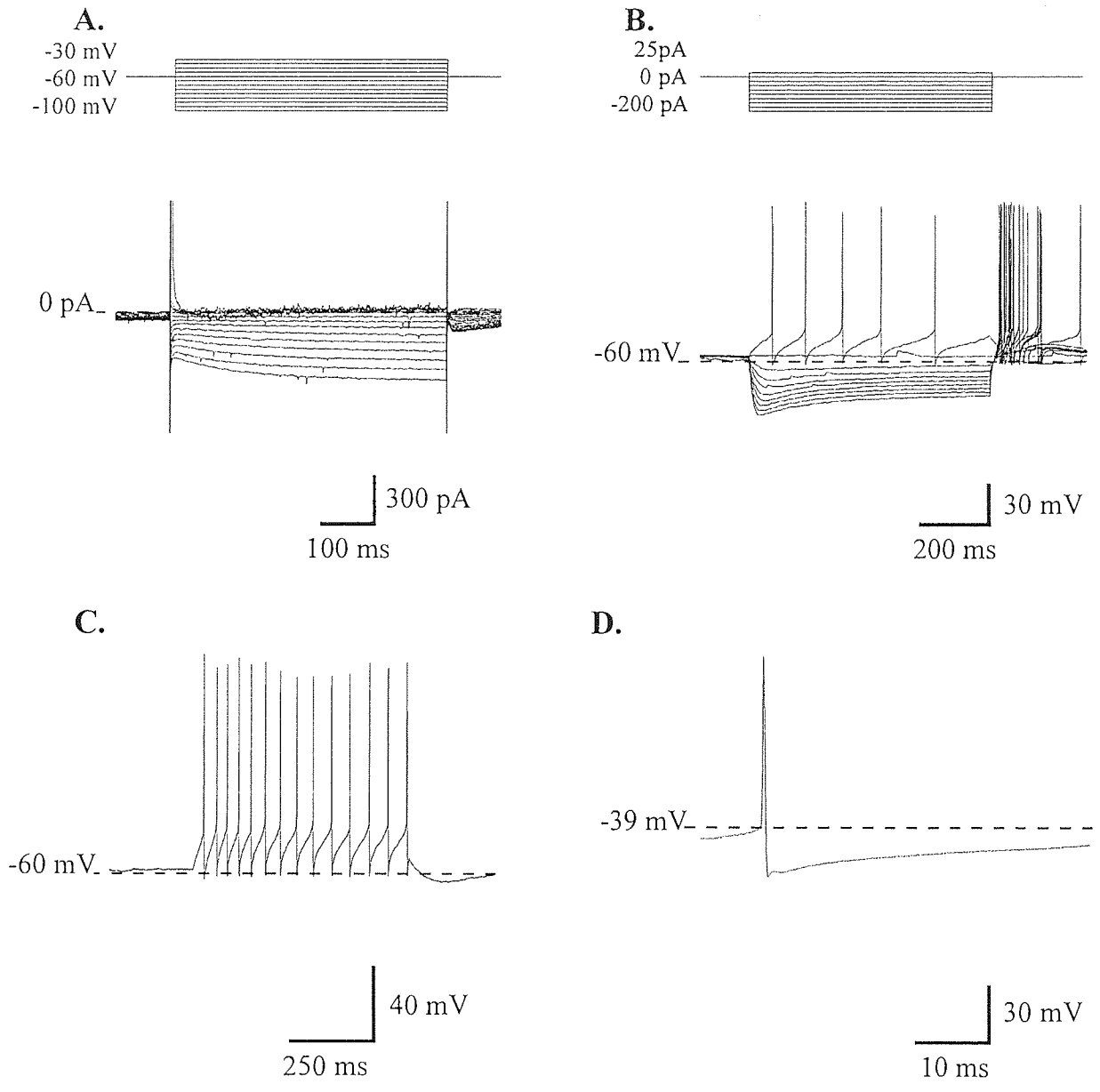

Figure 3.6: Example of a STN cell. A. Currents recorded in response to 5 mV hyperpolarising steps from a holding potential of -60 mV. Note the time- and voltage-dependent inward currents at hyperpolarised potentials indicative of the presence of I_h. **B.** Membrane potentials recorded in response to 25 pA current steps of 500 ms duration. Note the voltage 'sag' in response to hyperpolarising steps indicative of I_h. **C.** Membrane potential recorded in response to 50 pA current step, showing a small degree of adaptation. **D.** A single action potential from the same cell.

In current-clamp recordings with zero current injection, STN cells from MPTP mice were silent (n=40 of 51, 78 %) or fired action potentials at a frequency of 7.34 ± 1.99 Hz (n= 11 of 51, 22 %) before becoming silent. STN cells from normal mice were silent (n= 14 of 26, 54 %) or fired action potentials at a frequency of 3.36 ± 1.02 Hz (n= 12 of 26, 46 %) before again becoming silent.

As in normal mice, all STN neurones from MPTP-treated mice showed homogenous electrophysiological characteristics, consistent with a single population of STN cells. The mean input resistance of STN from MPTP-treated mice (251 ± 13.8 MΩ, n=51) was not significantly different from the mean input resistance of normal age matched STN neurones (222.5 ± 13.9 MΩ, n=26, P=0.18). The mean resting membrane potential in STN cells from MPTP mice (55.7 ± 1.0 mV, n=51) did not differ from the corresponding one in STN cells from normal mice (55.6 ± 1.4 mV, n=26, P=0.95).

The parameters of the action potentials in STN cells from MPTP-treated mice were also quantified and compared to those of normal age matched animals (table 3.2). The mean action potential amplitude from MPTP neurones was of 82.2 ± 0.7 mV (n=51) with a mean threshold for AP firing 31.0 ± 0.4 mV. APs were of short duration (0.58 ± 0.01 ms), and were followed by a mean AHP amplitude of 28.8 ± 0.5 mV. The mean action potential amplitude of normal age-matched STN neurones (n=26) was 84.0 ± 1.5 mV amplitude with an AP threshold of -32.1 ± 0.7 mV. APs were of short duration (0.64 ± 0.02 ms), and were followed by an AHP of 26.6 ± 0.7 mV in amplitude. No difference in AP amplitude (P=0.22) or AP threshold (P=0.12) was observed. However, there was a difference in action potential duration (P=0.001) and AHP amplitude (P=0.009).

	Normal mice (n=26)	MPTP mice (n=51)
IR (MΩ)	222.5 ± 13.9	251.0 ± 13.8
RMP (mV)	55.6 ± 1.4	55.7 ± 1.0
AP threshold (mV)	32.1 ± 0.6	31.0 ± 0.4
AP amplitude (mV)	84.0 ± 1.5	82.2 ± 0.7
AP duration (ms)	**0.64 ± 0.02**	**0.58 ± 0.01 (P=0.001)**
AHP amplitude (mV)	**26.6 ± 0.7**	**28.8 ± 0.5 (P=0.009)**

Table 3.3: Pooled data of IR, RMP and parameters of action potential in STN cells from MPTP and from normal age-matched mice. Note the significant difference in AP duration and AHP amplitude, indicated in bold.

3.3. Discussion

3.3.1. GP

For the first time, mouse GP cells were electrophysiologically characterised *in vitro* using whole-cell recordings. Two cell types were identified in mouse GP by the presence (or absence) of a voltage 'sag' (I_h) and rebound depolarisations in response to hyperpolarising current steps. Those cells showing evidence of I_h and rebound depolarisations were defined as type A cells while those lacking I_h and rebound depolarisations were defined as type B cells. These two mouse cell types may correspond to those found in rat (Cooper & Stanford, 2000).

As in rat GP, the proportion of the mouse type A cells is the largest (79 % in mouse and 63 % in rat). The second most abundant cell type in mouse is type B as in the rat GP. However, no evidence of type C cells was found in the mouse GP. In rat type C GP cells account for 5 % of the population. This discrepancy may be due to lower number of mouse GP cells recorded (83 versus 208).

Furthermore, mouse type A and B cells share comparable, input resistance, RMP and action potential parameters.

	Type A cells		Type B cells	
	Mouse	Rat	Mouse	Rat
IR (MΩ)	600.3 ± 44.5	558.9 ± 30.1	344.3 ± 58.9	311.5 ± 20.1
RMP (mV)	-53.1 ± 1.8	-66.3 ± 0.8	-56.5 ± 1.6	-58.1 ± 1.1
AP threshold (mV)	-37.4 ± 0.5	-42.1 ± 0.7	-37.2 ± 1.0	-42.9 ± 0.8
AP amplitude (mV)	75.8 ± 1.3	73.6 ± 1.3	68.8 ± 2.6	70.0 ± 1.0
AP duration (ms)	0.98 ± 0.06	1.04 ± 0.03	1.12 ± 0.11	0.73 ± 0.02
AHP amplitude (mV)	21.6 ± 0.8	25.5 ± 0.5	20.4 ± 1.8	26.7 ± 0.8

Table 3.4: Comparison of IR, RMP and parameters of action potential in GP cells in mouse and rat. Rat data taken from Cooper & Stanford, (2000).

The rebound depolarisations and action potential firing induced on repolarisation of the membrane have previously been thought to be due to deactivation of I_h and deinactivation of I_t (as the rebound was significantly reduced by bath application of $NiCl_2$ at 1 mM). However, I_t channels have not been detected in acutely isolated GABAergic neurones, although it is possible that these channels are dendritic and lost during preparation (Surmeier *et al.,* 1994), and no evidence of I_t was found in slice using the selective I_t antagonist mibefradil suggesting that the rebound is solely due to I_h (Chan et *al.,* 2004).

Type B GP cells did not show evidence of a voltage sag, indicative of a lack of I_h. However, this does not rule out the possibility that type B cells express I_h channels (Aponte *et al.,* 2006). If there is a high level of expression of I_h channels in the dendrites, whole-cell recordings may have not been sensitive enough to detect their function due to bad space clamping. Either patching the dendrites or coupling whole-cell recordings with single-cell RT-PCR may contribute to resolve this question. In addition, the existence of type B GP cells displayed a lower input resistance compared to type A GP cells, which is consistent with the presence of functional I_h channels in type B cells (Magee, 1998). Dendritic I_h may play an important role in sculpting the synaptic inhibitory and excitatory input to GP cells. I_h was shown to favor the resetting of pacemaking of GP cells by inhibitory striatal input, giving thus a mechanism by which the striatum may synchronise the activity of GP cells (Chan *et al.,* 2004). However, the role of I_h in integrating the excitatory synaptic input from STN remains to be characterized. In order to characterize the expression of I_h in GP cells, immunocytochemical experiments are under way in our laboratory. I_h channels have been found to be expressed pre-synaptically at axonal terminals allowing the modulation of pre-synatic GABA release (Boyes J, personel communication). In addition, there is evidence of tonic I_h modulating the activity of GP cells at rest *in vitro* (Chan *et al.,* 2004).

3.3.2. STN

Extracellular single-unit recordings of STN cells showed a spontaneous regular firing pattern in agreement with other studies in the STN *in vitro* (Flores *et al.,* 1995;

Abbott *et al.*, 1997; Zhu *et al.*, 2002a; Tofighy *et al.*, 2003; Wilson *et al.*, 2004). The regularity of firing suggests a lack of tonic modulation of STN activity by ongoing synaptic transmission in contrast to the irregular firing observed *in vivo* (Wichmann *et al.*, 1994). The firing rate followed a normal distribution indicating the existence of a homogenous population of STN cells. For the first time, mouse STN cells were characterised using whole-cell recordings *in vitro*. These recordings confirmed the existence of a single population of mouse STN cells, in agreement with previous studies in rat STN (Nakanishi *et al.*, 1987; Bevan *et al.*, 2000; Wigmore & Lacey, 2000). Previous studies have attempted to characterise STN populations with respect to the extent of this rebound depolarisation (Bevan *et al.*, 2002). However, accurate measurements of the extent of the rebound cannot be made in current clamp mode due to fluctuating membrane potentials and differences in cell input resistance.

Mouse STN input resistance, resting membrane potential and action potential parameters correspond with previous reports of rat STN input resistance (Beurrier *et al.*, 1999; Baufreton *et al.*, 2003), resting membrane potential (Otsuka *et al.*, 2001), action potential duration (Beurrier *et al.*, 1999) and spike threshold (Beurrier *et al.*, 1999).

Previously, it was reported that rat STN cells recorded by intracellular techniques fire spontaneously and sustain a burst activity, which is enhanced by hyperpolarisation (Beurrier *et al.*, 1999). However this finding has been challenged in other studies (Beurrier *et al.*, 2001; Otsuka *et al.*, 2001; Tofighy *et al.*, 2003) In this study there we found no evidence of spontaneous burst firing cells in naïve STN slices and burst firing could not be promoted by hyperpolarising current injections.

In previous studies (Nakanishi *et al.*, 1987; Otsuka *et al.*, 2001; Baufreton *et al.*, 2003), plateau potentials were elicited in response to a short depolarising current injection subsequent to a continuous hyperpolarisation of the membrane. This was not attempted in this study but this may not occur since the input resistance of STN cells in the study of Otsuka *et al.*,(2001) was larger than in the mouse STN. In addition, unlike type A GP cells, an ADP could not be triggered in response to depolarising current injection from resting membrane potential.

Using the non invasive extracellular single-unit technique, no evidence of spontaneous burst firing cells in naïve STN slices was found. This is in agreement with

other *in vitro* rat extracellular (Flores *et al.*, 1995; Abbott *et al.*, 1997; Zhu *et al.*, 2002a; Tofighy *et al.*, 2003; Wilson *et al.*, 2004) and perforated patch technique studies (Bevan & Wilson, 1999; Bevan *et al.*, 2000; Bevan *et al.*, 2002a; Bevan *et al.*, 2002b; Hallworth *et al.*, 2003), which have the advantage to avoid the dialysis the cell content into the pipette. Whole-cell recordings studies of STN cells are also consistent with this conclusion, although a progressive hyperpolarisation of STN cells is usually observed during the dialysis (Wigmore & Lacey, 2000; Baufreton *et al.*, 2001; Otsuka *et al.*, 2001; Zhu *et al.*, 2002b). Only one study described a spontaneous burst firing of rat STN cells (Beurrier *et al.*, 1999) using whole-cell and sharp microelectrode recordings.

3.3.3. STN from MPTP-treated mice

Following the observation of the emergence of low and irregular firing activity of STN cells in slices from MPTP-treated mice (Stanford IM, unpublished observations), intrinsic membrane properties of STN cells were examined using whole-cell recordings. This revealed that STN cells from MPTP-treated mice displayed no difference in most electrophysiological properties with the exception of the AP duration which was significantly reduced in MPTP-treated slices compared to STN cells from age-matched normal mice and AHP amplitude which was significantly increased in MPTP-treated slices compared to STN cells from age-matched normal mice. These results may indicate a functional change in a specific potassium channel such as the inward rectifier. However, more definitive studies are required.

Long term dopamine depletion may lead to changes in the expression and/or function of the channels underlying STN spontaneous subthreshold membrane oscillations. Currents underlying the hyperpolarising phase of STN membrane oscillations may be up-regulated. Such currents include large conductance calcium activated potassium channels (BK), SK, and the outwardly rectifying persistent outward current ($Kv_{3.1}$). A quantification of each of these currents in normal versus dopamine-depleted animals may be required to identify which conductances are altered during dopamine depletion. In particular, the irregularity of firing may be accounted for by an increased slow after-hyperpolarisation. Furthermore, the currents involved in the

depolarising phase of STN membrane oscillations may be altered following dopamine depletion. These currents include sodium persistent currents (Bevan *et al.*, 1999), probably I_h (Bevan *et al.*, 1999; Beurrier *et al.*, 2001) and may be I_t. Once again, these currents could be quantified and compared between dopamine-depleted animals and normal age-matched animals.

As major changes in the intrinsic properties of STN cells were not observed in MPTP-treated mice, the changes in STN firing pattern observed during dopamine depletion may arise from altered network activity such as that arising from STN-GP interactions. This will be the focus of study in the next chapter.

Chapter 4. A mouse brain slice with STN-GP connectivity does not sustain regenerative oscillatory activity

4.1. Introduction

According to the co-culture model of Plenz & Kitai, (1999), the STN and GP constitute a central pacemaker responsible for regenerative oscillatory activity. This activity is dependent upon reciprocal connectivity between STN and GP neurones and their respective intrinsic membrane properties (Plenz & Kitai, 1999). This view would gain further credibility if reproduced *in vitro*. Such a preparation would also allow further pharmacological and mechanistic studies.

4.1.1. Proposed mechanism of oscillatory activity in the STN-GP network

In the work of Plenz & Kitai, (1999), regenerative burst-firing was promoted by brief applications of GABA in STN in order to mimic pallidal synaptic input. This produced inhibition of STN cell activity followed by rebound burst which promoted oscillatory burst-firing. The proposed mechanism involved the de-inactivation of a low-threshold calcium conductance (I_t), such that on repolarisation of the STN cell membrane a rebound depolarisation was initiated. This rebound would then drive GP activity allowing further inhibition/rebound excitation of the STN. Therefore, it appeared that viable reciprocal connectivity between the GABAergic GP and glutamatergic STN was sufficient for the generation of rebound burst activity and hence regenerative oscillatory activity (Plenz & Kitai, 1999; Bevan *et al.*, 2000). Indeed, this appeared to be the case as STN activity reverted to tonic firing once the pallidal input to the STN was disconnected.

4.1.2. Further support for recurrent activity within the STN-GP network

Whether GABA transmission could recruit a STN rebound burst in rat slices was tested using the perforated patch-clamp configuration (Bevan *et al.*, 2000) which does not alter the intracellular concentration of chloride, the principal permeant ion of the

$GABA_A$ receptor. It appeared that the chloride driving force was large enough such that evoked IPSPs (from internal capsule) were able reset the phase of membrane oscillations and recruit STN rebound burst (Bevan *et al.*, 2000, 2002). In addition, rebound depolarisations have also been observed in the GP as evoked IPSPs (of GP or striatal origin) are able to reset the phase of spontaneous subthreshold membrane oscillations and produce GP rebound burst (Stanford, 2003).

In line with these observations, the modelling study of Terman *et al.*, (2002) proposed that regenerative burst activity could occur in the STN-GP network. This study suggested that during dopamine depletion, increased striatal activity might synchronise the activity of the GP through recruitment of GP rebound bursts. This synchronous GP activity would in turn hyperpolarise the STN sufficiently to generate STN rebound firing and initiate regenerative burst activity in the STN-GP network.

4.1.3. Previous *in vitro* electrophysiological studies

Single-unit extracellular recordings STN cells from rat slices have not provided evidence of spontaneous burst-firing, probably due to reduced reciprocal STN-GP connectivity in the rat slice preparation (Wilson *et al.*, 2004). A way to circumvent this problem was to reduce the distance between the two nuclei. In a 400 μm mouse slice preparation, the distance between the two structures is much reduced compared to rat slices (~ 1 mm instead of 1.5 mm) and may thus preserve the inter-nuclear network. In order to determine the best plane of section to maintain reciprocal STN-GP connectivity, morphological studies were performed using injection of biocytin pellets (in gelatin) in STN and GP. Evidence of biocytin reaction product was examined in three orientations, horizontal, 20° parasagittal and coronal planes. The most robust morphological connectivity between STN and GP was found in the 20 ° parasagittal plane (Wilson, 2004; Loucif *et al.*, 2005). This slice orientation was used in all subsequent recordings.

4.2. Results

4.2.1. Functional reciprocal connectivity between the STN and the GP

To show functional connectivity, whole-cell recordings in voltage- and current-clamp configurations were made in the GP while synaptic events were evoked by focal bipolar electrical stimulation of STN and *vice versa*. Connectivity between the GP and the STN was assumed if the evoked currents were larger than 20 pA and therefore clearly distinguishable from noise. It appears that there are no other GABA projections which course through the GP to the STN and no glutamatergic projections which course through the STN to the GP (Bolam P, personal communication). Thus, stimulating within the GP or STN will only activate efferents from these nuclei.

Single-shock electrical stimulation of the GP in the presence of the glutamate antagonists CNQX (10 μM) and DL-AP5 (50 μM) evoked postsynaptic currents in the STN (44 of 59 slices, 74 %, figure 4.1A) which reversed at -57 mV, close to the theoretical equilibrium potential of chloride (E_{Cl} = -56 mV as calculated by the Nernst equation). These currents were sensitive to the $GABA_A$ receptor antagonist bicuculline (10 μM, n=7), suggesting the presence of functional GABAergic connectivity from the GP to the STN.

Single-shock electrical stimulation of the STN in the presence of bicuculline (10 μM) evoked postsynaptic inward currents in the GP (22 of 33 slices, 66 %, figure 4.1B). These currents were sensitive to CNQX (10 μM) and DL-AP5 (50 μM, n=5), suggesting the presence of functional glutamatergic connectivity from the STN to the GP.

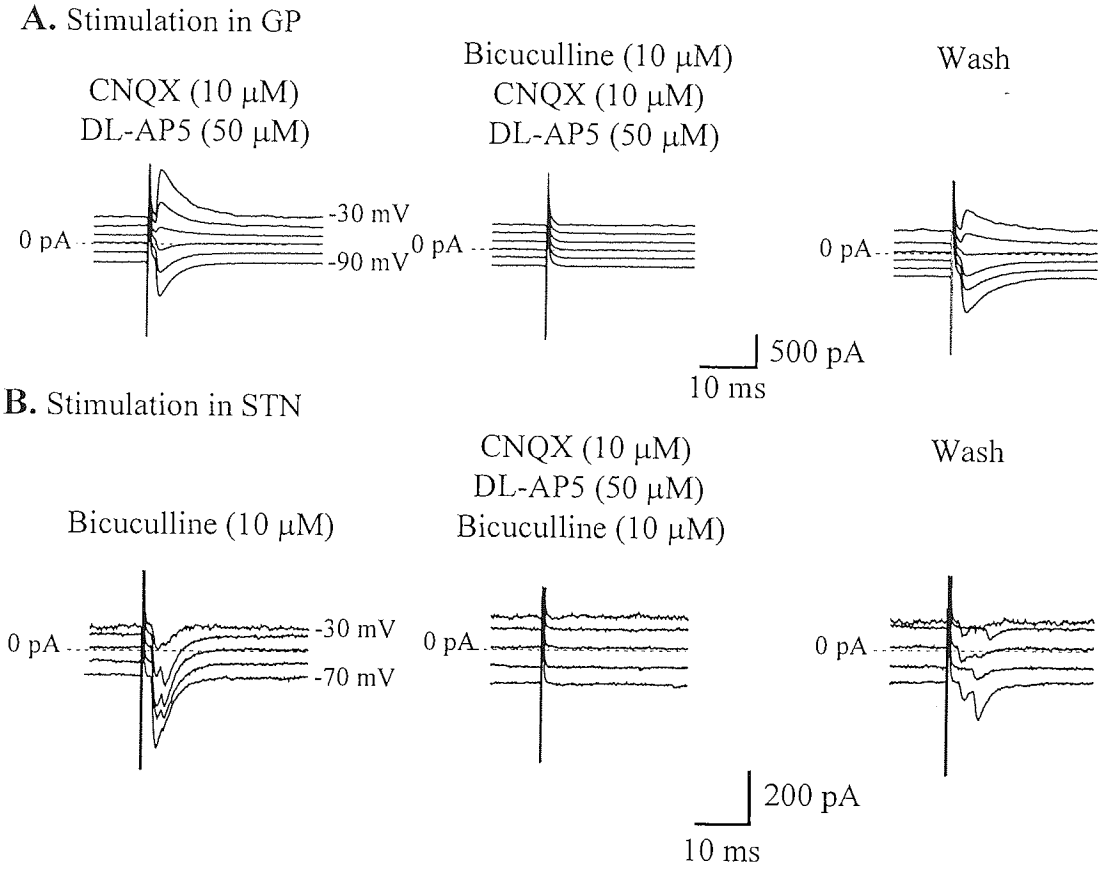

Figure 4.1: Electrical stimulation in GP or in STN evoked postsynaptic currents in STN or GP respectively. A. Single-shock electrical stimulation in the GP (in the presence of CNQX (10 μM) and DL-AP5 (50 μM)) evoked postsynaptic currents which reversed around –57 mV, close to the theoretical reversal potential of chloride (-56 mV) and were sensitive to the $GABA_A$ receptor antagonist bicuculline (10 μM). **B.** Single shock electrical stimulation in the STN (in the presence of bicuculline (10 μM)) evoked postsynaptic inward currents which were sensitive to CNQX (10 μM) and DL-AP5 (50 μM).

4.2.2. Stimulation in the GP induced a STN rebound burst

The proposed mechanism for the initiation of regenerative oscillatory activity between the STN and GP is based on the ability of the GP to promote rebound activity in the STN (Plenz & Kitai, 1999; Bevan *et al.,* 2000). An attempt was made to replicate the proposed mechanism in the mouse slice preparation. In current-clamp recordings, electrical stimulation of the STN evoked excitatory postsynaptic potentials (EPSPs) that were able to trigger action potentials in the GP (n=3, figure 4.2A). Electrical stimulation in the GP evoked inhibitory postsynaptic potentials (IPSPs) in STN (n=3, figure 4.2B). Single-shock stimulation evoked a single IPSP. By increasing the number of shocks, the IPSPs were able to summate and produce sufficient hyperpolarisation to produce rebound depolarisation and consequent action potential firing, consistent with the study of Bevan *et al.,* (2000). Thus, in the mouse slice preparation, the mechanism for the promotion of regenerative oscillatory activity is present.

4.2.3. Spontaneous excitatory and inhibitory synaptic currents

If the GP and STN are reciprocally connected, evidence for spontaneous release of GABA and glutamate should be observed. In voltage-clamp recordings at a holding potential of -45 mV, spontaneous postsynaptic currents were observed in the STN (sIPSCs in 85/150 cells, 57%; sEPSCs in 107/150 cells, 71%) and the GP (sIPSCs in 43/43 cells, 100%, sEPSCs in 26/43 cells, 60%), supporting further the existence of connectivity between the GP and the STN (figure 4.3). The amplitude and frequency were not quantified because of the small amplitude of the currents. sIPSCs in the GP must arise from intra-GP axon collaterals (Stanford, 2003) as GABAergic striatal MSNs are silent *in vitro* (Kawaguchi *et al.,* 1989). The sEPSCs observed in the STN are most likely to arise from activity in the cortex, thalamus or PPN (Smith *et al.,* 1998) or from intrinsic axon collaterals within the STN (Kita *et al.,* 1983) although their presence has not been confirmed (Hammond & Yelnik, 1983; Sato *et al.,* 2000b; Wilson *et al.,* 2004).

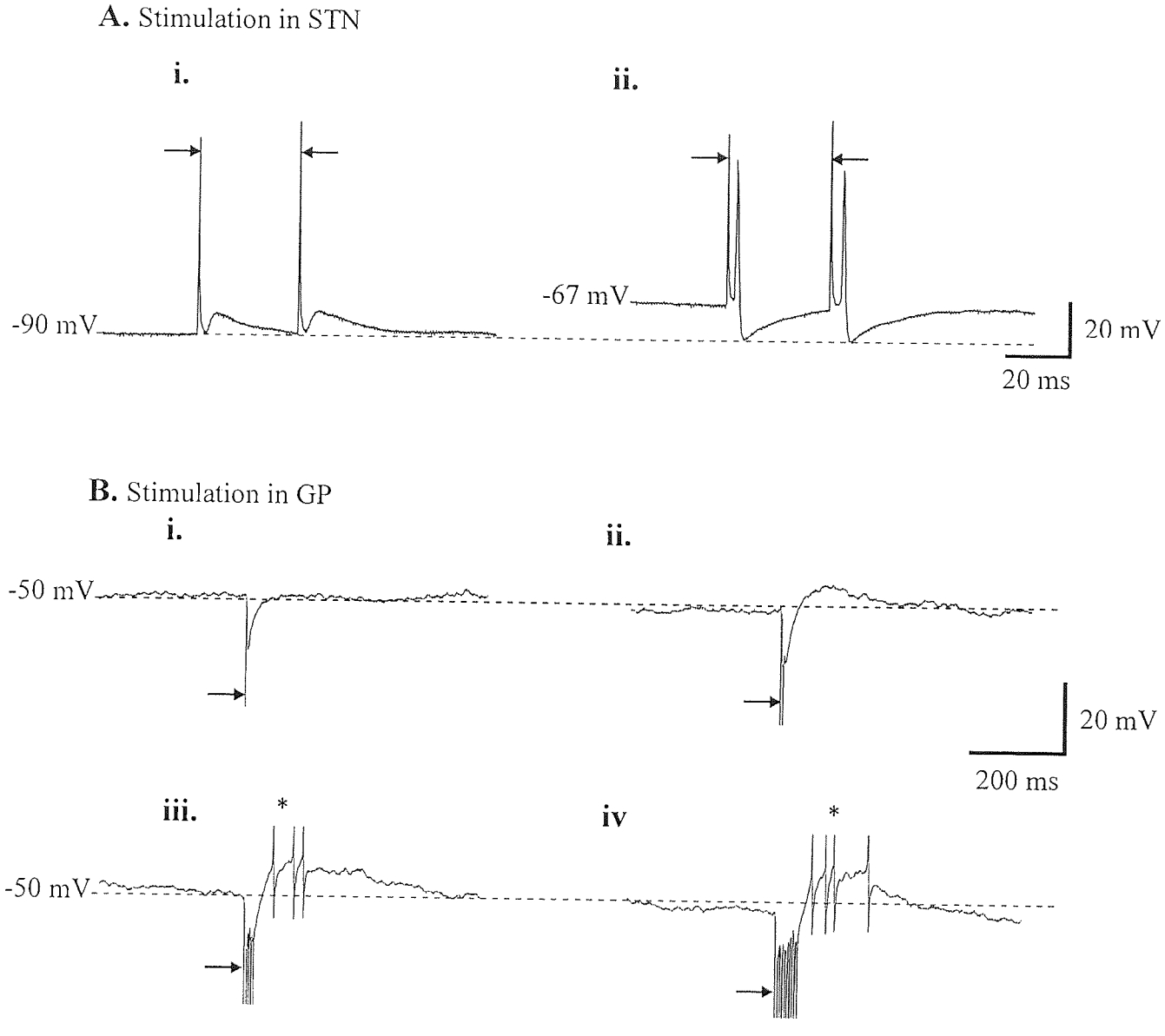

Figure 4.2: Electrical stimulation in STN evoked EPSPs followed by spikes in GP while electrical stimulation in GP evoked rebound depolarisation followed by action potential firing in STN. A. Membrane potential from a GP cell in response to single-shock stimulation in STN. The shock was able to promote an EPSP **(i)** and action potential firing **(ii)**. **B.** Membrane potential from a STN cell in response to stimulation in GP. **i.** Single shock stimulation evoked a single IPSP. **ii.** Double-shock stimulation (5 ms interval) evoked IPSPs followed by small rebound depolarisation. **iii. iv.** The rebound depolarisation promoted action potential firing in response to 5- and 10- shock stimulation (at 200 Hz) **(iii** and **iv** respectively). Arrows denote electrical stimulation artefact. Action potentials are truncated (*) for clarity.

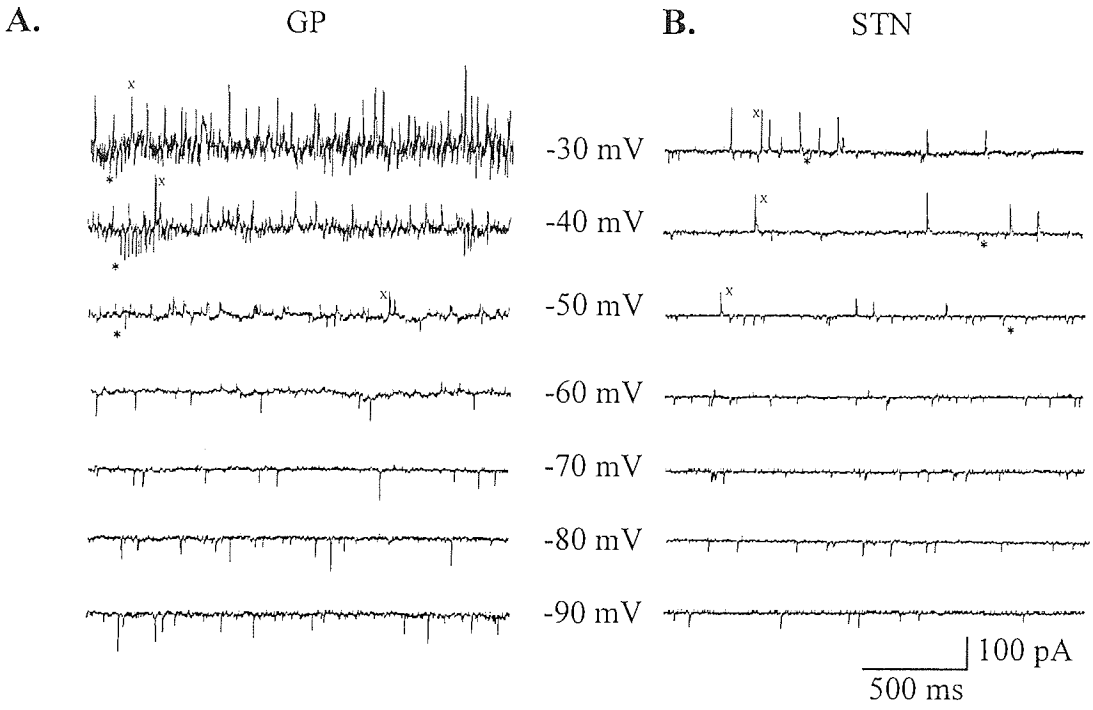

Figure 4.3: Spontaneous inhibitory and excitatory postsynaptic currents. Voltage clamp recordings in GP (**A**) and STN cells (**B**) showing sIPSCs and sEPSCs at holding potentials from -90 mV to -30 mV. sIPSCs are indicated by the presence of reversal potential between -50 mV and -60 mV and outward currents at membrane potentials more depolarised than the reversal potential (ˣ). sEPSCs are indicated by the presence of inward currents at all membrane potentials recorded (*).

4.2.4. Lack of effect of GABA and glutamate antagonists

Chapter 3 provided evidence of the regular pattern of STN single-unit activity in the mouse slice with no spontaneous burst activity. In order to test whether the connectivity present within the slice influences the rate or pattern of firing, GABA or glutamate antagonists were bath applied. In these experiments the $GABA_A$ antagonist picrotoxin was used as bicuculline methiodide has previously been shown to induce burst-firing activity through its action at SK channels (Johnson & Seutin, 1997; Wilson *et al.*, 2004; Wilson, 2004). Application of picrotoxin (50 μM) produced no effect on the firing rate (n=11, P=0.42, figure 4.4A). Application of CNQX (10 μM) and DL-AP5 (50 μM) also had no effect on the firing rate (n=9, P=0.1, figure 4.4B) as did an inhibitor of AMPA receptor desensitisation cyclothiazide (50 μM) (n=5, P=0.30, figure 4.4C). These data suggest that the spontaneous inhibitory and excitatory activity previously recorded in the whole-cell experiments (figure 4.3) does not influence the rate or pattern of STN cell firing.

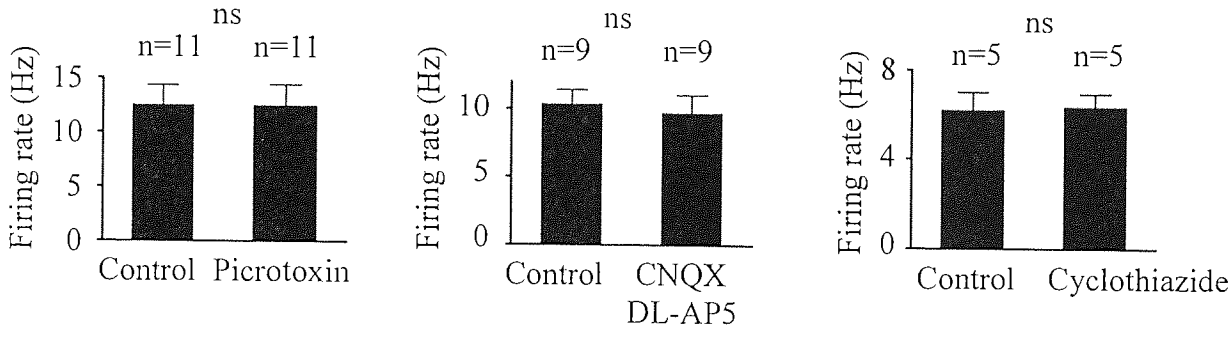

Figure 4.4: Pooled data showing a lack of effect of the antagonists of $GABA_A$ and fast glutamatergic transmission on extracellularly recorded STN activity. Lack of effect of picrotoxin (50 μM), CNQX (10 μM) and DL-AP5 (50 μM) and cyclothiazide (50 μM).

4.2.5. A lack of correlated (synchronous) activity in the naive slice

Although single cells only show regular firing the STN-GP network may still promote correlated activity. This point was addressed by performing simultaneous extracellular single-unit recordings of 33 pairs of STN cells obtained from 17 slices. A representative example is given in figure 4.5. The recorded activity and associated cross-correlogram indicated the absence of synchronous activity in the mouse slice in normal conditions.

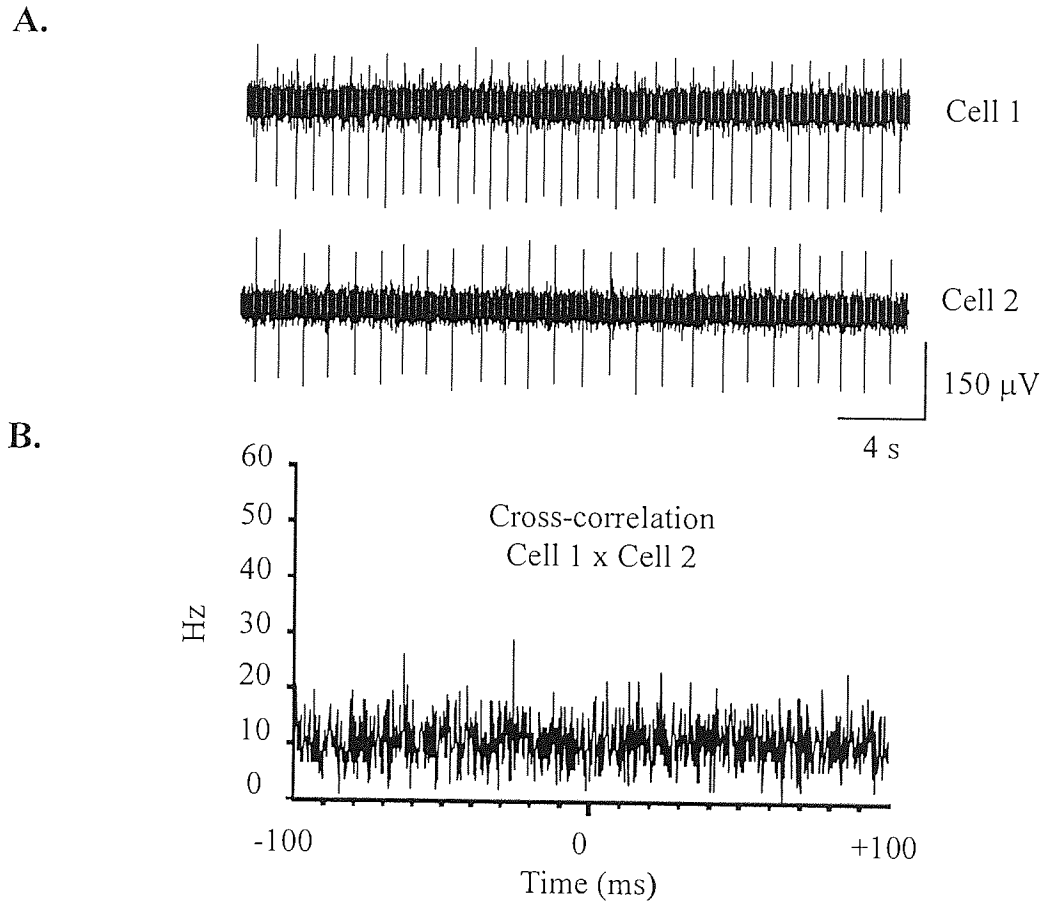

Figure 4.5: Extracellular single-unit recordings of a pair of STN cells did not show correlated activity. A. Raw data showing a pair of STN cells recorded simultaneously using two separate recording electrodes. **B.** Cross-correlogram (Spike2, version 5.11) of the two STN cells showing a lack of correlation.

4.2.6. No evidence of burst-firing in slices from MPTP-treated mice

No evidence of spontaneous regenerative burst firing was observed in the STN-GP network slices from normal mice. This may be because of the requirement for long-term adaptive changes following dopamine depletion. To test this hypothesis, recordings from STN from MPTP-treated mice were performed. Whole-cell current clamp recordings of 51 STN cells (16 slices) with an intracellular solution containing EGTA (0.5 mM) were made from slices obtained from MPTP-treated mice. However, even in dopamine depleted slices, STN cells did not show evidence of regenerative burst firing, ruling out the hypothesis that long-term changes following dopamine depletion might be required to initiate regenerative burst-firing.

4.2.7. Pharmacological promotion of burst-firing in the STN

Previous results have shown a lack of evidence of modulation of STN activity by ongoing synaptic GABA and glutamate release and no occurrence of spontaneous burst-firing in normal slices preserving STN-GP connectivity. In an attempt to replicate the bursting activity observed in STN neurones during dopamine depletion *in vivo,* and increase the activity of GP cells thus promoting GABA release (Lisman, 1997), a series of pharmacological manipulations was carried out.

4.2.8. Enhancement of metabotropic glutamate receptor mediated activity

As the group I /II metabotropic glutamate receptor agonist 1-S-3R-ACPD has been shown to promote burst-firing in STN (Beurrier *et al.,* 1999; Awad *et al.,* 2000), extracellular single-unit recordings were made in the presence of this drug. STN neurones with a stable basal firing rate were recorded (mean firing rate of 10.16 ± 1.32 Hz, n=24 in 4.5 mM external potassium aCSF solution). Application of 1-S-3R-ACPD (100 μM, 3 min) produced a transient increase in the firing rate followed by desensitisation (to steady state). Application of different concentrations of 1-S-3R-ACPD (1, 3, 10, 30 and 100 μM) induced a dose-dependent increase in the firing rate

(quantified at the steady state) with an EC_{50} of 7.6 μM and a maximum increase of ~ 480 % (figure 4.6AB), in agreement with the work of Abbott *et al.*, (1997).

Application of 1-S-3R-ACPD (100 μM, n=8; 30 μM, n=4) for 15 min failed to change the pattern of STN neuronal activity (figure 4.6C). Analysis of the pattern revealed only a change in the rate of firing from 14.11 ± 2.84 Hz in control to 21.37 ± 4.52 Hz (n=8, P=0.014) in the presence of the drug at 100 μM and from 13.32 ± 2.60 Hz in control to 27.73 ± 2.28 Hz (n=4, P=0.016) in the presence of the drug at 30 μM.

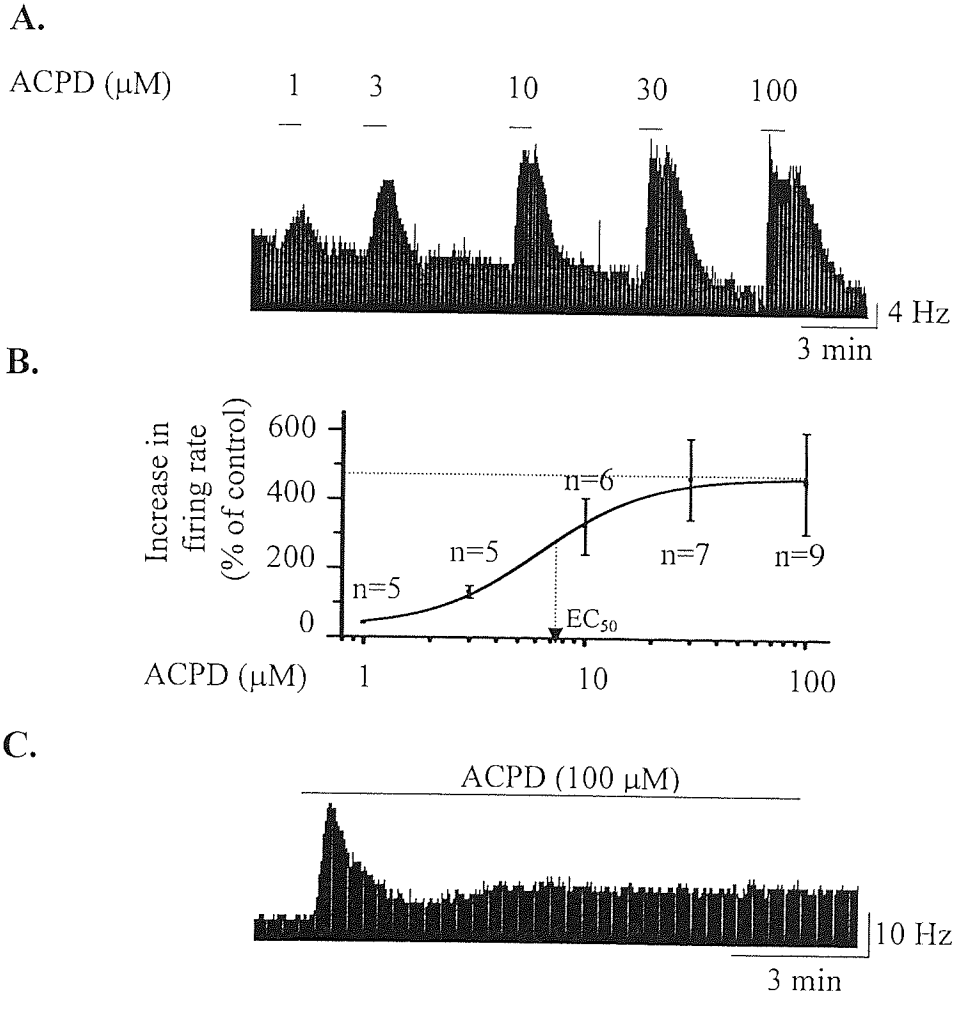

Figure 4.6: 1-S-3R-ACPD failed to promote burst-firing in STN cells. A. Rate-meter recording showing that 1-S-3R-ACPD induced a dose-dependent increase in the firing rate of STN cells. **B.** Dose-response curve of 1-S-3R-ACPD showing a maximum increase in firing rate of 480 % and an EC_{50} of 7.6 μM. **C.** Rate-meter recording showing that application of 1-S-3R-ACPD (100 μM) for 15 min did not promote burst-firing of a STN cell.

4.2.9. Bath application of NMDA and apamin

Previously, the ionotropic glutamate receptor agonist NMDA alone was shown to promote burst firing in dopamine neurones (Seutin *et al.*, 1993) and recently in rat STN cells (Zhu *et al.*, 2004). In order to promote bursting activity, extracellular single-unit recordings of STN neurones were made in the presence of NMDA (20 μM), bath applied for 10 minutes. The action of NMDA alone was highly variable, increasing the mean firing rate by 317 ± 249 % (n=4). However, in each case there was no effect on the pattern of activity and no promotion of burst firing (figure 4.7).

Apamin, a blocker of potassium SK channels, has been shown to enhance NMDA-mediated burst firing in dopaminergic neurones (Seutin *et al.*, 1993) and in rat STN neurones (Wilson *et al.*, 2004). In order to promote bursting activity in STN neurones NMDA (20 μM) was bath applied in a conjunction with apamin (50 and 100 nM) (figure 4.8).

Using the whole-cell technique, burst firing was observed in approximately half of the cells tested, 14 of 37 cells (38 %) for 50 nM apamin and 15 of 26 cells (58 %) for 100 nM apamin. The intracellular solution contained reduced EGTA (0.5 mM) in order to preclude cessation of burst activity during dialysis. When the patch pipette solution contained the fast calcium chelator BAPTA (10 mM) (Tsien, 1980), the bursting activity was progressively abolished within 15 minutes following breakthrough in all bursting cells, showing that the NMDA/apamin induced burst is dependent on intracellular calcium (figure 4.9).

The burst analysis revealed, for a concentration of apamin of 50 nM, a mean interburst frequency of 0.46 ± 0.10 Hz, an average number of spikes per burst of 31.26 ± 8.81 and an average interspike interval (ISI) of 32.3 ± 5.3 ms (n=14). When apamin was used at a concentration of 100 nM the parameters were not different than those observed with 50 nM apamin (interburst frequency of 0.42 ± 0.07 Hz, n=15, P=0.72; average number of spikes per burst of 28.6 ± 6.8, n=15, P=0.81; average ISI of 25.5 ± 3.5 ms, n=15, P=0.29).

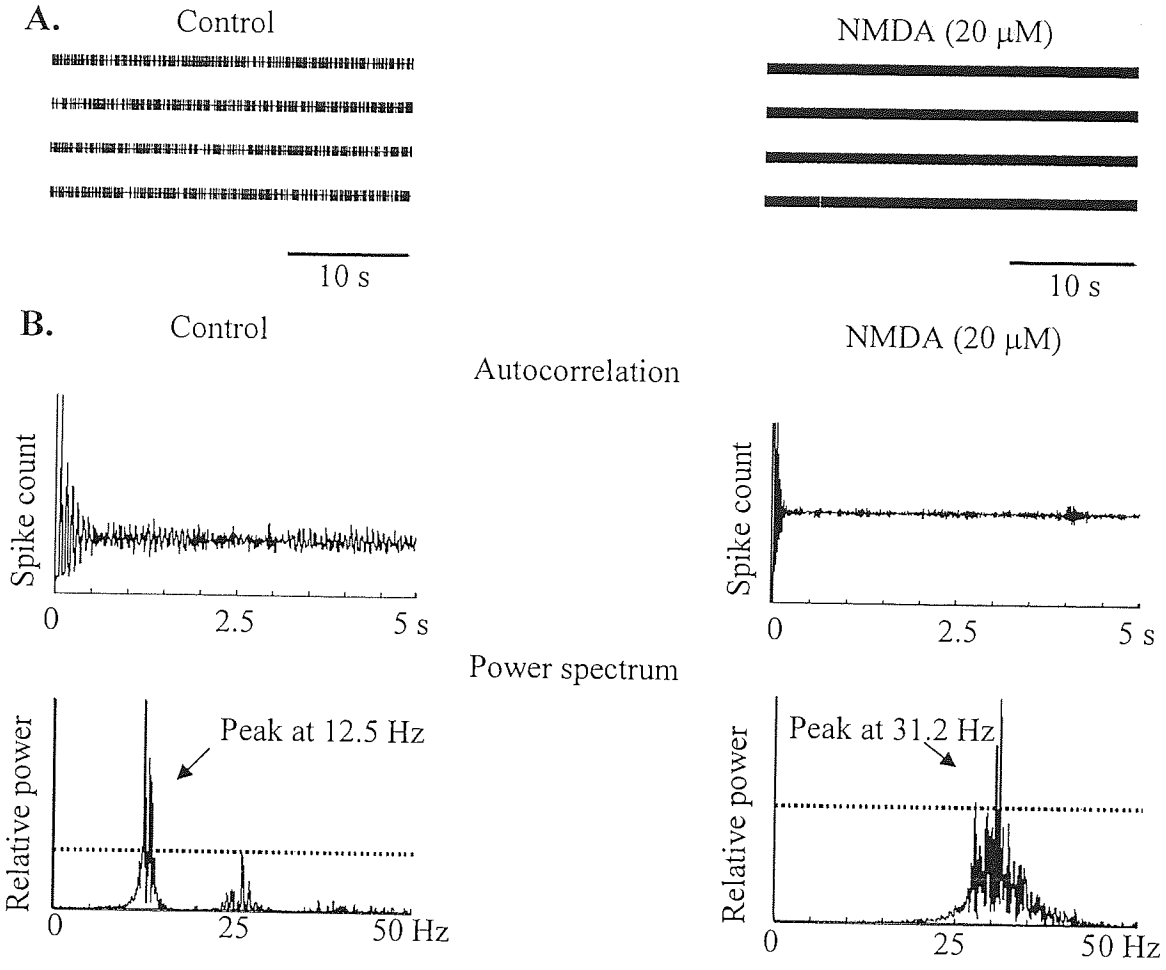

Figure 4.7: NMDA did not promote burst firing in an extracellularly recorded STN cell. Data in control (left) and following NMDA (20 μM) application (right). **A.** 2-min recordings showing that NMDA increased the firing rate but did not change the regular pattern of the discharge. **B.** Autocorrelogram (top) and Lomb power spectrum (bottom) showing that NMDA increased firing rate from 12.5 to 31.2 Hz. Dashed lines represent a significance level of $P< 0.05$.

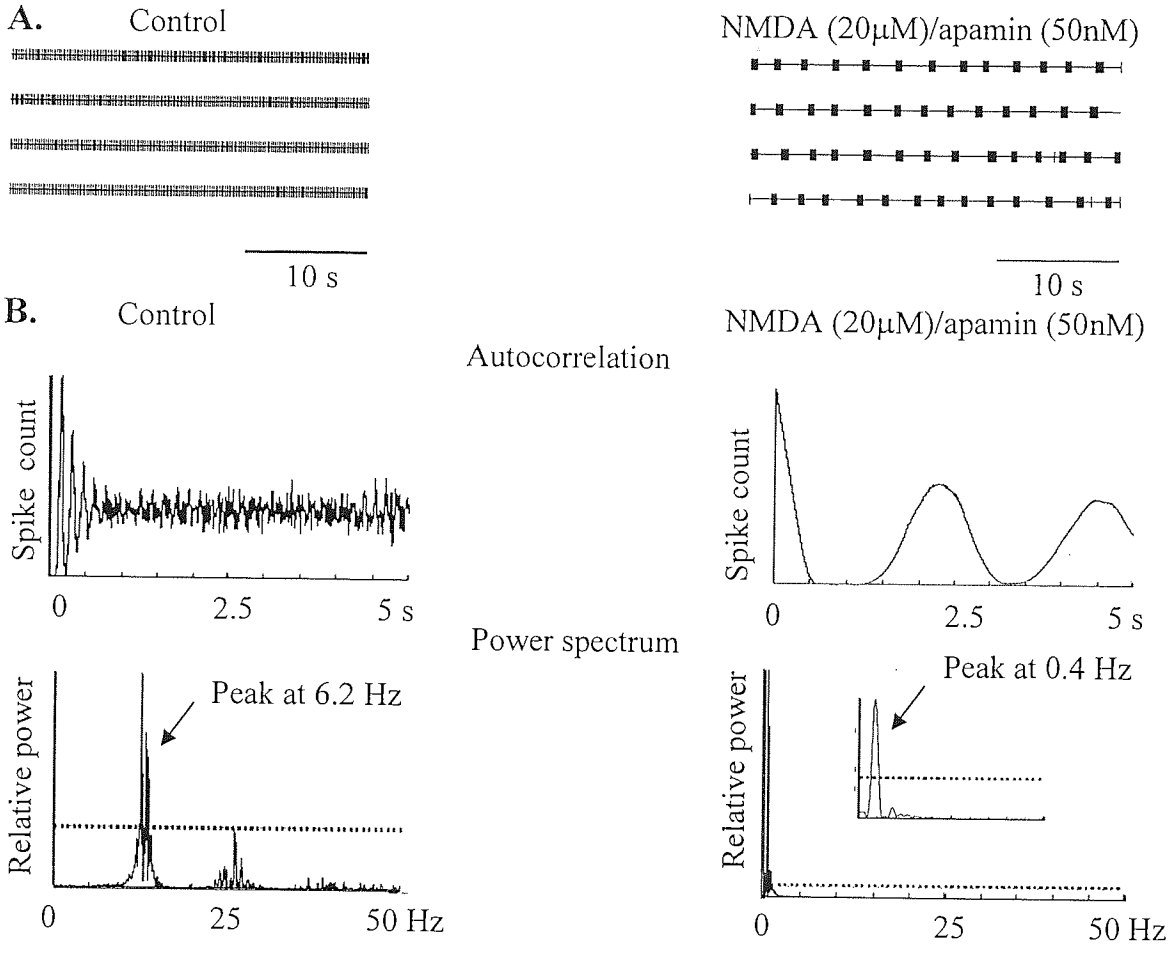

Figure 4.8: NMDA co-applied with apamin promoted burst-firing in an extracellularly recorded STN cell. Data in control (left) and following NMDA (20 μM) and apamin (50 nM) application (right). **A.** 2-min recordings showing that NMDA/apamin promoted burst-firing. **B.** Autocorrelogram (top) and Lomb power spectrum (bottom) showing that application of NMDA/apamin induced an oscillation at 0.4 Hz. Dashed lines represent a significance level of $P< 0.05$.

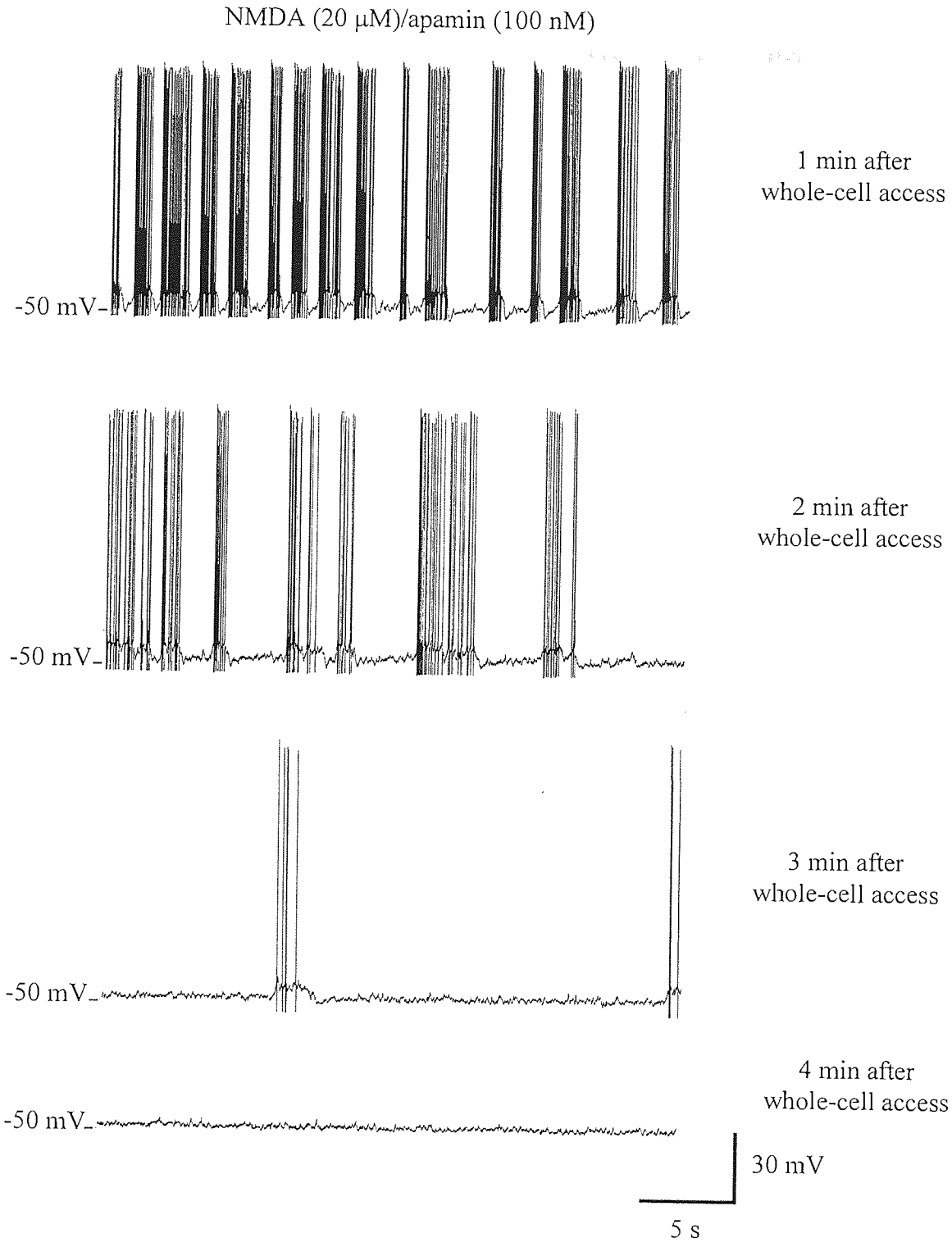

Figure 4.9: The NMDA/apamin induced burst in STN was dependent on intracellular calcium. Whole-cell current-clamp recordings from a STN cell following 1, 2, 3 and 4 minutes of dialysis with intracellular BAPTA (10 mM). Note the suppression of the burst-firing activity over time.

4.2.10. TTX application revealed plateau potentials underlying burst activity

Whole-cell recordings of STN neurones in the presence of the blocker of sodium channels TTX (1 μM) and with an internal solution containing EGTA (0.5 mM) unmasked plateau potentials (n=4, figure 4.10A) suggest that the burst is not generated by network activity. Plateau potentials were present within a voltage window between -40 mV and -70 mV. The frequency of the plateaus increased with depolarisation ($P<0.0001$, r=0.81) while their amplitude was increased by hyperpolarisation ($P<0.0001$, r=-0.82) (figure 4.10BC).

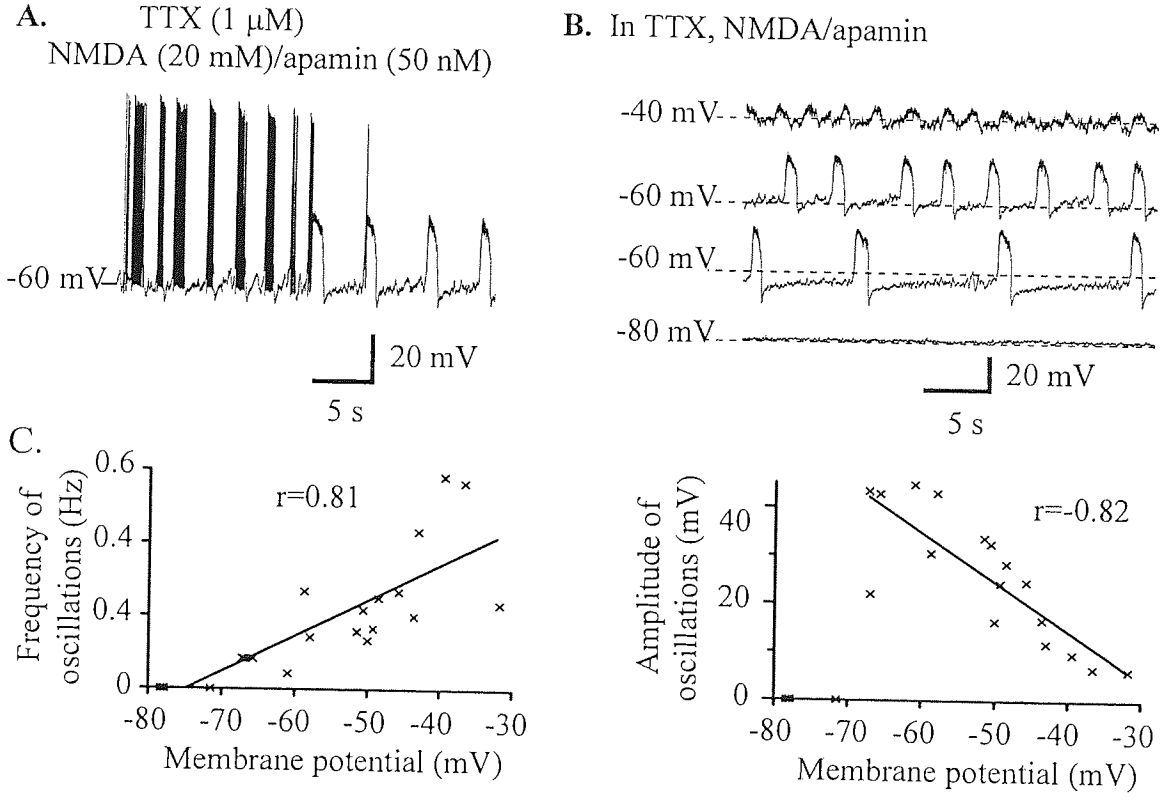

Figure 4.10: The NMDA/apamin induced burst in STN was independent of network activity. A. Current clamp whole-cell recording of a STN cell showing that application of TTX (1 μM) uncovered plateau potentials. **B.** TTX-resistant membrane oscillations are voltage-dependent. **C.** Pooled data showing that membrane hyperpolarisation reduced the frequency and increased the amplitude and of TTX-resistant plateau potentials.

4.2.11. Investigation of the role of GABA and glutamate during the NMDA/apamin induced burst-firing in STN

As NMDA/apamin application promoted burst-firing in GP cells (Stanford IM, unpublished observations) as well as in STN cells, burst-activity may increase both GABA and glutamate release (Lisman, 1997). Since the present slice maintains some of the inhibitory (from GP) and excitatory connectivity, the possibility of ongoing modulation of the pharmacologically induced burst firing by synaptic inputs in STN was explored.

First, the $GABA_A$ antagonist picrotoxin (50 μM) was applied. However, picrotoxin produced no significant change in the interburst frequency (P=0.40), the number of spikes per burst (P=0.49) and the average ISI within burst (P=0.53) (n=6, figure 4.11). To examine whether a modulatory effect of fast glutamatergic transmission, CNQX (10 μM) was applied. The analysis of the burst parameters also failed to show a change in the interburst frequency (P=0.88), the number of spikes per burst (P=0.19) and the ISI within the burst (P=0.21) (n=5, figure 4.12).

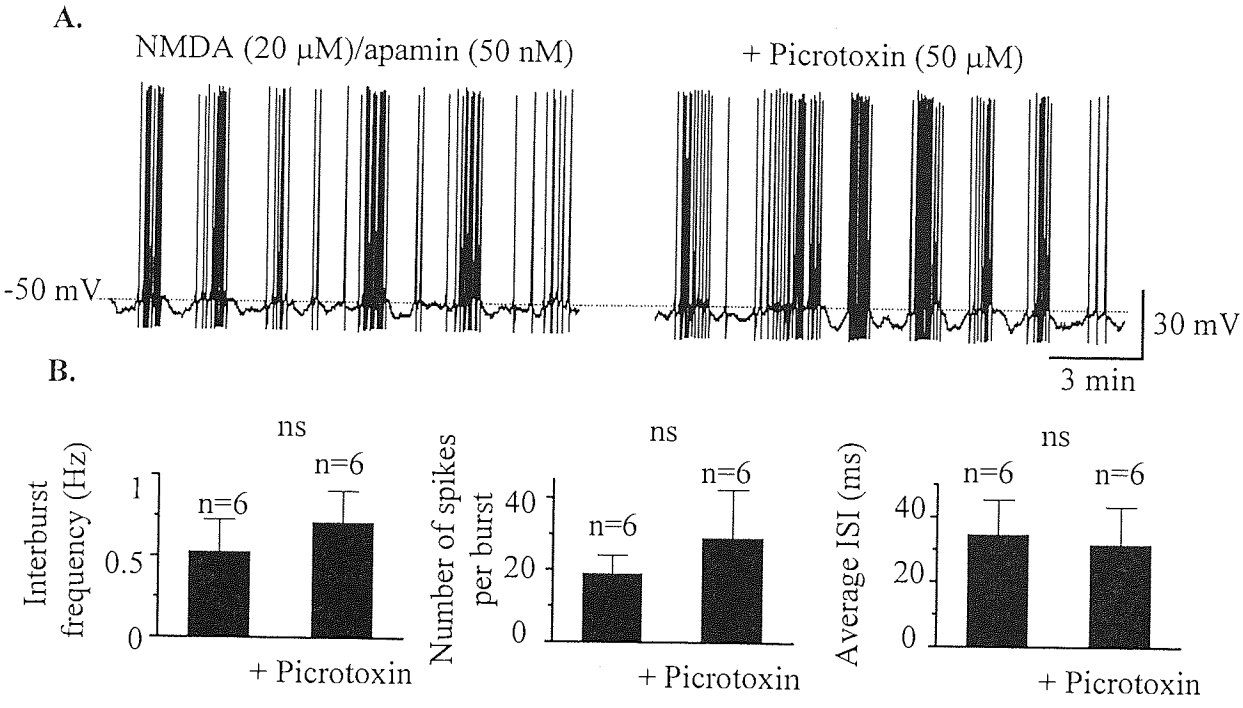

Figure 4.11: NMDA/apamin induced burst firing in STN was not modulated by spontaneous synaptic GABA release. A. Whole-cell current clamp recordings of a STN cell in NMDA (20 μM)/apamin (50 nM) and following perfusion the $GABA_A$ antagonist picrotoxin (50 μM). **B.** Pooled data showing the lack of effect of picrotoxin on the NMDA/apamin induced interburst frequency, the number of spikes per burst and the average ISI within burst.

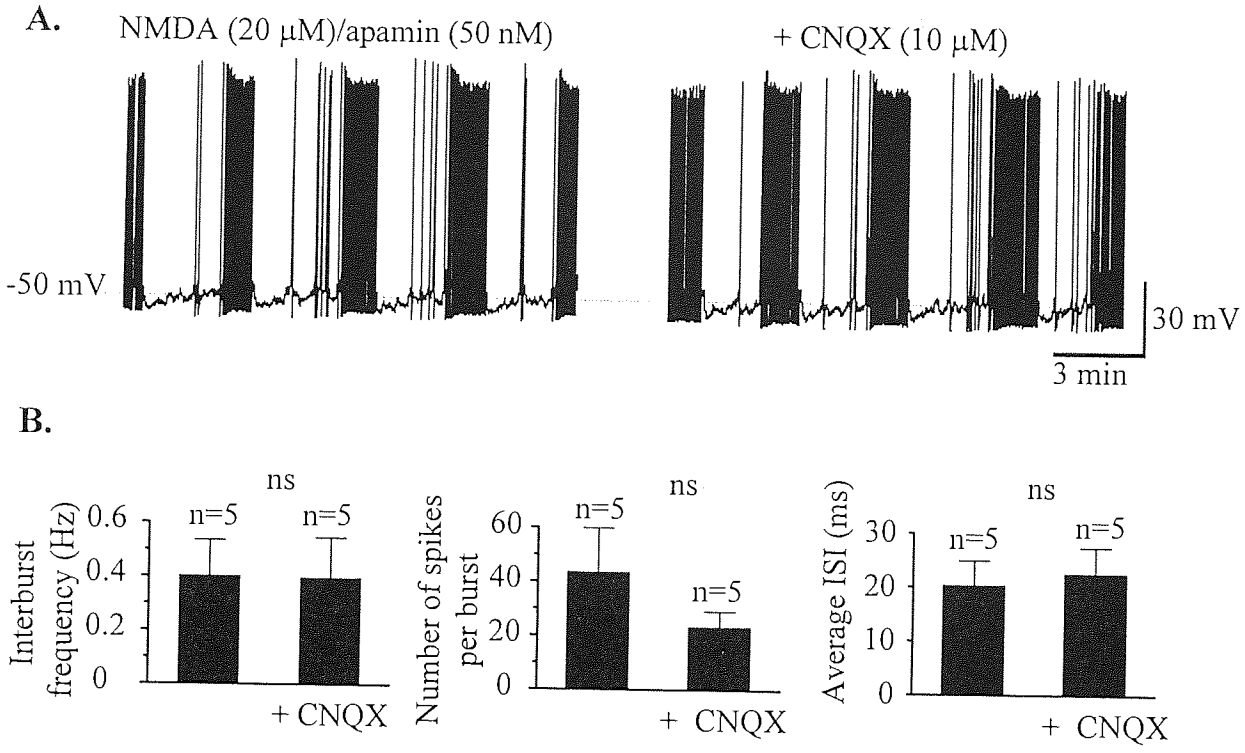

Figure 4.12: NMDA/apamin induced burst firing in STN was not modulated by spontaneous synaptic glutamate release. A. Whole-cell current clamp recordings in NMDA (20 μM)/apamin (50 nM) and following perfusion of the antagonist of fast glutamatergic transmission CNQX (10 μM). **B.** Pooled data showing the lack of effect of CNQX on the NMDA/apamin induced interburst frequency, the number of spikes per burst and the average ISI within burst.

4.2.12. Lack of synchrony during NMDA/apamin induced burst firing

Single-unit recordings of neuronal activity were made from 6 pairs of STN cells. In each pair, the regular activity in control conditions was uncorrelated as was the bursting activity induced by NMDA (20 μM) and apamin (100 nM) application.

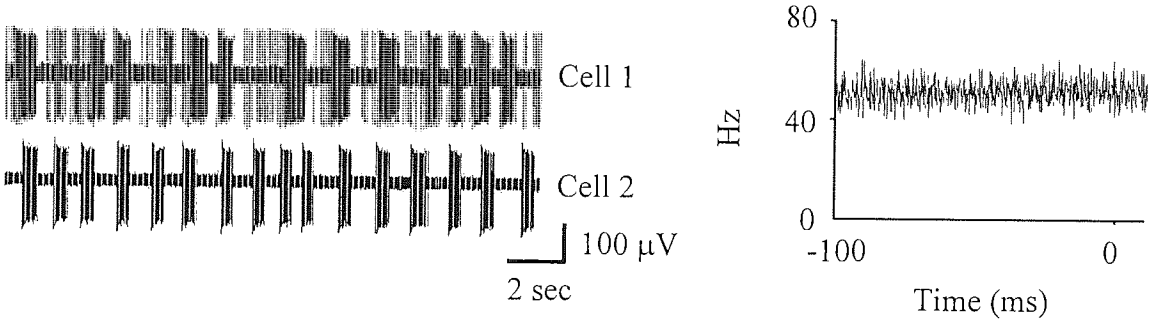

Figure 4.13: Paired recordings in the STN showed uncorrelated activity. Simultaneous single-unit recording from paired STN neurones in the presence of NMDA (20 μM) and apamin (100 nM) and the associated cross-correlogram showing a lack of correlation between the two burst-firing cells.

4.3. Discussion

4.3.1. Lack of network activity

In order to study cellular mechanisms by which abnormal patterned activity arises in basal ganglia, in the STN-GP network in particular, an *in vitro* model is required. This chapter showed that in a 20° parasagittal mouse slice preparation, functional reciprocal STN-GP connectivity was preserved. This has been proposed to be a prerequisite for the initiation and promotion of a regenerative burst activity between the STN and GP using an organotypic co-culture (Plenz & Kitai, 1999).

In this mouse preparation, a spontaneous regular single spike firing of STN cells was observed, in agreement with the regular firing reported in rat slices using extracellular recordings (Abbott *et al.*, 1997; Tofighy *et al.*, 2003; Wilson *et al.*, 2004; Zhu *et al.*, 2002a) and perforated patch-clamp (Bevan & Wilson, 1999). This spontaneous firing has been shown to be due to intrinsic spontaneous membrane oscillations (Bevan & Wilson, 1999). It appeared, however, that synaptic GABA and glutamate release did not play a role in modulating the activity of STN cells both in naïve slices and following pharmacological promotion of burst activity using NMDA and apamin. The lack of functional inhibitory influence on the activity of STN cells may be accounted for by the presence of large proportion (68 %) of silent GP cells and by the slow firing of other GP cells (<8 Hz) (Cooper & Stanford, 2000). Alternatively, the burst induced by NMDA and apamin may not be susceptible to synaptic modulation as it is generated independently from network activity.

Although the proposed mechanism for initiation and promotion of regenerative burst activity were evident in the mouse slice preparation, STN cells did not show evidence of spontaneous regenerative oscillatory activity, unlike the proposed finding of Plenz & Kitai, (1999) using organotypic culture of GP and STN. Furthermore, the lack of synchronous activity within the STN argues against the presence of intra-STN collaterals, in agreement with the report of Wilson *et al.*, 2004. The numerous sEPSCs recorded in STN cells may therefore arise from other nuclei such as the cortex, thalamus or PPN (Smith *et al.*, 1998).

It appears likely that the extent of connectivity in the STN-GP network in the mouse preparation is not great enough to sustain oscillatory activity. Nevertheless, it is possible that a small proportion of the STN-GP network may be able to sustain regenerative oscillatory activity. Alternatively, the regenerative oscillatory activity seen in organotypic culture may have been due to abnormal hyperconnectivity of the STN-GP network in organotypic culture (Plenz *et al.,* 1998). The burst activity in the mouse preparation was induced using a non physiological agent, apamin, in conjunction with glutamate. The use of more physiological agents such as agonists of cholinergic and kainate receptors may have induced burst firing that could initiate a regenerative activity. Such a burst activity might have been more susceptible to modulation by spontaneous synaptic activity. It is also possible that the initiation of a regenerative oscillatory activity may depend on the frequency of the induced burst, favouring certain frequencies over others, the frequency of the NMDA/ apamin induced being inappropriate for initiation of oscillatory activity. In addition, promotion of an oscillatory activity may be dependent on a fine control of the temperature, the humidity and therefore the pH. The present study used a submerged-type recording chamber, which may have compromised any potential oscillatory activity. Instead, the use of an interface-type chamber may may increase the probability of observing an oscillatory activity. Additionally, the lack of evidence of spontaneous burst activity in the STN from slices of MPTP-treated mice rules out the possibility that the lack of spontaneous regenerative burst in the STN-GP network in the normal mouse preparation is due to the requirement of long-term adaptive changes following dopamine depletion. However, these MPTP-treated mice did not show obvious motor deficits questioning therefore the relevance of this animal model in the investigation of the changes underlying the pathology of Parkinson's disease. Yet, these mice show a reduced dopamine content in the striatum, although, one can not be certain that the extent of dopamine depletion is constant and reproducible for each animal. Correlating dopamine loss and electrophysiological characteristics may help in solving this problem. To circumvent this model issue, an alternative animal model could be set by injecting 6-OHDA in mice. This would need immunochemical, behavioural and functional studies to validate

such a model. If changes comparable to that seen in 6-OHDA rats are found, investigation of oscillatory activity could be carried on.

Taken together, these data point towards the conclusion that other anatomical structures (in addition to the STN and GP) may be required to drive burst activity in the STN-GP network. Such structures may include cortex (Magill *et al.*, 2000, 2001) or the striatum (Tseng *et al.*, 2001a).

4.3.2. A pharmacological model of bursting

A pharmacological model of burst-firing was sought in an attempt to increase spontaneous synaptic release of GABA and glutamate in the GP-STN network (Lisman, 1997). NMDA alone did not promote burst firing in STN neurones, in disagreement with the work of Zhu *et al.*, (2004). However, co-application of NMDA and apamin (50-100 nM) induced burst firing in about 50 % of the cells. This is consistent with reports showing that apamin, a blocker of SK channels, enhances NMDA-mediated burst firing in dopaminergic neurones (Seutin *et al.*, 1993) and rat STN neurones (Wilson *et al.*, 2004). Accordingly, modulation of SK channels using other agents such as TEA-Cl (Wilson *et al.*, 2004), bicuculline methiodide (Johnson & Seutin, 1997) and 1S, 3R ACPD (Beurrier *et al.*, 1999; Awad *et al.*, 2000) also enhance NMDA-mediated burst firing. Surprisingly, 1S, 3R ACPD did not promote burst firing in STN mouse slice.

The slow oscillation frequency of the burst firing induced by NMDA and apamin in the mouse preparation is in the same range as seen using co-culture (0.4-1.2 Hz, Plenz & Kitai, 1999) and in 6-OHDA-lesioned rats (0.5-1.5 Hz, Magill *et al.*, 2000, 2001; Tseng *et al.*, 2001a). It is however lower than that observed in MPTP-treated monkeys or patients with PD (4-7 and 10-15 Hz, Bergman *et al.*, 1994; Brown *et al.*, 2001).

CHAPTER 5. Actions of dopamine and 5-HT on mouse STN cells *in vitro*

In this chapter the postsynaptic actions and pharmacology of the neurotransmitter, dopamine, on single STN neurones were characterised using whole-cell and extracellular single-unit recordings in the STN-GP connected mouse slice preparation. In addition this chapter explored the action and pharmacology of 5-HT on STN neurones using extracellular single-unit recordings.

5.1. Dopamine in the STN

A key feature of the classical model of BG function is the concept that dopamine acts exclusively in the striatum (Alexander & Crutcher, 1990). However, anatomical studies have shown that both the GP (Lindvall & Björklund, 1979; Lavoie *et al.*, 1989; Smith & Parent, 1989) and the STN (Cossette *et al.*, 1999; Gauthier *et al.*, 1999; Hassani *et al.*, 1997; Prensa *et al.*, 2000; Smith & Kieval, 2000) receive direct dopaminergic projections from the SNc. Due to the small number of fibres, this projection has been assumed to play a minor role (Hassani *et al.*, 1997; Hedreen, 1999; Francois *et al.*, 2000). However, this view has now been challenged by further molecular, behavioural and electrophysiological studies.

In addition to synaptic vesicles, Cragg *et al.*, (2004) demonstrated that vesicules are present in axonal elements not associated with syanpses, suggesting that volume transmission of dopamine in the STN coexist alongside point to point synaptic transmission.

Dopamine receptors belong to the family of seven transmembrane domain G-protein coupled receptors. Five distinct dopamine receptors have been characterised and subdivided into two subfamilies, D1- (D1 and D5) and D2-like (D2, 3 and 4), on the basis of their biochemical and pharmacological properties (Vallone *et al.*, 2000). The transduction pathways activated by D1- and D2-like receptors include an increase or a decrease in cyclic adenonosine monophosphate (cAMP) levels leading to an increase or a decrease in cell excitability respectively. The coupling between dopamine receptors

and cAMP pathways involves the activation of the $G\alpha_s$ subunit of G-proteins by dopamine D-1 like receptors and activation of $G\alpha_{i/o}$ subunit by D2-like receptors. The transduction cascades between the cAMP and the cell response remain to be characterised. In addition, dopamine receptors may also interact with $G_{\beta\gamma}$ subunits of G-proteins (Neve *et al.,* 2004). The cell responses to dopamine receptor activation include modulation of potassium and calcium currents (Yan et *al.,* 1997; Zhu *et al.,* 2002b).

Binding studies have shown evidence of D1- and D2-like dopamine receptors in the STN (Boyson *et al.,* 1986; Johnson *et al.,* 1994; Kreiss *et al.,* 1996; Flores *et al.,* 1999). In addition, *in situ* hybridisation studies have reported the presence of mRNA for D2 and D3 receptors (Bouthenet *et al.,* 1991; Flores *et al.,* 1999), although no evidence of D1 mRNA was found (Mansour *et al,* 1991). Dopamine receptors have been shown to be involved in the regulation of normal muscle tone, as local intra-subthalamic administration of a non-selective dopamine receptor antagonist produces rigidity (Hemsley *et al.,* 2002). In addition, in intact rats, local application of D1 receptor agonists has been reported to induce orofacial dyskinesia, which is enhanced following nigro-striatal lesions (Parry *et al.,* 1994; Mehta *et al.,* 2000) suggesting that the nigro-subthalamic projection may be involved in the development of dyskinesia induced by dopaminergic medication. In contrast, blockade of D1 receptors in STN was found to result in akinesia in rats (Hauber, 1998).

Electrophysiological studies *in vivo* have produced no consensus concerning the nature of the action of dopamine in STN. An early study reported mixed inhibitory and excitatory effects in the STN (Campbell *et al.,* 1985). Another study has shown that local application of dopamine in STN produced an excitation (Mintz *et al.,* 1986). Later on, an excitation has also been shown following systemic injection, and local application, of the mixed D1/D2 agonist apomorphine (Kreiss *et al.,* 1996) an effect mimicked by systemic injection or local application of D1, but not D2, receptor agonists (Kreiss *et al.,* 1996). Following nigro-striatal lesions, the effect of apomorphine reverted to an inhibitory one, an effect mimicked by dopamine D1 agonists, while the D2 receptor agonist quinpirole exerted an excitatory effect when administered after D1 agonists (Kreiss *et al.,* 1997). In contrast, Hassani & Feger (1999) revealed that intra-subthalamic injection of apomorphine and selective dopamine D_1 and D_2 dopamine

receptor agonists decreased the firing rate of STN cells in intact rats. However, in 6-OHDA-lesioned rats, apomorphine and D_2 receptor agonists increased the firing rate (Hassani & Feger, 1999). Recently, selective destruction of the nigro-subthalamic pathway (by local intra-subthalamic injection of 6-OHDA) has revealed a decrease in the firing rate of STN neurones, supporting the existence of an excitatory influence of dopamine on STN cells (Ni *et al.*, 2001a).

Electrophysiological studies *in vitro* produced a considerable support for an excitatory role of dopamine, although no consensus emerged with respect to the receptor subtype(s) involved. Fast-scan cyclic voltammetry experiments have provided evidence of spontaneous dopamine release in rat STN slices (Cragg *et al.*, 2004). In addition, dopamine was shown to induce a direct postsynaptic excitation of STN neurones (Zhu *et al.*, 2002b; Tofighy *et al.*, 2003), an excitation which has been reported to be mediated by D2 receptors through a reduction of a resting potassium conductance (Zhu *et al.*, 2002b). Interestingly, D1 receptor agonists failed to produce a significant excitation in normal rats but significantly increased STN firing rate following nigro-striatal lesions (Zhu *et al.*, 2002a). In contrast, another group has reported that D1 receptor agonists increase the firing rate of rat STN cells (Baufreton *et al.*, 2005). In addition to the direct postsynaptic action, dopamine has been reported to act on presynaptic receptors in STN to reduce synaptic glutamate and GABA transmission (Shen & Johnson, 2000).

5.2. Results

5.2.1. Dopamine excited STN cells

The action of dopamine in STN was investigated using extracellular single-unit recordings in mouse brain slices. Dopamine (30 μM) induced an excitation in all cells with an absolute change in firing rate of 12.0 ± 0.6 Hz (n=69, $P<0.0001$, figure 5.1AB). The effect of dopamine was quantified throughout the study as absolute change in firing rate (in Hz), as the percentage increase of basal firing rate was negatively correlated with regard to the basal firing rate ($P=0.0004$, n=69, figure 5.1C). The absolute change in firing rate was independent from the basal firing rate ($P=0.29$, n=69, figure 5.1D).

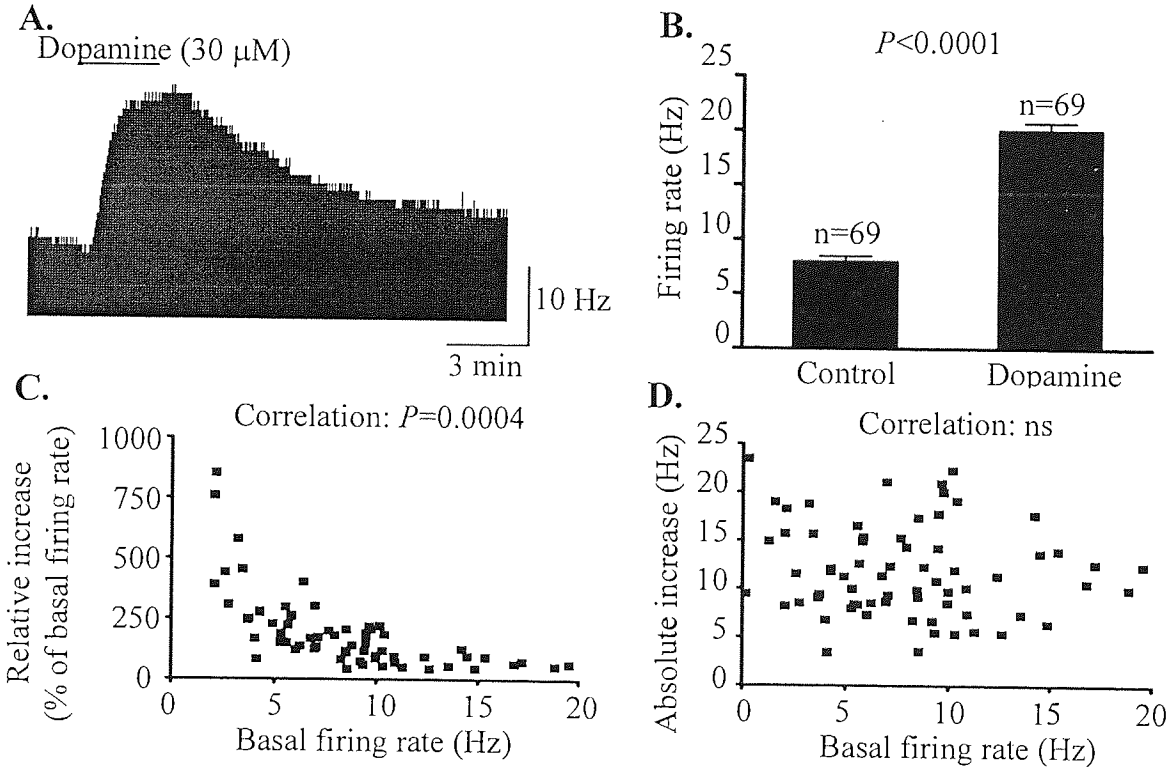

Figure 5.1: Dopamine excited STN cells. A. Rate-meter recording of a STN neuronal activity showing that dopamine (30 μM) increased the firing rate from 9 to 21 Hz. **B.** Pooled data showing that dopamine induced an absolute increase of 12.0 ± 0.6 Hz. **C.** The relative increase in firing rate (in % of control) was negatively correlated with the basal firing rate ($P=0.0004$). **D.** The absolute increase in firing rate (in Hz) was independent of the basal firing rate ($P=0.29$).

5.2.2. Dopamine induced excitation was independent of synaptic transmission

To examine whether the excitation induced by dopamine resulted from changes in GABA or glutamate neurotransmitter release, dopamine (30 μM) was applied in the presence of the $GABA_A$ receptor antagonist picrotoxin (50 μM) and antagonists of fast glutamatergic receptor transmission CNQX (10 μM) and DL-AP5 (50 μM). As shown in chapter 4, these antagonists had no effect on the basal STN cell firing rate. Furthermore, the absolute increase in firing rate induced by dopamine (9.80 ± 1.36 Hz) was not affected by the antagonists of $GABA_A$ and fast glutamatergic transmission (9.62 ± 1.22 Hz, n=9, P=0.37, figure 5.2), suggesting that the excitatory effect of dopamine is mediated through postsynaptic action and has little to do with glutamate or GABA release within the STN.

5.2.3. D1-like and D2-like receptor agonists mimicked the action of dopamine

No consensus on the subtypes of the receptors involved in the dopamine induced excitation emerged from previous studies. Therefore, an attempt was made to determine the receptor subtyes involved in mediating the dopamine induced excitation of STN cells. In an attempt to mimic the excitatory action of dopamine, the D1-like receptor agonist SKF38393 (10 μM) and the D2-like receptor agonist quinpirole (10 μM) were bath applied. Both drugs induced comparable responses. SKF38393 induced a mean absolute increase of 6.48 ± 0.65 Hz (n=17 cells, P<0.0001, figure 5.3AB). Washout of SKF38393 was slow, and irreversible in some cases. Quinpirole produced a reversible mean absolute increase of 6.37 ± 0.48 Hz (n=35, P<0.0001, figure 5.3AB).

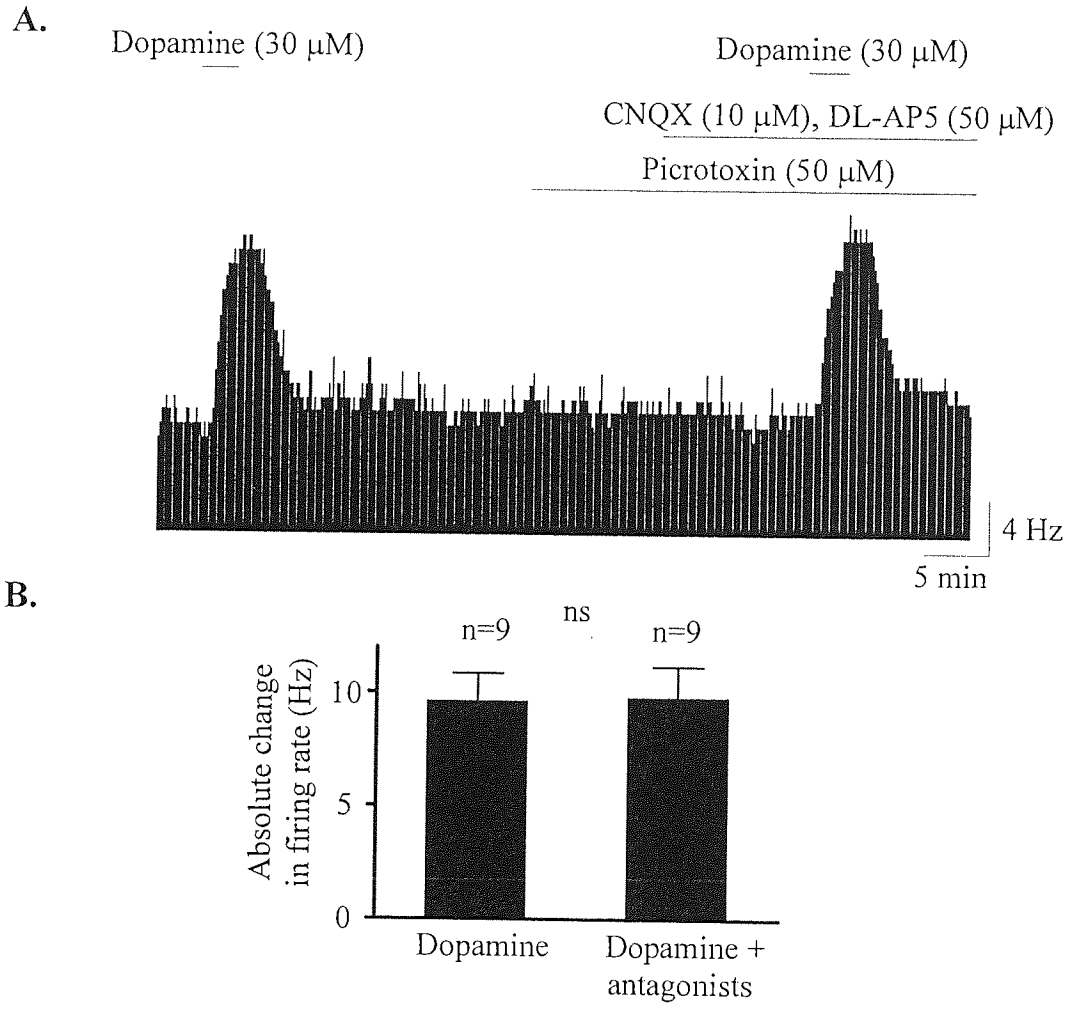

Figure 5.2: Dopamine induced excitation was independent of GABA and glutamate transmission. A. Rate-meter recording showing that co-application of picrotoxin (50 μM), CNQX (10 μM) and DL-AP5 (50 μM) did not affect the excitation induced by dopamine (30 μM). **B.** Pooled data showing the lack of effect of antagonists on the dopamine induced excitation.

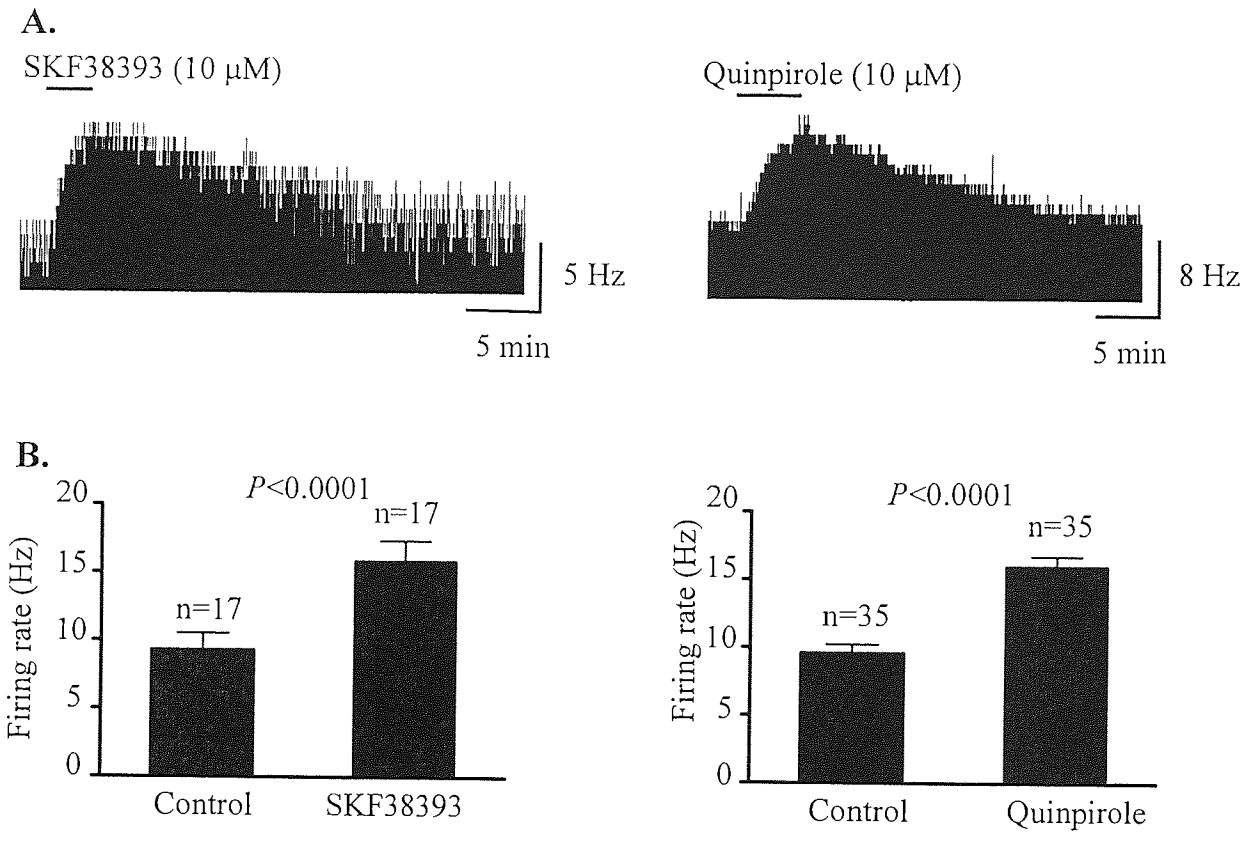

Figure 5.3: SKF38393 and quinpirole mimicked the excitation induced by dopamine. A. Rate-meter recordings of the increase in firing rate induced by SKF38393 (10 μM) and quinpirole (10 μM). **B.** Pooled data showing the excitatory actions of SKF38393 and quinpirole on STN cells.

5.2.4. SKF38393 and dopamine showed additive effects

Previously, it has been shown that the responses to D1-like and D2-like receptor agonists when co-applied in GP are potentiated (Walters *et al.*, 1987; Ruskin *et al.*, 1999). In order to test whether this is the case in the STN, dopamine was applied alone and then in the presence of the D1-like receptor agonist SKF38393 (figure 5.4AB). Dopamine (30 μM) alone induced an absolute increase of 12.18 ± 2.08 Hz (n=6) while SKF38393 alone induced an increase of 7.29 ± 1.29 Hz (n=6). In presence of SKF38393, application of dopamine (in order to activate D2-like receptors) induced an absolute increase of 3.93 ± 1.09 Hz (n=6). Although we expected a slightly larger affect of the second application of dopamine, these results are consistent with the additive effects of D1-like and D2-like receptors in the STN. Thus, no evidence of potentiation was observed.

5.2.5. SKF38393 occluded the quinpirole effect

Quinpirole alone produced an absolute increase of 6.34 ± 0.29 Hz (n=6) while SKF38393 applied alone produced an absolute increase of 6.16 ± 1.19 Hz (n=6), consistent with the results presented in figure 5.3CD. However, in the presence of SKF38393, application of quinpirole produced an absolute increase of 1.61 ± 0.24 Hz (n=6), significantly smaller than the increase induced by quinpirole alone (P=0.0002, n=6). This suggests that, in this set of experiments, the D1 agonist SKF38393 occludes the effect of the D2 agonist quinpirole.

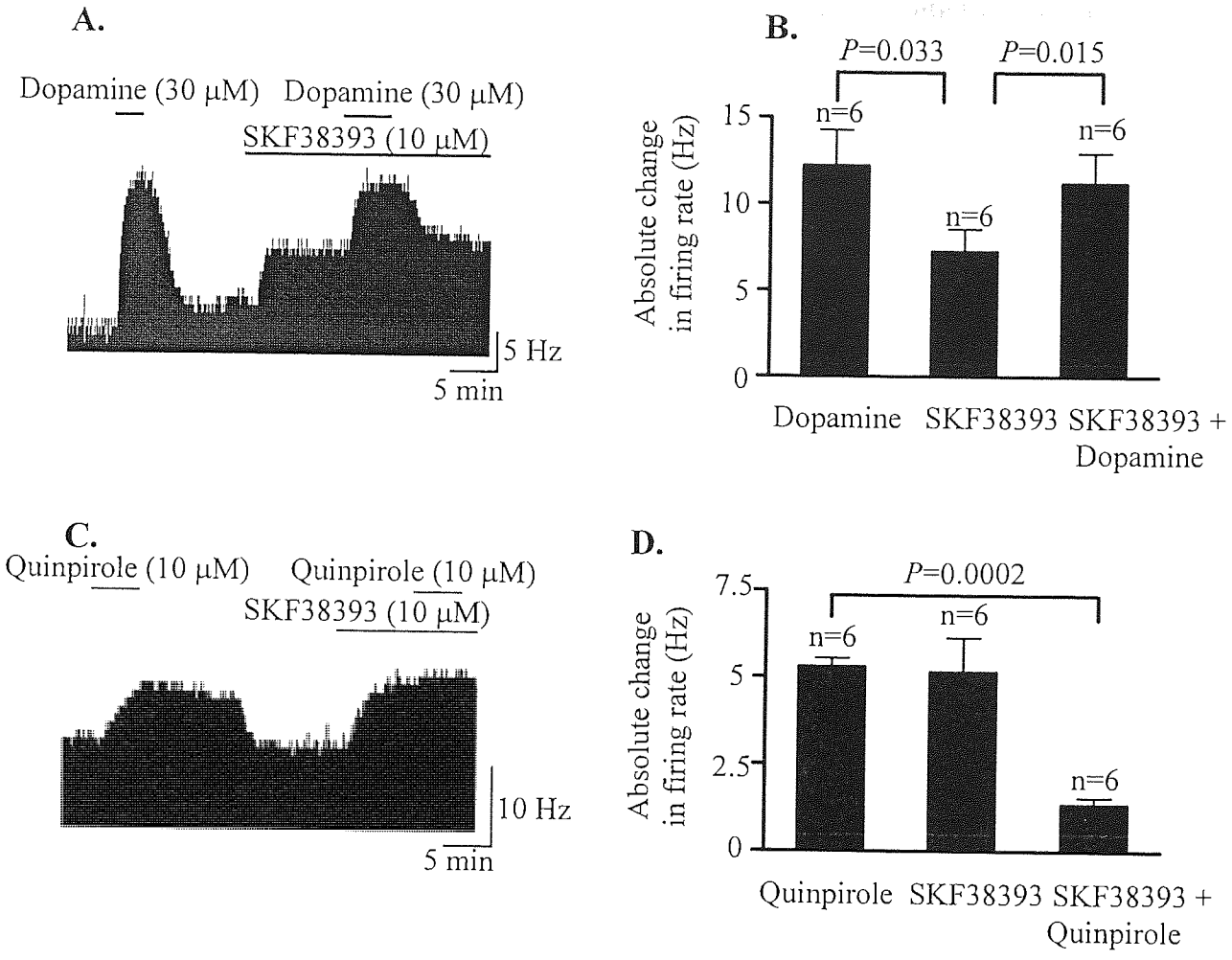

Figure 5.4: Co-application of D1- and D2- like receptor agonists. A. Rate-meter recording of STN cell activity showing application of dopamine (30 μM) and dopamine in the presence of SKF38393 (10 μM). **B.** Pooled data showing apparent additive effects of D1 and D2 receptor activation **C.** Rate-meter recording showing the effect of quinpirole (10 μM) alone and in the presence of SKF38393 (10 μM). **D.** Pooled data showing the apparent occlusion of quinpirole effect by SKF38393.

5.2.6. The D1-like receptor antagonist SCH23390 partially inhibited the dopamine induced excitation

The D1-like antagonist SCH23390 (2 μM) reduced the absolute increase induced by dopamine by 8.15 ± 1.56 Hz (n=7, *P*=0.001) confirming that the action of dopamine is at least partly mediated through D1-like receptors (figure 5.5AB). Application of SCH23390 (2 μM) alone resulted in small absolute increase in the basal firing rate of 2.10 ± 1.01 Hz (n=6, *P*=0.046). This SCH23390 induced excitation was prevented by 15 minutes pre-application of the 5-HT_{2C} receptor antagonist RS102221 (500 nM) (n=8), consistent with an agonist effect of SCH23390 on 5-HT_{2C} receptors (Seeman & Van Toll, 1994).

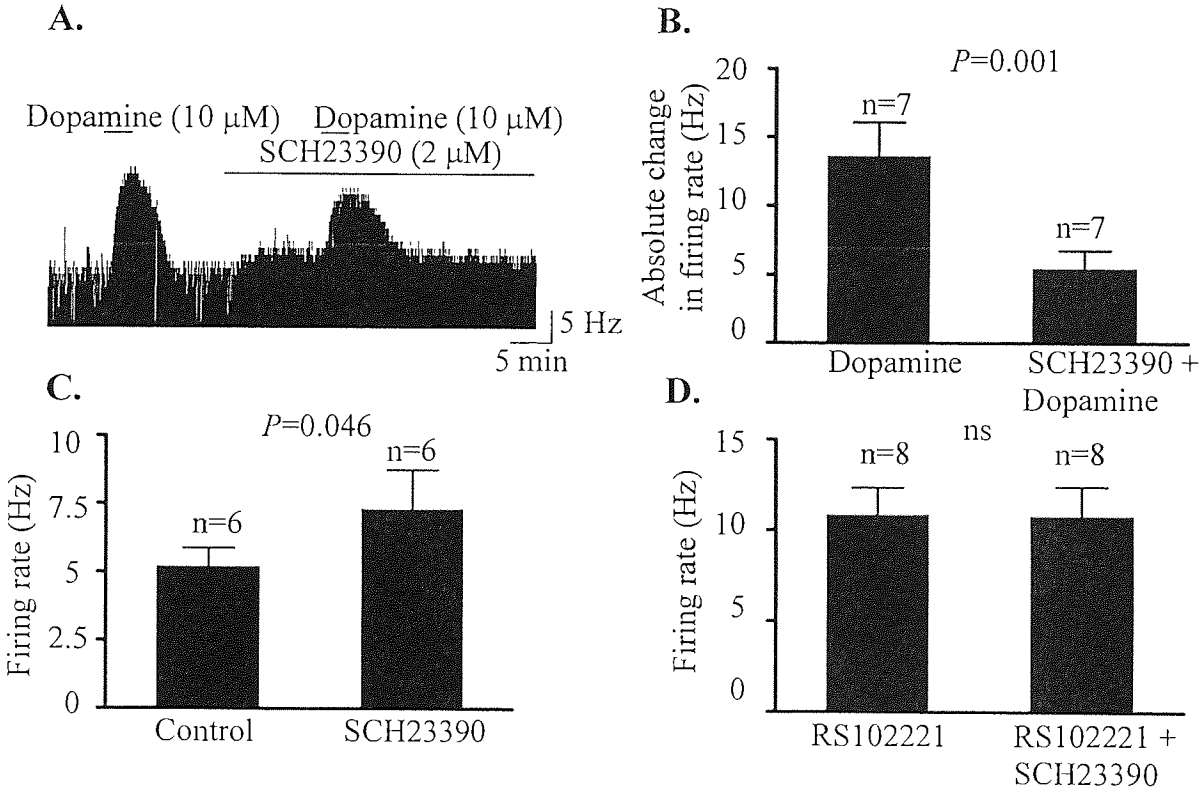

Figure 5.5: SCH23390 produced a 5-HT_{2C} mediated excitation while inhibiting the dopamine induced excitation. A. Rate-meter recording of STN cell activity showing that the D1 antagonist SCH23390 (2 μM) alone increased the basal firing rate and partially inhibited the dopamine (30 μM) induced excitation. Pooled data showing the effect of SCH23390 on the dopamine induced excitation (**B**) the increase in STN basal firing rate induced by SCH23390 (**C**) and the effect of the 5-HT_{2C} antagonist RS102221 (500 nM) (**D**).

5.2.7. Lack of effect of D2-like receptor antagonists

The D2-like antagonists sulpiride (n=7, *P*=0.48) and eticlopride (n=6, *P*=0.28) failed to affect the response of STN cells to dopamine (figure 5.6). This result fits with the apparent D1-like receptor mediated occlusion presented in figure 5.4D and is also consistent with the study in rat STN of Tofighy *et al.*, (2003).

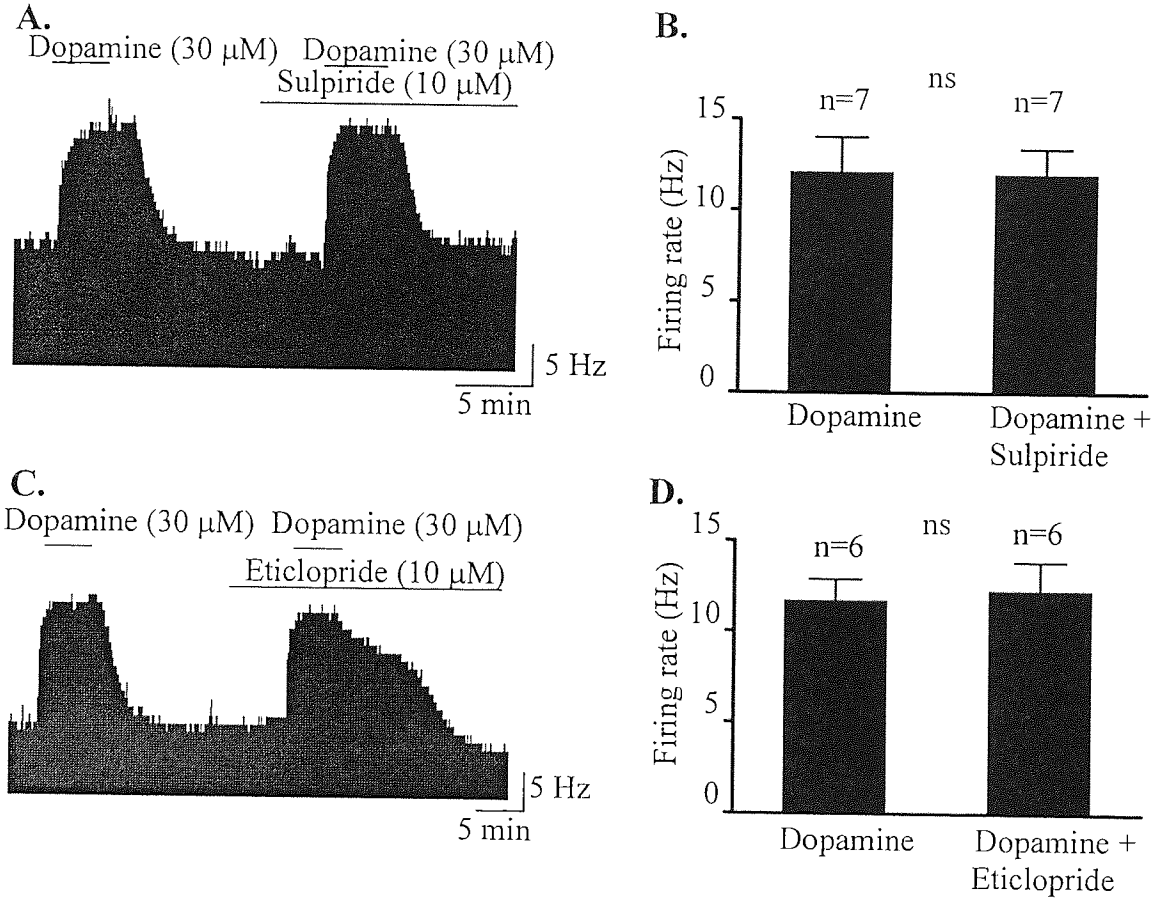

Figure 5.6: The D2 antagonists sulpiride and eticlopride failed to affect the dopamine induced excitation. A. C. Rate-meter recordings of extracellular STN cell activities showing the lack of effect of sulpiride (10 μM) and eticlopride (10 μM) on the dopamine (30 μM) induced increase in firing rate. **B. D.** Pooled data indicating the lack of effect of the D2-like receptor antagonists.

Co-application of both D1 and D2 antagonists SCH23390 (2 μM), eticlopride (10 μM) and sulpiride (10 μM), in the presence of RS102221, reduced the dopamine response by 6.57 ± 1.77 Hz (n=7, *P*=0.0049, figure 5.7) but did not abolish the response, in agreement with the study of Tofighy *et al.*, (2003).

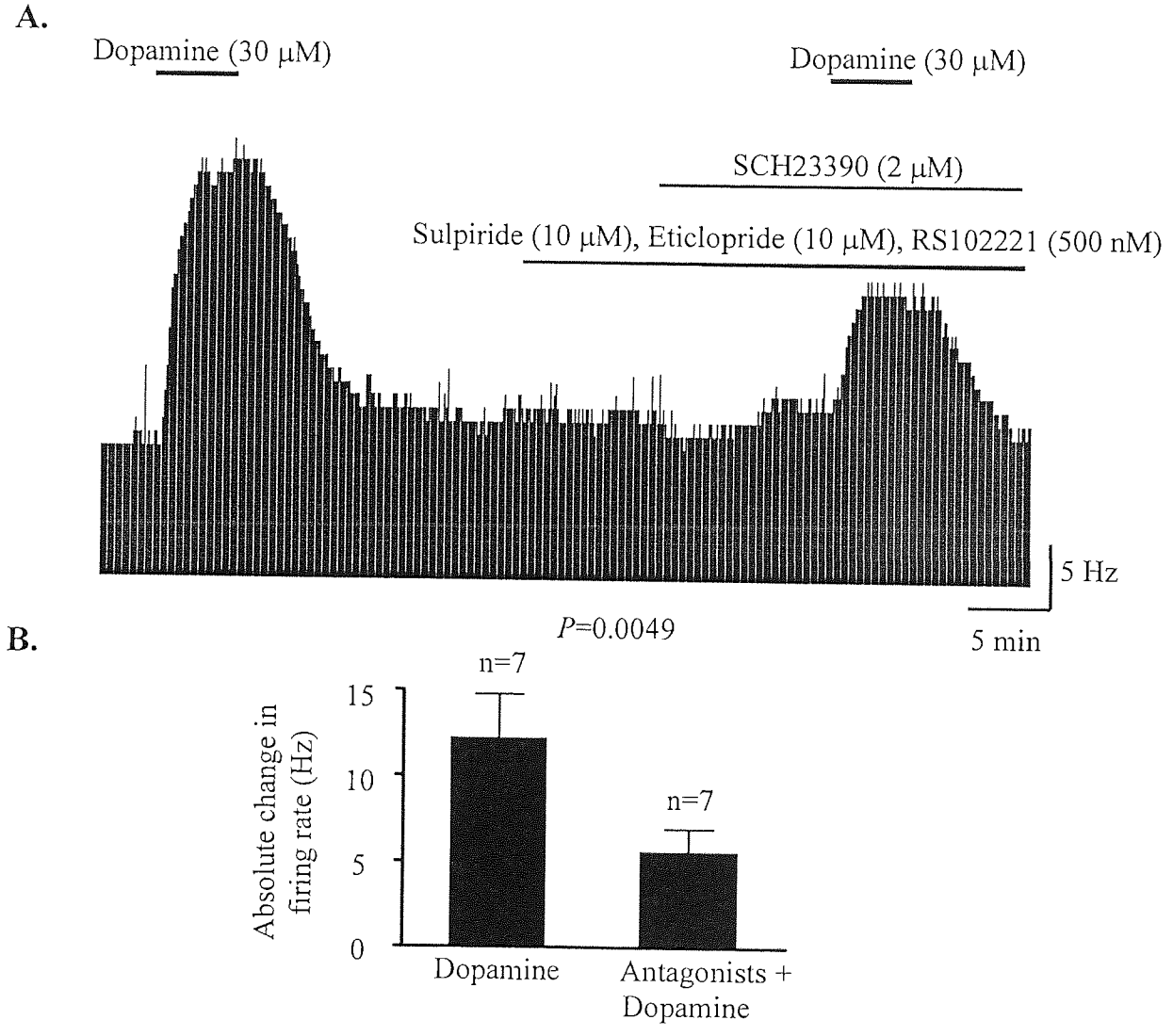

Figure 5.7: A combination of D1-like and D2-like antagonists did not abolish the dopamine induced excitation of STN cells. A. Rate-meter recordings of STN cell activity. **B.** Pooled data showing that D1 and D2 antagonists together did not completely antagonise the dopamine induced excitation in STN.

5.2.8. The quinpirole effect was not mediated by D2-like receptors

As previously described, the D1-like receptor antagonist SCH23390 (2 μM) increased the firing rate through action at $5HT_{2C}$ receptors. However, when the agonist SKF38393 was added in the presence of SCH23390 no further excitation was observed (n=7, *P*=0.38, figure 5.8A). However, the increase in firing rate induced by D2 receptor agonist quinpirole was not significantly suppressed by the D2-like receptor antagonist sulpiride (10 μM, n=4, *P*=0.06) and was only partially reduced by eticlopride (10 μM, n=5, *P*=0.0049) consistent with the results of Tofighy *et al.*, (2003) where the excitation caused by quinpirole were evident in the presence of sulpride, eticlopride and the non-selective antagonist (+) butaclamol.

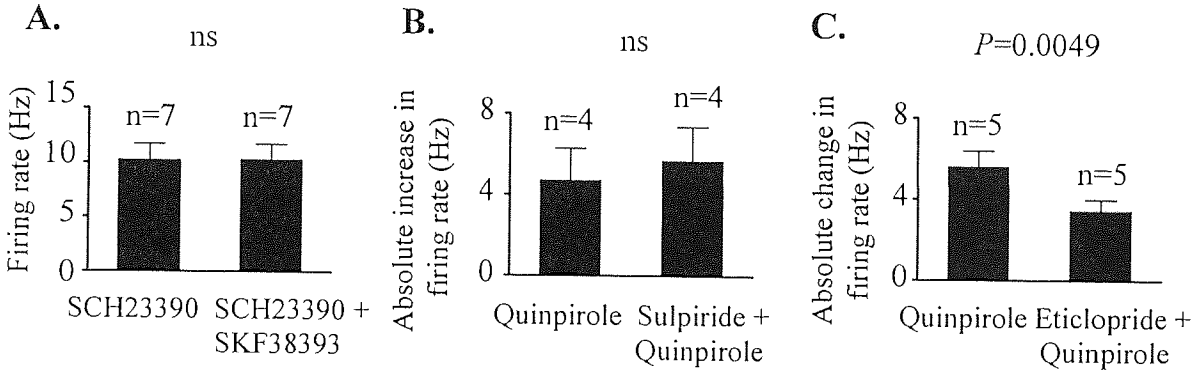

Figure 5.8: Lack of, or weak, effect of D2-like receptor antagonists. A. Pre-application of the D1 antagonist SCH23390 (2 μM) prevented the SKF38393 (10 μM) induced increase in STN firing rate. **B. C.** Pre-application of sulpiride (10 μM) or eticlopride (10 μM) had no effect or a weak effect on the quinpirole induced increase in STN firing rate respectively.

5.2.9. Current-clamp recordings of the action of dopamine

Following the extracellular studies presented above, the action of dopamine was studied using the whole-cell technique in order to describe the specific membrane effects and, in particular, the modulation of intrinsic ionic conductances. In all experiments 0.5 mM EGTA was included in the patch pipette.

The effect of dopamine (30 μM) on membrane potential was studied in 12 STN cells in current-clamp configuration. Dopamine increased the firing rate from 0.68 ± 0.42 Hz to 8.58 ± 2.32 Hz in 4 regular firing cells, while in a further 3 cells, initially quiescent, action potentials were induced at a rate of 1.65 + 1.39 Hz. In a further 2 cells a membrane depolarisation of +4 and +5mV was observed; while in 3 cells dopamine had no effect. Unlike the study of Tofigy *et al.*, (2003) the nature of the dopamine effect did not correlate with the series resistance.

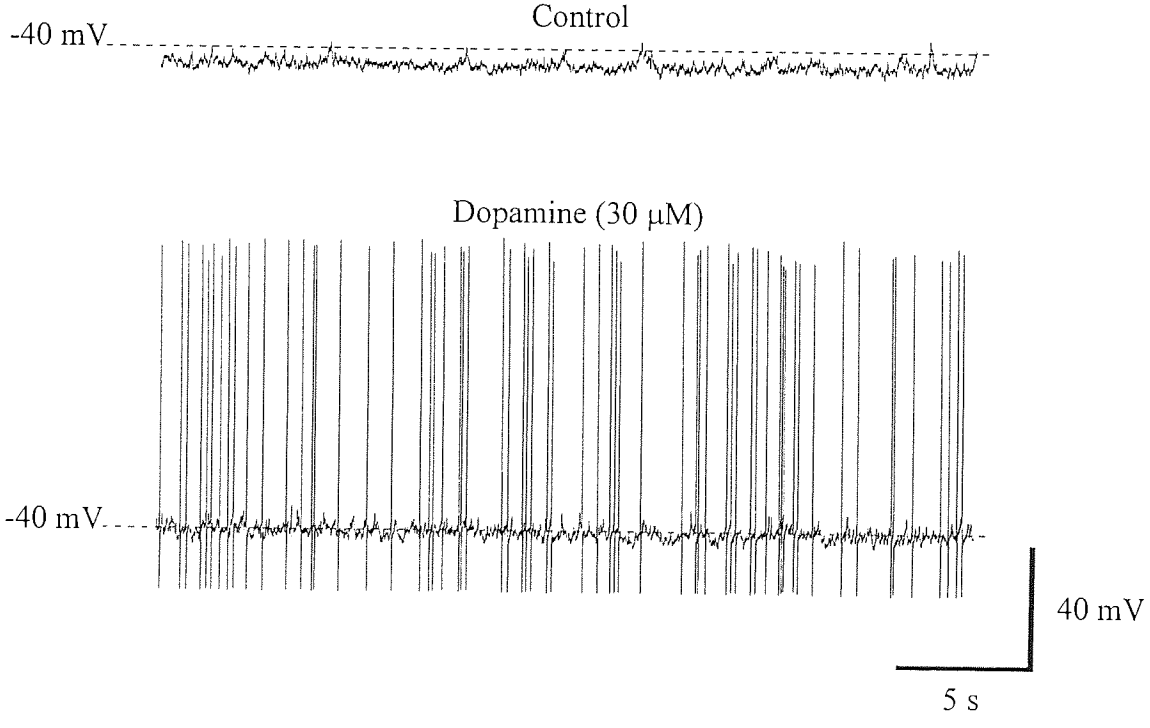

Figure 5.9: Dopamine induced depolarisation and action potential firing in STN cells.

5.2.10. Voltage-clamp protocol used to examine the effect of dopamine

In voltage-clamp, membrane currents were evoked from a holding potential of -60 mV, in a series of 500 ms duration voltage steps (incremented by 5 mV), from -130 mV to -40 mV. Instantaneous currents were measured as the difference between the holding current and the current measured immediately after the initial capacitive transient. I_h currents were measured as the difference between the instantaneous current and the steady state current measured at the end of the voltage step (figure 5.10).

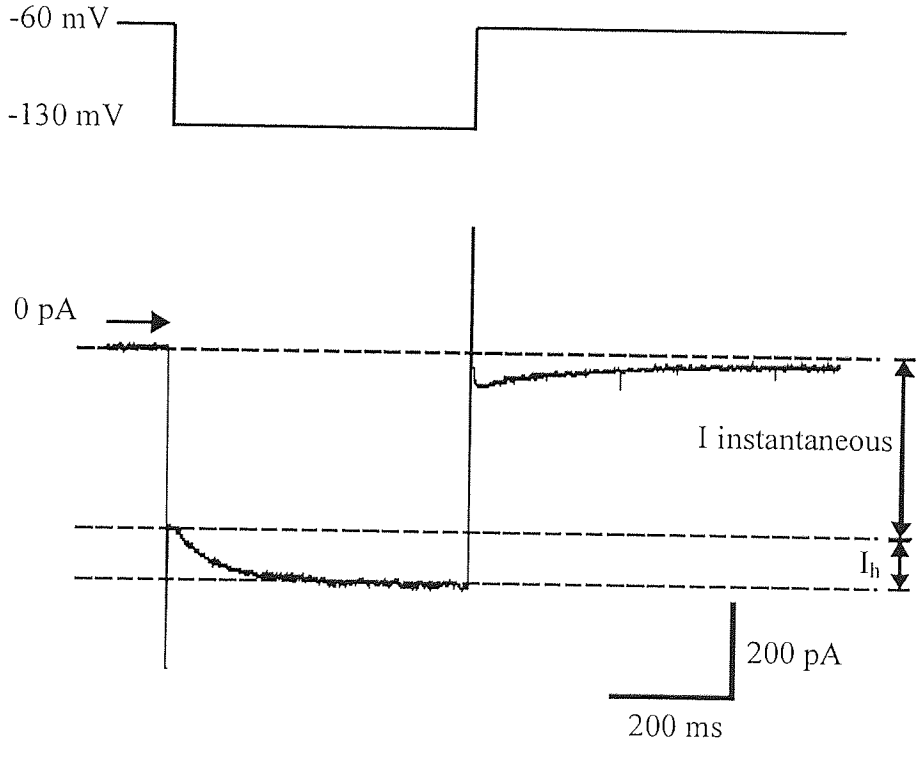

Figure 5.10: Measurement of instantaneous current and I_h using step voltage clamp recordings. Membrane currents (bottom) were evoked from a holding potential of -60 mV in response to a current step from -130 mV of 500 ms duration (top). Note the criteria used to measure the instantaneous current and the I_h current.

5.2.11. Voltage clamp recordings of the effect of dopamine

Consistent with a depolarising action of dopamine observed using extracellular and current clamp recordings, at a holding potential of -60 mV dopamine (30 μM) produced an inward shift in the holding current of -52 ± 17 pA in all cells tested (P=0.01, n=10). Instantaneous current-voltage relationships revealed that dopamine produced two types of conductance change. In 9 of 10 cells, dopamine increased the slope of the current-voltage relationship indicating an increase of conductance which reversed at -68 mV (figure 5.11). In 1 of 10 cells, dopamine decreased the slope of the current-voltage relationship indicating a reduction of conductance which reversed at -80 mV.

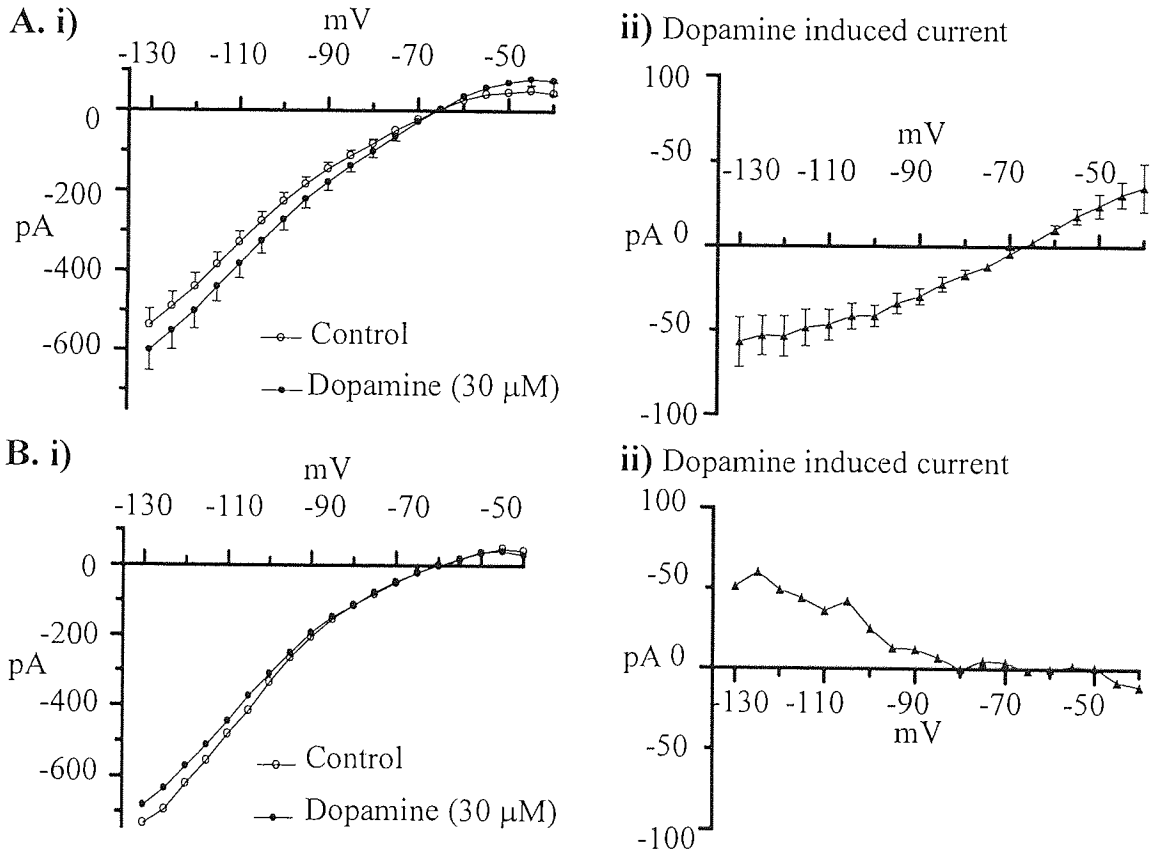

Figure 5.11: Dopamine produced two types of conductance changes. Instantaneous current-voltage relationships in control (open circles) and dopamine (30 μM) (filled circles) and dopamine induced currents (triangles). **A.** Pooled data showing that dopamine increased membrane conductance which reversed at -68 mV (9 of 10 cells) **B.** In 1 of 10 cells, dopamine decreased membrane conductance which reversed at -80 mV.

5.2.12. Ramp voltage clamp protocol used to examine the effect of dopamine

To aid further in the identification of the currents modulated by dopamine, membrane currents were evoked using a ramp protocol. From a holding current of -60 mV, membrane currents were evoked by a step hyperpolarisation to -140 mV followed by a ramp depolarisation (50 mV/s) up to -20 mV. Then, the membrane potential was immediately stepped back to the holding potential of -60 mV (figure 5.12).

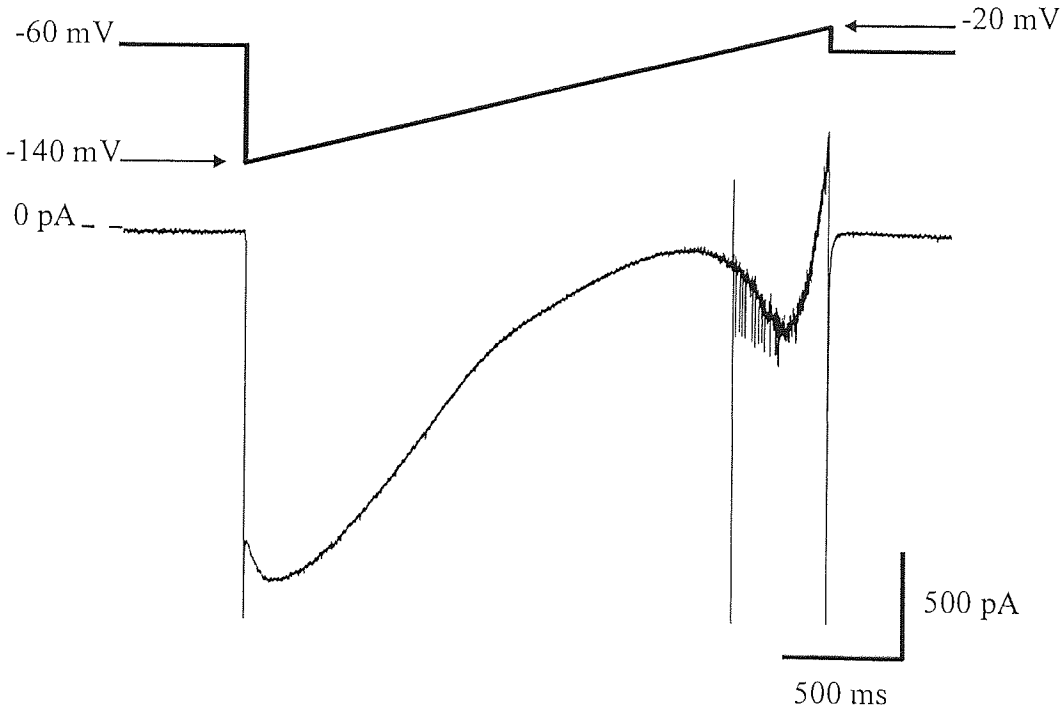

Figure 5.12: Measurement of membrane currents using voltage ramps. Membrane currents were evoked by a 50 mV/s ramp from -140 mV to -20 mV from a holding potential of -60 mV. Note the inward current and action currents observed at depolarised potentials.

5.2.13. Ramp voltage clamp recordings of the effect of dopamine

In order to avoid activation of action currents, recordings were made in the presence of TTX (1 μM). Bath application of dopamine (30 μM) induced an inward current of -67.1 ± 10.6 pA at a holding potential of -60 mV (n=17). This inward current was accompanied by an increase in conductance of 0.89 ± 0.18 pS which reversed at -33.7 ± 2.6 mV (n=12 of 17 cells, figure 5.13A). In two cells, an inward current was accompanied by a decrease in conductance of 1.2 nS and 1.44 nS which reversed at -108 mV and -87.3 mV respectively close to the theoretical reversal potential of potassium -105 mV, consistent with the closure of a potassium conductance (figure 5.13B). In three cells the inward current was accompanied by no change in conductance and no reversal was observed over the voltage range tested.

5.2.14. Action of SKF38393 and quinpirole in ramp voltage clamp recordings

Using the voltage ramp protocol, application of the D1-like agonist SKF38393 (10 μM) induced an inward current of -51.1 ± 15.2 pA at a holding potential of -60 mV (n=10). In 9 of 10 cells (in one cell there was no effect), the inward current was accompanied by an increase in conductance of 0.94 ± 0.14 nS which reversed at -38.6 ± 4.8 mV (figure 5.14A). Application of the D2-like receptor agonist quinpirole (10 μM) induced an inward current of -69.3 ± 13.8 pA at a holding potential of -60 mV accompanied by a decrease in conductance of -3.1 ± 0.61 nS which reversed at -97.4 ± 8 mV (n=4, figure 5.14B).

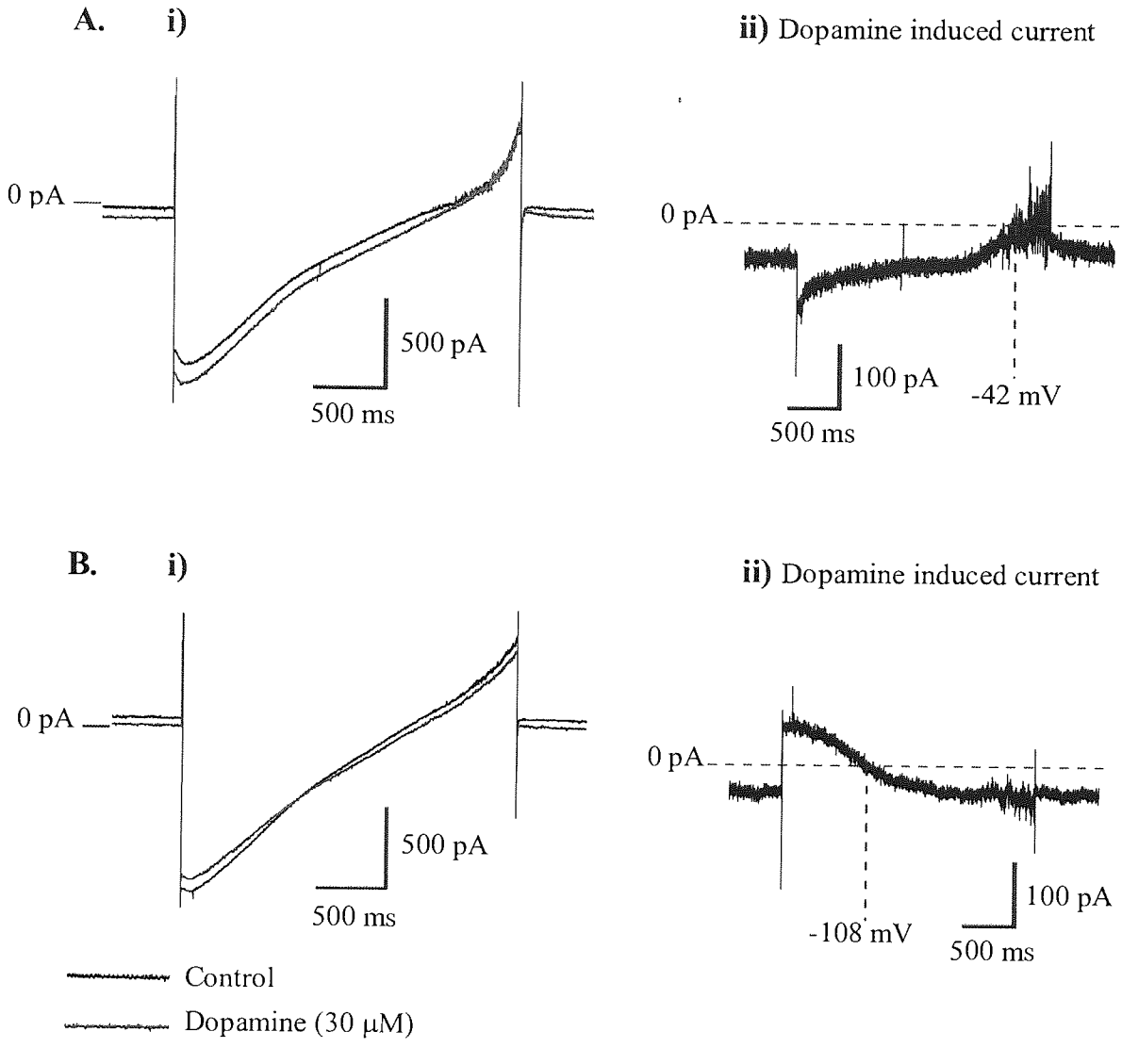

Figure 5.13: Dopamine produced two types of conductance changes. Current traces are shown in control (black) and in the presence of dopamine (red). **A.** Representative example of dopamine (30 μM) causing an inward shift in the holding current which is accompanied by an increase in conductance which reversed at -42 mV. **B.** In one cell dopamine induced an inward shift of the holding current which was accompanied by a decreased in the conductance which reversed at -108 mV.

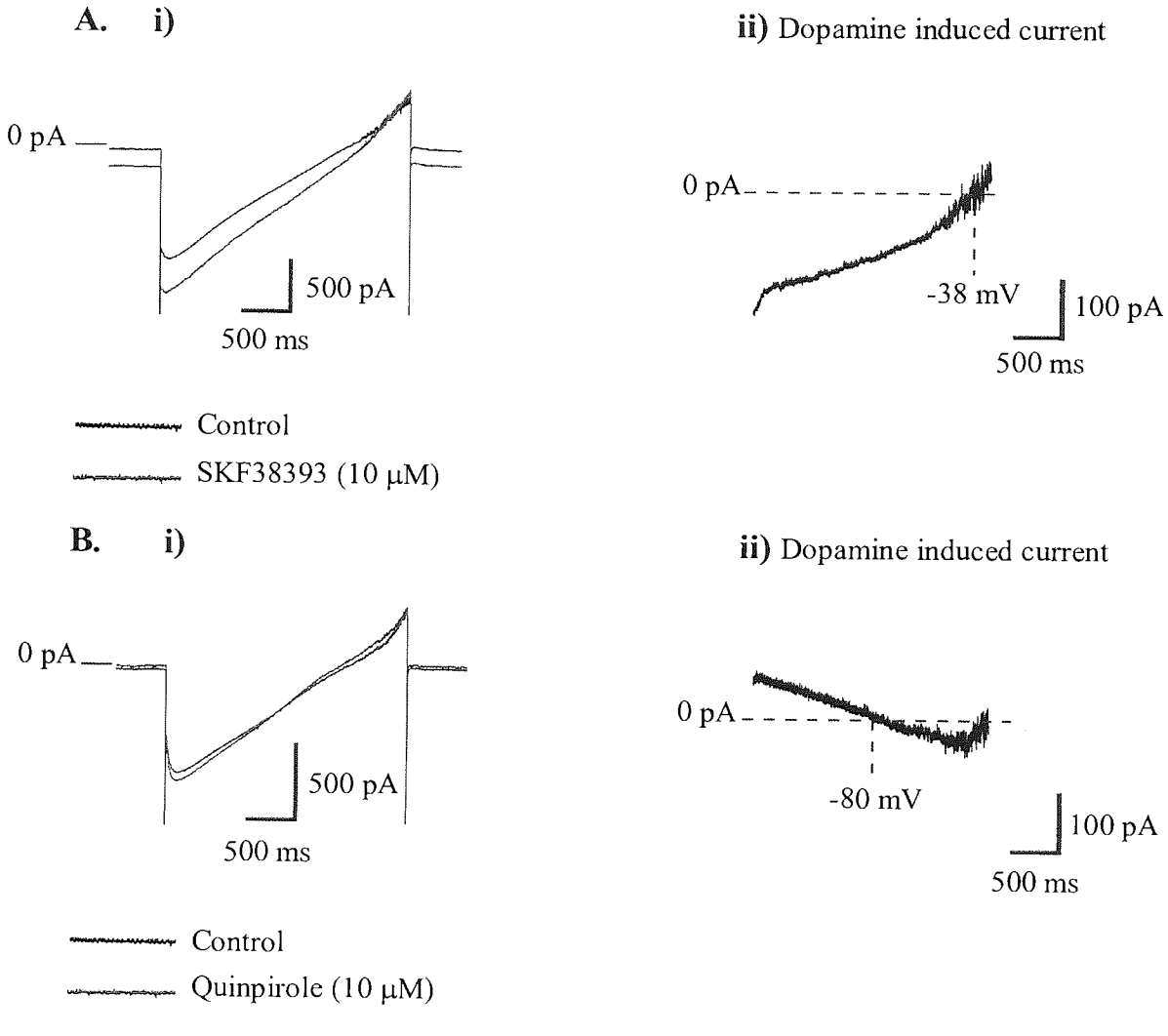

Figure 5.14: SKF38393 and quinpirole mimicked dopamine induced conductance changes. Current traces are shown in control (black) and in the presence of D1-like receptor agonists (red). A. The D1-like receptor agonist SKF38393 (10 μM) caused an inward shift in the holding current which is accompanied by an increase in conductance which reversed at -38 mV. B. The D2-like receptor agonist quinpirole (10 μM) induced an inward shift of the holding current which was accompanied by a decrease in the conductance which reversed at -80 mV.

5.2.15. Dopamine modulation of I_h in voltage clamp recordings

It was noted from membrane currents induced by the ramp protocols that application of either dopamine or SKF38393 reduced the time- and voltage- dependent current, I_h. This is clearly evident at the initial segments of the subtracted current-voltage relationships and is probably responsible for the non-linear conductance over the voltages tested (see figure 5.13). The reduction in I_h was confirmed by using a step protocol from holding potential of -60 mV first to -125 mV and then in 5 mV incremental steps back to -60 mV. I_h was recorded at all potentials more negative than -65 mV with dopamine significantly inhibiting this current at all membrane potential less than -80 mV (figure 5.15B). In many studies a reduction in I_h is accompanied by a change of voltage dependency (McCormick & Pape, 1990b). However, in this study I_h conductance was only reduced at potentials less than -80 mV (figure 5.15C).

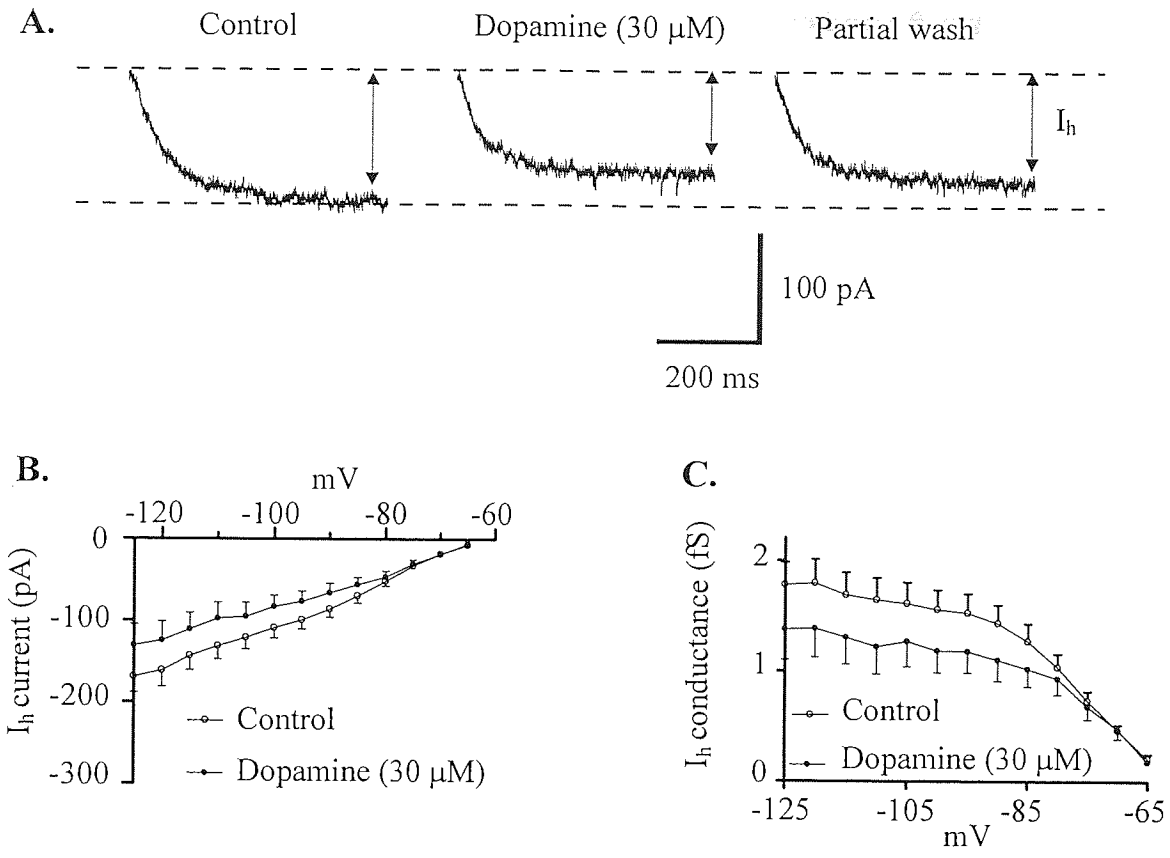

Figure 5.15: Dopamine reduced the amplitude of I_h current. A. Current traces at a holding potential of -125 mV showing that dopamine (30 μM) reduced I_h amplitude. **B.** Current-voltage relationship (n=10) showing I_h current in control (open circles) and in the presence of dopamine (filled circles). Note the reduction in I_h amplitude by dopamine. **C.** I_h conductance as a function of membrane potential in control and dopamine. I_h conductance (g) was calculated using the following formula:
g=I_h amplitude (1/(command potential- estimated reversal potential of I_h)). The reversal potential was estimated to -30 mV.

5.2.16. Action of dopamine on the NMDA/apamin induced burst firing

The effect of dopamine on the burst activity induced by NMDA and apamin was investigated. The action of dopamine (30 μM) on the NMDA/apamin induced burst firing was examined in 10 STN cells using single-unit extracellular recordings. In 5 of these cells, the firing pattern switched from burst to tonic regular/firing upon dopamine application. These cells initially had an oscillatory frequency of 0.99 ± 0.29 Hz, with 29.11 ± 4.09 spikes per burst and a mean ISI within burst of 11.06 ± 3.08 ms which reverted to tonic firing at 36.52 + 3.75 Hz upon the addition of dopamine (figure 5.16). In the remaining 5 cells, application of dopamine had no effect on the bursting parameters.

The action of dopamine (30 μM) on the NMDA/apamin induced burst was studied in 7 STN cells using the whole-cell recording technique in current-clamp mode. In 2 of 7 cells, a burst pattern (as detected by the algorithm of Kaneoke & Vitek, (1996)) became tonic upon dopamine application (figure 5.17). In the remaining 5 cells dopamine had no effect on the oscillatory frequency (n=5, P=0.25), the number of spikes per burst (n=5, P=0.62) and the average ISI within burst (n=5, P=0.62). In addition, the effect of dopamine on TTX-resistant plateau potentials underlying the burst activity (see chapter 4) was examined. Dopamine (30 μM) induced an increase in the frequency of the plateaus while decreasing their amplitude as a result of membrane depolarisation and this was reversible by direct hyperpolarisation (n=2, figure 5.17).

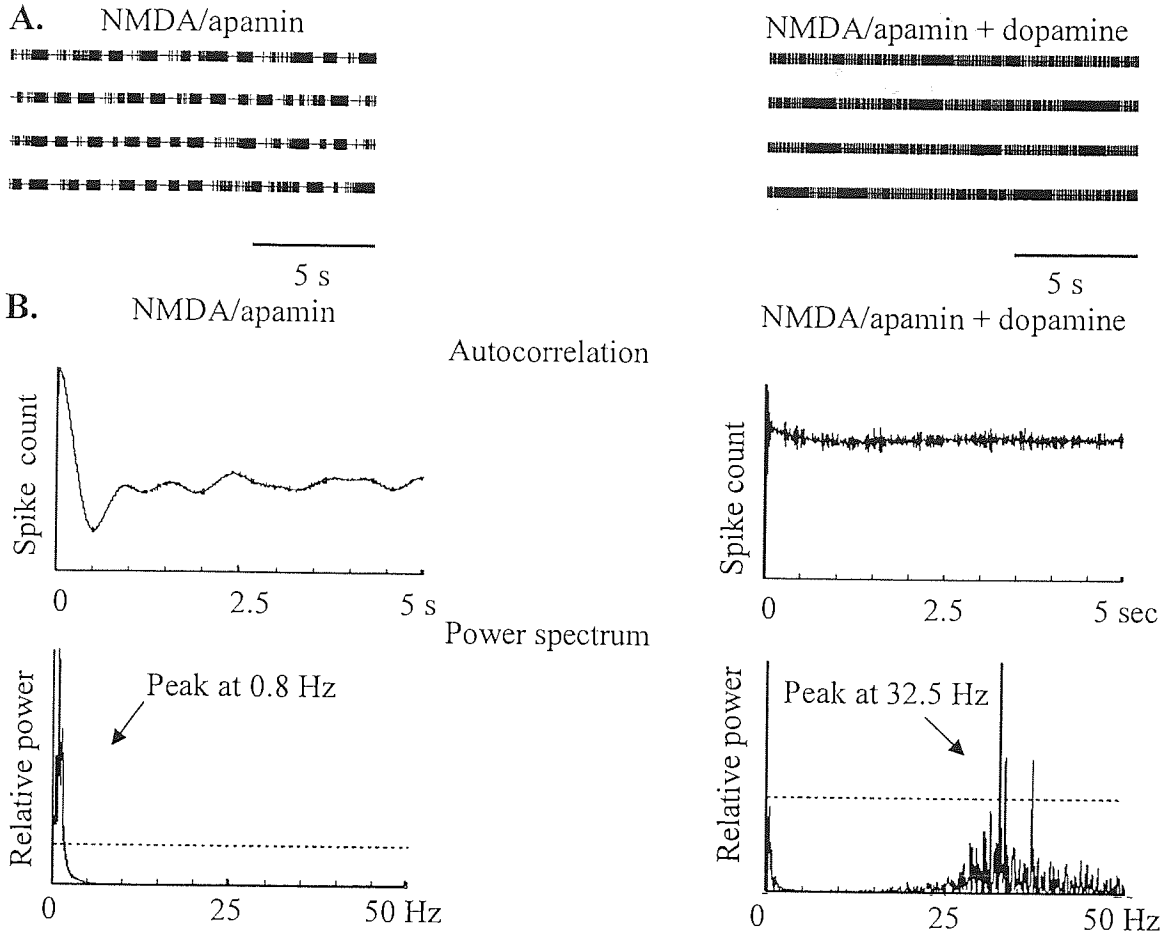

Figure 5.16: Dopamine attenuated the burst-firing induced by NMDA and apamin. **A.** Discharge recordings showing that dopamine switched burst-firing into a regular discharge. **B.** Autocorrelogram (top) and Lomb power spectrum (bottom) showing that dopamine reduced the burst oscillatory frequency inducing tonic activity at 32.5 Hz. Dashed lines represent a significance level of $P< 0.05$.

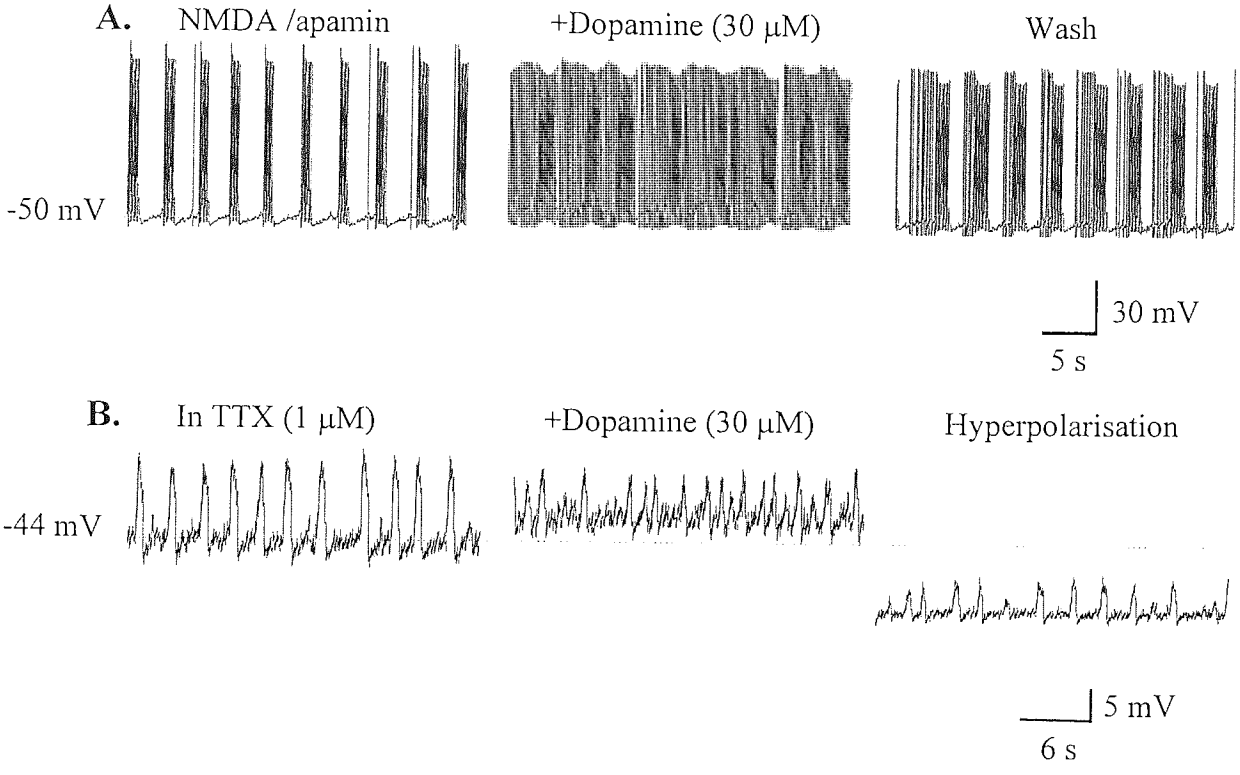

Figure 5.17: Dopamine attenuated burst-firing induced by NMDA and apamin. A. Whole-cell recording showing burst-firing in before, during application of dopamine (30 μM) and following the washout. Note that dopamine changed the pattern of the burst activity. **B.** TTX-resistant plateau potentials underlying the burst activity showing that dopamine increases their frequency and reduced their amplitude as a result of a depolarising effect. Note that this effect is partially reversible upon membrane hyperpolarisation.

5.3. Discussion

5.3.1. Pharmacology of the dopamine induced excitation

In support of previous studies (Mintz *et al.*, 1986; Tofighy *et al.*, 2003; Cragg *et al.*, 2004), dopamine caused an excitation of STN cells. This was due to a direct (post-synaptic) membrane depolarisation, independent of glutamate or GABA synaptic activity.

In the mouse slice, the action of dopamine was mediated through D1-like and D2-like receptors as it was mimicked by SKF38393 and quinpirole respectively. However, as in the rat STN (Tofighy *et al.*, 2003), D2 antagonists did not block the excitation observed. Dopamine receptor pharmacology within the STN is particularly puzzling because it is not sensitive to the classical agonists and antagonists (Shi *et al.*, 1997; Tofighy *et al.*, 2003). Previous studies have found 1) no effect of D2 agonists (Kreiss *et al.*, 1996, 1997), 2) no effect of D1 agonists (Zhu *et al.*, 2003; Tofighy *et al.*, 2003) and 3) no effect of the D2 antagonists sulpiride or eticlopride (Tofighy *et al.*, 2003, and this study). The lack of effect of D2 antagonists could be explained by the results shown in figure 5.4 in which SKF38393 occludes the effect of quinpirole. If this is the case, only a D1 receptor response would be observed and D2 antagonists would have little effect. Furthermore, dopamine produced a mean conductance increase of 0.89 nS comparable to the average increase in conductance of 0.94 nS induced by SKF38393, whereas quinpirole produced a mean conductance decrease of 3.1 nS.

Spontaneous release of dopamine has been demonstrated in rat STN slice up to 50 nM (Cragg *et al.*, 2004). As the EC_{50} for dopamine at D2, and D3 receptors (Werner *et al.*, 1996; Levant, 1997) are 200-500 nM and for D1 receptors in high nM to low μM range (Demchyshyn *et al.*, 2000), a small degree of tonic activation of D1 and D2 receptors might be expected.

5.3.2. Ionic conductances involved in the dopamine induced excitation

The dopamine induced depolarisation involved two ionic mechanisms. Indeed, the coupling of dopamine receptors to dual mechanisms is not unusual and has been observed in striatal cholinergic cells (Aosaki *et al.,* 1998) and has been suggested in other neurotransmitter systems including 5-HT, noradrenalin, and substance P (Larkman and Kelly 1992; Shen & North, 1992a, 1992b; Koyano *et al.,* 1993; Guerineau *et al.*, 1994, 1995; Aosaki & Kawaguchi, 1996). In addition, there may be two STN neuronal populations with respect to the expression and function of dopamine receptors.

In the majority of cells, application of dopamine produces an increased conductance which reverses around -34 mV. In only two cells, a decrease in conductance was observed which reverses around the theoretical potassium reversal potential (-105 mV). A previous study has showed a dopamine induced depolarisation in the STN which was due to a D2 receptor mediated decrease in potassium conductance (Zhu *et al.,* 2002). Indeed, the dopamine induced decrease of membrane conductance was mimicked by the D2-like receptor agonist quinpirole. However, in most cells, the effect of dopamine was mimicked by SKF38393. This action was blocked by SCH23390 and flufenamic acid, an inhibitor of cation channels, indicating a dopamine D1-receptor mediated increase of a non-specific cation conductance (Stanford IM, unpublished observations). In addition, experiments in mice, rats and using the efficient calcium chelator BAPTA (10 mM) revealed consistent observations suggesting the lack of calcium dependency of the dopamine induced cation current.

Thus, in mouse STN, dopamine acts mainly through D1 receptors via an increase in a calcium independent non-specific cation conductance. This result is in agreement with a recent work showing a D1 mediated increase of firing rate in STN slices (Baufreton *et al.,* 2005) but in contrast to previous studies revealing a lack of effect of D1 receptor agonists (Zhu *et al.,* 2002, Tofighy *et al.,* 2003). It is interesting to note that the effect of D1 receptor agonists becomes significant upon dopamine depletion (Zhu *et al.,* 2002), suggesting an alteration of dopamine receptor pharmacology following long-term dopamine depletion.

5.3.3. Effect of dopamine on I_h

This study provides evidence of a dopamine mediated reduction in I_h amplitude in STN cells. Reduction of I_h by dopamine is not unprecedented and has been shown in cells of the rat VTA (Jiang *et al.,* 1993) and in rod photoreceptors (Akopian & Witkovsky, 1996). However, a dopamine mediated increase in I_h has been observed in other cell types such as in the cells of layer V of enthorinal cortex (Rosenkranz & Johnston, 2006) and in layer I interneurones of the cortex (Wu & Hablitz, 2005) or in rat lateral geniculate nucleus (Govindaiah & Cox, 2005).

The anomalous inward rectifier I_h has been known to contribute to the resting membrane potential and cell excitability in many cell types (McCormick & Pape, 1990a). However, in STN cells, I_h current has been shown not to be involved in the generation of spontaneous membrane oscillations (Bevan *et al.,* 1999) suggesting that I_h has no effect at membrane potentials close to the resting state. However, I_h would have the tendency to limit membrane hyperpolarisation and this property would be enhanced in the dopamine depleted state and may therefore contribute to the recruitment of rebound firing and thus promote correlated activity. In addition, I_h may also contribute to synaptic integration of excitatory inputs.

5.3.4. Effect of dopamine on the burst induced by NMDA and apamin

In this study, dopamine induced a membrane depolarisation such that the patterned activity of the pharmacologically induced burst (by NMDA and apamin) tends towards a tonic activity. This effect appears to be due to the modulation of underlying TTX-resistant plateau potentials. Thus, dopamine appears to depolarise the membrane potential out the voltage range for burst firing activity and into a range favouring tonic activity. This observation is in agreement with membrane depolarisation increasing the regularity of firing of STN cells (Beurrier *et al.,* 1999) and the ability of dopamine to regularise the irregular firing pattern of STN cells in slices from 6-OHDA-lesioned rats (Zhu *et al.,* 2002a). Furthermore, dopamine D1- and D2- like agonists have previously

been shown to affect the pattern of spontaneous or evoked burst activity (Baufreton *et al.*, 2003, 2005).

5.4. Action of 5-HT on extracellular single-units recorded in the STN

5.4.1. 5-HT in the STN

5-HT receptors are classified into seven receptor families (5-HT_{1-7} receptors). 5-$HT_{1, 2, 4-7}$ receptors are seven transmembrane G-protein coupled receptors while 5-HT_3 receptors are a ligand-gated ion channel (Barnes & Sharp, 1999). 5-HT projections from the dorsal raphe nucleus to the STN appear as a fine, evenly distributed network (Mori *et al.*, 1985). Receptor binding and mRNA for many of the 14 characterised 5-HT receptors have been found in BG (Poppeiano *et al.*, 1994) including 5-HT_{1A}, 5-HT_4 and 5-HT_{2C} receptors in the STN, modulation of which has previously reported to have potential therapeutic benefit in PD and other movement disorders (Nicholson & Brotchie, 2002). In addition, antagonists of the 5-HT_{1A} receptor suppress levodopa induced dyskinesia in animal models (Bibbiani *et al.*, 2001) while antagonism at the $5HT_{2C}$ receptor reduces orofacial dyskinesias (Eberle-Wang *et al.*, 1996; Barwick *et al.*, 2000). Furthermore, antagonism at 5-HT receptors is thought to make a major contribution to the low incidence of extra-pyramidal side effects observed with atypical neuroleptics (Mehta *et al.*, 2001).

Previous *in vitro* studies have reported that 5-HT induced excitations of STN activity were blocked by the non-selective 5-HT_2 antagonist mianserin (Flores *et al.*, 1995) and more recently by 5-HT_{2C} and 5-HT_4 receptor antagonists (Xiang *et al.*, 2005). However, mixed excitatory/inhibitory responses and inhibitory responses alone were also noted (Flores *et al.*, 1995), and these remain uncharacterised.

5.4.2. 5-HT induced excitations and inhibitions of STN cells

The effect of 5-HT was examined in STN cells using extracellular recordings. In most STN cells (n=19 of 21, 90 %), 5-HT application produced a dose-dependent

increase in firing rate with an EC_{50} of approximately 2.7 μM and a maximum increase of 216 % (figure 5.18). In two cells (10 %), 5-HT (3 and 30 μM) induced an inhibition which was prevented by pre-application with the $5\text{-}HT_{1A}$ antagonist WAY100135 (1 μM, not shown).

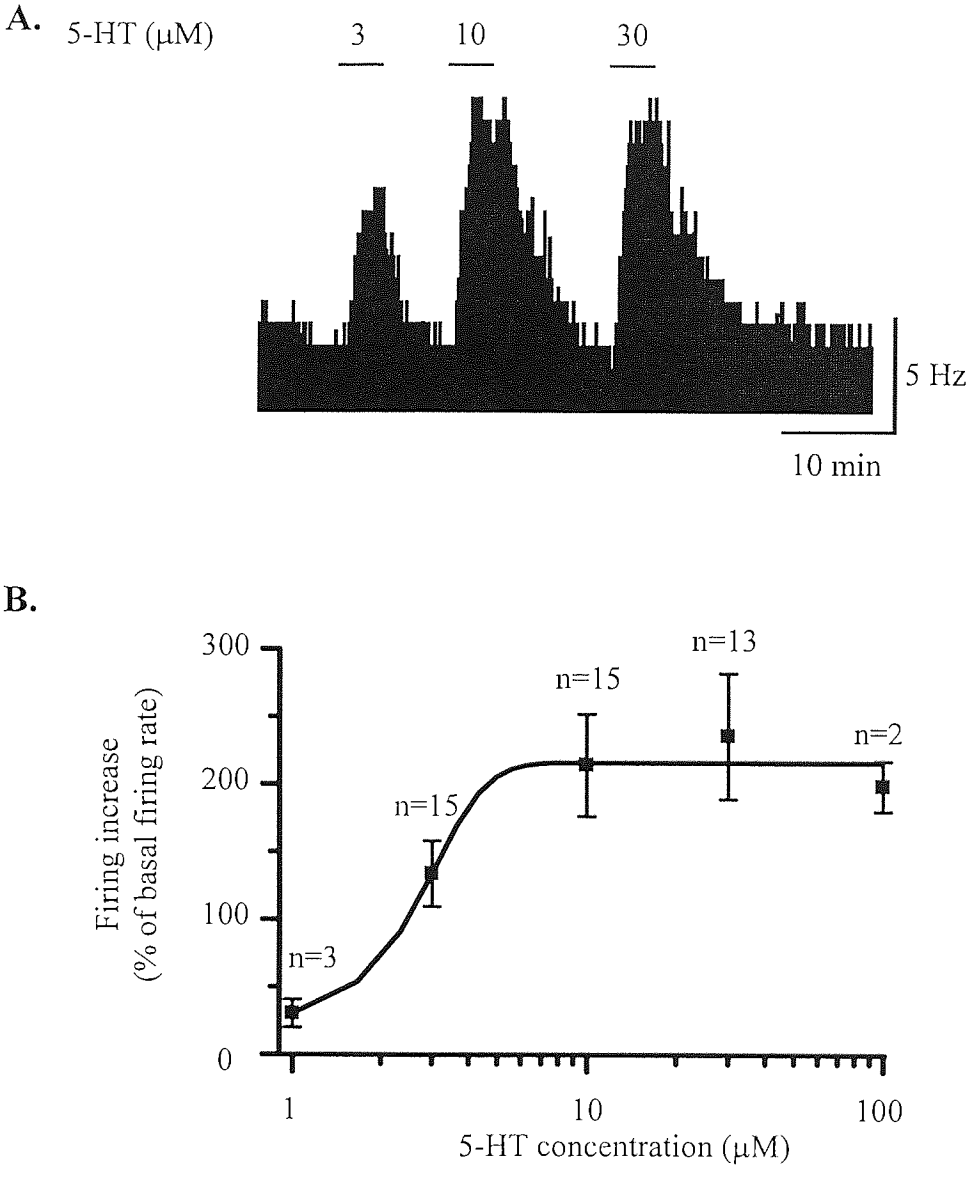

Figure 5.18: 5-HT induced excitation of STN neurones. A. Rate-meter recording of STN cell activity showing that 5-HT increased STN firing rate. B. Dose-response curve showing a dose-dependent increase in firing rate with an EC_{50} of 2.7 μM and a maximum response of 216 %.

5.4.3. Pharmacology of 5-HT in STN cells

The pharmacology of 5-HT induced excitation and inhibition was investigated using antagonists of 5-HT_{2C} receptors (RS102221, 500 nM), 5-HT_4 receptors (GR113808, 500 nM) and 5-HT_{1A} receptors (WAY100135, 1 μM). Previous studies in this laboratory have shown that the excitation induced by 5-HT was mimicked by the non-selective 5-HT_2 receptor agonist α-methyl-5-HT (10 μM). The 5-HT excitation was found to be partially inhibited by the 5-HT_{2C} antagonist RS102221 (500 nM). RS102221 also reduced the excitatory effect of α-methyl 5-HT (a non selective 5-HT_2 agonist).

The receptor mediating the remaining excitation was investigated using GR113808 (500 nM), an antagonist at 5-HT_4 receptors (figure 5.18). Significant differences were only observed using 5-HT at 10 μM. RS102221 (500 nM) alone reduced the excitation induced by 5-HT (10 μM) by 79.3 ± 12.3 % (P=0.03, n=6), GR113808 (500 nM) alone reduced the response to 5-HT (10 μM) by 49.7 ± 11.2 % (P= 0.016, n=6), Co-application of both antagonists reduced the excitation induced by 5-HT (10 μM) by 108.6 ± 18.3 % (P=0.0007, n=6) (see Stanford *et al.*, 2005 for the full study).

5.4.4. Discussion

5-HT application in STN produced concentration-dependent increases in firing rate in most STN cells, and inhibition in a very small proportion of cells. The excitatory effect was mediated mainly by 5-HT_{2C} receptors with a small contribution made by 5-HT_4 receptors while the inhibitory effect was mediated by the 5-HT_{1A} receptor. This study conflicts with that of Xiang *et al.*, 2005 who reported the majority of the excitation to be mediated by 5-HT_4 receptors. In summary, these results indicate that 5-HT induced excitation and inhibition in the STN are separate entities and most likely to arise as a consequence of independent, direct postsynaptic receptor mediated effects at 5-HT_{2C}, 5-HT_4 and 5HT_{1A} receptors. Furthermore, the combined action of RS102221 and GR113808 in blocking 5-HT induced excitation and the block of the inhibitory

responses by WAY100135 revealing excitation which was subsequently reduced by RS102221, indicates that more than one 5-HT receptor subtype may be expressed on individual STN neurones. Thus, there may well be sub-populations of STN cells which may be classified according to their 5-HT receptor complement.

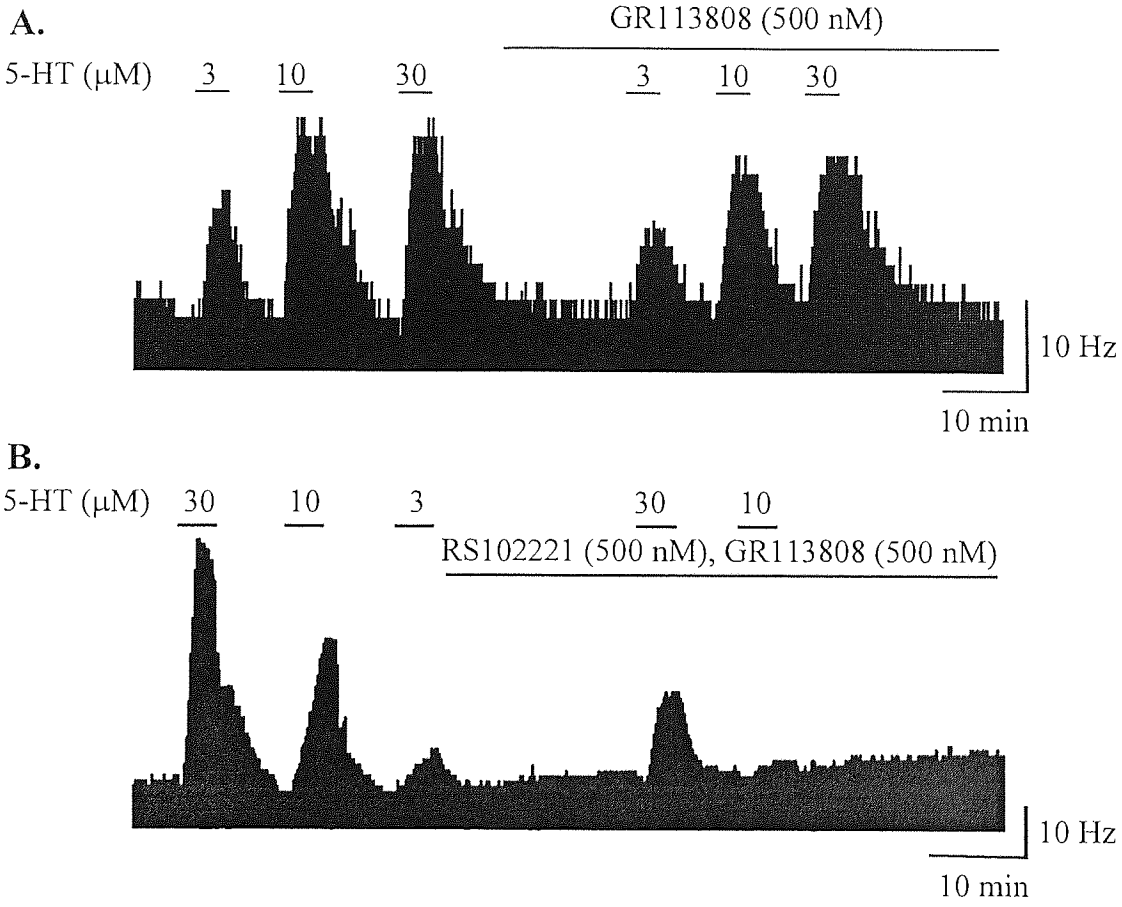

Figure 5.19: RS102221 and GR113808 antagonised the effect of 5-HT. A. Rate-meter recording showing that the excitatory effect of 5-HT is slightly reduced by the application of the 5-HT_4 antagonist GR113808 (500 nM). **B.** Rate-meter showing that co-application of the RS102221 (500 nM) and GR113808 further reduced the 5-HT response.

CHAPTER 6. General discussion

6.1. Relevant questions concerning the pattern of activity in BG

The classical model of BG function has been used to understand movement disorders such as PD (Alexander & Crutcher, 1990). However, one important limitation of this model is that it is based upon the rate rather than the pattern of firing. As the only glutamatergic excitatory nucleus within the BG, the STN and its integration with the inhibitory GP has received particular attention with regard to the generation of patterned activity. This patterned activity correlates with the PD symptoms of rigidity and akinesia (Nini *et al.,* 1995). Moreover, the STN has been implicated in the generation of pathological oscillations as surgical lesion or DBS relieves the symptoms. In order to understand further the function of BG in both the normal and the pathological state, important questions remain. These questions may include 1) By what mechanisms do these oscillations arise in BG nuclei? 1) What oscillation frequencies are pathological? and 3) How are pathological oscillations facilitated by dopamine depletion?

6.2. A role for the cortex in the generation of oscillatory activity in the STN

Previous studies have indicated that regenerative oscillatory activity may arise in networks of reciprocally connected STN-GP neurones (Plenz & Kitai, 1999). Indeed, using rat organotypic co-culture, synchronous oscillatory activity at low frequency (around 1 Hz) between STN and GP has been observed while the proposed mechanism relied on the existence of (GP-derived) IPSPs driving rebound STN firing exciting the GP (Plenz & Kitai, 1999). This GP-driven rebound activity has been reproduced in rat slices containing STN and internal capsule (Bevan *et al.,* 2000, 2002).

This thesis describes the development of a mouse brain slice preparation which preserved functional connectivity between the STN and the GP and could directly test the proposed mechanism of Plenz & Kitai, (1999). The mouse STN was composed of a homogenous population of cells and the GP contained at least two cell types. Both STN and GP cells exhibited intrinsic membrane properties which may predispose them to

sustain regenerative bursting activity. However, although functional reciprocal connectivity was preserved, no spontaneous regenerative oscillatory activity between STN and GP was observed, both in control slices and in slices in which low frequency oscillatory burst-firing was pharmacologically induced (using bath application of NMDA and apamin). This burst firing appeared unaffected by GABA and glutamate antagonists consistent with its generation by intrinsic membrane properties. However, the lack of evidence for regenerative network activity in the mouse preparation may suggest that the network required for such an activity is not present within the slice and that other anatomical structures from cortico-BG-thalamo-cortical loop are required. Accordingly, *in vivo* experiments suggest that the cortex may drive synchronous activity in anaesthetised rodents (Magill *et al.*, 2000, 2001, 2004) whilst in awake rodents, cortical activity leads oscillatory activity in STN and GP (Magill *et al.*, 2005; Sharott *et al.*, 2005b).

Further evidence that the cortex itself having a major role in modulating activity within BG nuclei and in particular the STN comes from experiments in which transcranial magnetic stimulation of primary motor cortex which alleviates the parkinsonian symptoms in the MPTP-treated monkey (Drouot *et al.*, 2004) and PD patients (Pagni *et al.*, 2005) raising the possibility of future non-invasive therapies. Thus, future experiments may focus on the cortical input of STN such as motor cortex, pre-motor and somatosenory cortex. The ideal mechanistic studies would involve an *in vitro* preparation with maintained connectivity between the motor cortex and the STN, but this does not appear possible. However, studies on the frequencies of oscillation that may be sustained within superficial (layers I and II) and deep layers (V and VI) of the motor cortex are underway in our laboratory (Yamawaki N, personal communication).

6.3. Delta oscillations

Low frequency synchronous oscillations between STN and GP have been observed in organotypic co-culture (Plenz & Kitai, 1999) and anaesthetised dopamine-depleted rats (Magill *et al.*, 2000). However, in human and non-human primates,

synchronous neuronal oscillations occur at delta (4-10 Hz) and beta (10-30 Hz) and gamma (60-100 Hz) frequencies (Bergmann *et al.*, 1994; Nini *et al.*, 1995).

The 4-10 Hz oscillations appear to correlate with the frequency of muscle tremor in PD (Bergman *et al.*, 1994; Hutchison *et al.*, 1997) although oscillations at this frequency can be observed in the absence of clinical symptoms (Levy *et al.*, 2001). Interestingly, surgical targeting of the thalamus has positive benefits in the relief of tremor (see Krack *et al.*, 1999 for review) implicating neuronal activity (and possible spindle activity, Bal *et al.*., 1995) within the thalamus as the source of this pathology.

6.4. Beta oscillations: physiological or pathological?

Synchronous beta (10-30 Hz) oscillations occur in sensorimotor, pre-motor and primary motor cortex (Murthy & Fetz; 1992; Sanes & Donoghue, 1993; Engel *et al.*, 2001; Neuper & Pfurtscheller, 2001) and in many other brain areas. However until recently, no evidence of beta oscillations was found in BG (Nini *et al.*, 1995; Bergman *et al.*, 1998; Raz *et al.*, 2001). However, using local field potential recordings, *beta* oscillations have been observed in healthy monkeys (Courtemanche *et al.*, 2003), rats (Vorobyov *et al.*, 2003; Berke *et al.*, 2004) and patients without PD (Sochurkova & Rektor, 2003).

In patients with PD, synchronous beta (10-30 Hz) activity is more evident in the STN, pallidum and cortex (Brown *et al.*, 2001; Cassidy *et al.*, 2002) and constitutes a hallmark of the disease. There appears to be an inverse relationship between neuronal synchronisation at the beta frequency and motor function. In PD patients withdrawn from dopamine therapy, oscillations at beta frequencies between the STN, GPi, and cortex are prominent but are reduced by dopamine replacement therapy (Brown *et al.*, 2001; Levy *et al.*, 2002; Cassidy *et al.*, 2002), or DBS of the STN (Brown *et al.*, 2004), which both improve motor symptoms. Comparable changes are seen in awake 6-OHDA-lesioned rats as the power and coherence of beta oscillations in STN and cortex are increased compared to normal rats while apomorphine administration decreases the power and coherence of oscillatory activity (Sharott *et al.*, 2005a). Furthermore, STN stimulation at tremor and beta frequencies intensifies the symptoms of PD (Moro *et al.*,

2002; Timmerman *et al.*, 2004; Fogelson *et al.*, 2005). Conversely, beta oscillations also appear to be suppressed, prior to, and during voluntary movements (Cassidy *et al.*, 2002; Levy *et al.*, 2002a; Priori *et al.*, 2002) and are reduced following environmental cues informative of subsequent movement demands (William *et al.*, 2003; Williams *et al.*, 2005; Kuhn *et al.*, 2004; Doyle *et al.*, 2005).

6.5. Gamma oscillations: the motor carrier

Synchronous gamma (30-100 Hz) oscillations in cortex have been suggested to serve as a mechanism which allows the integration of spatially distributed sensory cortical networks (the so-called "binding" theory) (Brecht *et al.*, 1999; Neuenschwander *et al.*, 1999, 2002; Engel & Singer, 2001). Similarly, cortical synchronous gamma oscillations may carry motor information by linking spatially distributed sites involved in voluntary movement (Brown & Marsden, 2001). This activity is increased during motor preparation and focused attention (Pfurtscheller *et al.*, 1993) and coherent with a similar activity in the activated muscle (Brown *et al.*, 1998).

Gamma oscillations were detected in the STN of healthy rats (Brown *et al.*, 2002, Magill *et al.*, 2005) and PD patients treated with levodopa (Brown *et al.*, 2001). An increase in the power of LFP oscillations above 60 Hz is evident following voluntary movement (Cassidy *et al.*, 2002; Foffani *et al.*, 2003) and dopaminergic medication (Brown *et al.*, 2001) This gamma activity in BG is phase-locked to a similar activity in the motor cortex (Cassidy *et al.*, 2002; Williams *et al.*, 2002) suggesting the encoding of movement.

6.6. Dopamine in the STN

Following the discovery of direct nigro-subthalamic dopamine projection (Hassani *et al.*, 1997; Prensa *et al.*, 2000; Smith & Kieval, 2000) and evidence for D1- and D2-like dopamine receptors in the STN (Boyson *et al.*, 1986; Johnson *et al.*, 1994; Kreiss *et al.*, 1996; Flores *et al.*, 1999), the prevailing view that dopamine acts solely in the striatum has been re-evaluated.

This study has shown a direct postsynaptic dopamine mediated excitation of STN cells via D1- and D2-like receptors. The depolarisation was found to be mediated by two mechanisms. The first mechanism, involving an increase in membrane conductance, was mimicked by the D1 agonist SKF39393, an effect consistent with an increase of a non-specific cation conductance, while the second involved a decrease in a potassium conductance which was mimicked by the D2 agonist quinpirole. This latter D2-like effect is consistent with the work of Zhu *et al.,* (2002b), a study in which no D1-like effect was observed.

Dopamine also decreases the amplitude of I_h in STN cells. In many cell types, tonic activation of I_h is involved in setting the resting membrane potential at a relatively depolarised potential, although this has not been shown in the STN (Bevan *et al.,* 1999). I_h is known to be involved in mediating rhythmic activity of thalamo-cortical cells (McCormick & Pape, 1990b), thus it is that the enhanced I_h during dopamine depletion may favour oscillatory activity. An enhanced I_h would also have tendency to synchronise synaptic activity due to its voltage dependence which tends to depolarise upon membrane hyperpolarisation and inactivate upon membrane depolarisation. Thus, the decay time of large incoming hyperpolarising events (such as GABA) would be reduced, so tightening the temporal window over which summation of events may take place and thus allow enhanced synchronous rebound firing in a population of STN neurons. However, at least *in vitro,* experiments using dopamine depleted animals (with MPTP) only served to decrease and disrupt regular STN firing rate (Wilson *et al.,* 2005).

In the present NMDA/apamin pharmacological model of burst-firing activity in the STN, dopamine produced depolarisation and reduced the tendency to burst in favour of a more regular pattern of firing. Consistently, dopamine is known to regularise the irregular firing pattern of STN cells in slices from 6-OHDA-lesioned rats (Zhu *et al.,* 2002a) and from MPTP-treated mice (Stanford IM, unpublished observations) while quinpirole has been shown to regularise spontaneous burst-firing cells (Baufreton *et al.,* 2005). However, this study also indicates that D1 receptor agonists depolarise and increase STN firing rate while D5 receptors enhance burst firing (Baufreton *et al.,* 2005). Indeed, a previous study reported that it is D5 receptor activation which prolongs

the duration of plateau potentials underlying spontaneous burst firing in STN via an increase in L-type calcium conductance (Baufreton *et al.,* 2003).

In summary, the results presented in this thesis demonstrate that an *in vitro* slice preparation, which preserves STN-GP neuronal connectivity, cannot sustain regenerative oscillatory activity. This suggests that the mechanisms by which pathological oscillatory activity arises *in vivo* may be much more complex than a simple interaction between STN, excitatory - GP, inhibitory cells, and that other structures from the cortico-BG-thalamocortical loop are likely to be involved. This thesis also demonstrates that STN cells themselves can sustain oscillatory burst activity which is depedendent on intrinsic properties. Many intrinsic STN cell membrane conductances, including a non-specific cation conductance, a potassium conductance and I_h have been shown to be modulated by dopamine and this implies that STN cellular characterisitics may alter in the dopamine-depleted state. These data further support the view that dopamine has an important functional role outside of the striatum.

References

Abosch A., Hutchison WD., Saint-Cyr JA., Dostrovsky JO., & Lozano AM. 2002. Movement-related neurons of the subthalamic nucleus in patients with Parkinson disease. *J Neurosurg.* **97**, 1167-72.

Abbott A., Wigmore MA., & Lacey MG. 1997. Excitation of rat subthalamic nucleus neurones in vitro by activation of a group I metabotropic glutamate receptor. *Brain Res.* **766**, 162-7.

Aguirre JA., Kehr J., Yoshitake T., Liu FL., Rivera A., Fernandez-Espinola S., Andbjer B., Leo G., Medhurst AD., Agnati LF., & Fuxe K. 2005. Protection but maintained dysfunction of nigral dopaminergic nerve cell bodies and striatal dopaminergic terminals in MPTP-lesioned mice after acute treatment with the mGluR5 antagonist MPEP. *Brain Res.* **1033**, 216-20.

Aghajanian GK., & Rasmussen K. 1989. Intracellular studies in the facial nucleus illustrating a simple new method for obtaining viable motoneurons in adult rat brain slices. *Synapse.* **3**, 331-8.

Akopian A., & Witkovsky P. 1996. D2 dopamine receptor-mediated inhibition of a hyperpolarization-activated current in rod photoreceptors. *J Neurophysiol.* **76**, 1828-35.

Albin RL., Young AB., & Penney JB. 1989. The functional anatomy of basal ganglia disorders. *Trends Neurosci.* **12**, 366-75.

Alexander GE., & Crutcher MD. 1990. Functional architecture of basal ganglia circuits: neural substrates of parallel processing. *Trends Neurosci.* **13**, 266-71.

Alexander GE., Crutcher MD., & Delong M R. 1990. Basal ganglia-thalamocortical circuits: parallel substrates for motor, oculomotor, "prefrontal" and "limbic" functions. *Prog. Brain Res.* **85**, 119-46.

Allers KA., Kreiss DS., & Walters JR. 2000. Multisecond oscillations in the subthalamic nucleus: effects of apomorphine and dopamine cell lesion. *Synapse.* **38**, 38-50.

Allers KA., Bergstrom DA., Ghazi LJ., Kreiss DS., & Walters JR. 2005. MK-801 and amantadine exert different effects on subthalamic neuronal activity in a rodent model of Parkinson's disease. *Exp Neurol.* **191**, 104-18.

Aosaki T., & Kawaguchi Y. 1996. Actions of substance P on rat neostriatal neurons in vitro. *J Neurosci.* **16**, 5141-53.

Aosaki T., Kiuchi K., & Kawaguchi Y. 1998. Dopamine D1-like receptor activation excites rat striatal large aspiny neurons in vitro. *J Neurosci.* **18**, 5180-90.

Aponte Y., Lien CC., Reisinger E., & Jonas P. 2006. Hyperpolarization-activated cation channels in fast-spiking interneurons of rat hippocampus. *J Physiol.* **574**, 229-43.

Araki T., Mikami H., Matsubara Y., Imai Y., Mizugaki M., & Itoyama Y. 2001. Biochemical and immunohistological changes in the brain of 1-methyl-4-phenyl-1,2,3,6-tetrahydropyridine (MPTP)-treated mouse. *Eur J Pharm.* **12**, 231-8.

Arbuthnott GW., & Crow TJ. 1971. Relation of contraversive turning to unilateral release of dopamine from the nigrostriatal pathway in rats. *Exp Neurol.* **30**, 484-91.

Arbuthnott GW., & Ungerstedt U.1970. Quantitative recording of rotational behavior in rats after 6-hydroxy-dopamine lesions of the nigrostriatal dopamine system. *Brain Res.* **24**, 485-93.

Arbuthnott GW., & Ungerstedt U. 1975. Turning behavior induced by electrical stimulation of the nigro-neostriatal system of the rat. *Exp Neurol.* **47**,162-72.

Arkadir D., Morris G., Vaadia E., & Bergman H. 2004. Independent coding of movement direction and reward prediction by single pallidal neurons. *J Neurosci.* **24**, 10047-56.

Awad H., Hubert GW., Smith Y., Levey AI., & Conn PJ. 2000. Activation of metabotropic glutamate receptor 5 has direct excitatory effects and potentiates NMDA receptor currents in neurons of the subthalamic nucleus. *J Neurosci.* **20**, 7871-9.

Bacci JJ., Absi el H., Manrique C., Baunez C., Salin P., & Kerkerian-Le Goff L. 2004. Differential effects of prolonged high frequency stimulation and of excitotoxic lesion of the subthalamic nucleus on dopamine denervation-induced cellular defects in the rat striatum and globus pallidus. *Eur J Neurosci.* **20**, 3331-41.

Bal T., & McCormick DA. 1993. Mechanisms of oscillatory activity in guinea-pig nucleus reticularis thalami in vitro: a mammalian pacemaker. *J Physiol.* **468**, 669-91.

Bal T., von Krosigk M., & McCormick DA. 1995. Synaptic and membrane mechanisms underlying synchronized oscillations in the ferret lateral geniculate nucleus in vitro. *J Physiol.* **483**, 641-63.

Bar-Gad I., Elias S., Vaadia E., & Bergman H. 2004. Complex locking rather than complete cessation of neuronal activity in the globus pallidus of a 1-methyl-4-phenyl-1,2,3,6-tetrahydropyridine-treated primate in response to pallidal microstimulation. *J Neurosci.* **24**, 7410-9.

Bar-Gad I., Heimer G., Ritov Y., & Bergman H. 2003. Functional correlations between neighboring neurons in the primate globus pallidus are weak or nonexistent. *J Neurosci.* **23**, 4012-6.

Barwick VS., Jones DH., Richter JT., Hicks PB., & Young KA. 2000. Subthalamic nucleus microinjections of 5-HT_2 receptor antagonists suppress stereotypy in rats. *Neuroreport.* **11**, 267-70.

Baufreton J., Garret M., Dovero S., Dufy B., Bioulac B., & Taupignon A. 2001. Activation of GABA(A) receptors in subthalamic neurons in vitro: properties of native receptors and inhibition mechanisms. *J Neurophysiol.* **86**, 75-85.

Baufreton J., Garret M., Rivera A., de la Calle A., Gonon F., Dufy B., Bioulac B., & Taupignon A. 2003. D5 (not D1) dopamine receptors potentiate burst-firing in neurons of the subthalamic nucleus by modulating an L-type calcium conductance. *J Neurosci.* **23**, 816-25.

Baufreton J., Zhu ZT., Garret M., Bioulac B., Johnson SW., & Taupignon AI. 2005. Dopamine receptors set the pattern of activity generated in subthalamic neurons. *Faseb J.* **19**, 1771-7.

Belforte JE., & Pazo JH. 2004. Turning behaviour induced by stimulation of the 5-HT receptors in the subthalamic nucleus. *Eur J Neurosci.* **19**, 346-55.

Belluscio MA., Kasanetz F., Riquelme LA., & Murer MG. 2003. Spreading of slow cortical rhythms to the basal ganglia output nuclei in rats with nigrostriatal lesions. *Eur J Neurosci.* **17**, 1046-52.

Benabid AL. 2003. Deep brain stimulation for Parkinson's disease. *Curr Opin Neurobiol.* **13**, 696-706.

Benabid AL., Benazzouz A., Limousin P., Koudsie A., Krack P., Piallat B., & Pollak P. 2000. Dyskinesias and the subthalamic nucleus. *Ann Neurol.* **47**, S189-92.

Benabid AL., Wallace B., Mitrofanis J., Xia C., Piallat B., Fraix V., Batir A., Krack P., Pollak P., & Berger F. 2005. Therapeutic electrical stimulation of the central nervous system. *C R Biol.* **328**, 177-86.

Benazzouz A., Boraud T., Feger J., Burbaud P., Bioulac B., & Gross C. 1996. Alleviation of experimental hemiparkinsonism by high-frequency stimulation of the subthalamic nucleus in primates: a comparison with L-Dopa treatment. *Mov Disord.* **11**, 627-32.

Benazzouz A., Gross C., Feger J., Boraud T., & Bioulac B. 1993. Reversal of rigidity and improvement in motor performance by subthalamic high-frequency stimulation in MPTP-treated monkeys. *Eur J Neurosci.* **5**, 382-9.

Bentivoglio M., van der Kooy D., & Kuypers HG. 1979. The organization of the efferent projections of the substantia nigra in the rat. A retrograde fluorescent double labeling study. *Brain Res.* **174**, 1-17.

Bergman H., & Deuschl G. 2002. Pathophysiology of Parkinson's disease: from clinical neurology to basic neuroscience and back. *Mov Disord.* **17**, S28-40.

Bergman H., Feingold A., Nini A., Raz A., Slovin H., Abeles M., & Vaadia E. 1998. Physiological aspects of information processing in the basal ganglia of normal and parkinsonian primates. *Trends Neurosci.* **21**, 32-38.

Bergman H., Wichmann T., & DeLong MR. 1990. Reversal of experimental parkinsonism by lesions of the subthalamic nucleus. *Science.* **249**, 1436-8.

Bergman H., Wichmann T., Karmon B., & Delong MR. 1994. The primate subthalamic nucleus. II. Neuronal activity in the MPTP model of parkinsonism. *J Neurophysiol.* **72**, 507-20.

Bergmann O., Winter C., Meissner W., Harnack D., Kupsch A., Morgenstern R., & Reum T. 2004. Subthalamic high frequency stimulation induced rotations are differentially mediated by D1 and D2 receptors. *Neuropharm.* **46**, 974-83.

Bergstrom DA., & Walters JR. 1984. Dopamine attenuates the effects of GABA on single unit activity in the globus pallidus. *Brain Res.* **310**, 23-33.

Bergstrom DA., Bromley SD., & Walters JR. 1982. Apomorphine increases the activity of rat globus pallidus neurons. *Brain Res.* **238**, 266-71.

Berke JD., Okatan M., Skurski J., & Eichenbaum HB. 2004. Oscillatory entrainment of striatal neurons in freely moving rats. *Neuron.* **43**, 883-96.

Bernheimer H., Birkmayer W., Hornykiewicz O., Jellinger K., & Seitelberger F. 1973. Brain dopamine and the syndromes of Parkinson and Huntington. Clinical, morphological and neurochemical correlations. *J Neurol Sci.* **20**, 415-55.

Beurrier C., Congar P., Bioulac B., & Hammond C. 1999. Subthalamic nucleus neurons switch from single-spike activity to burst-firing mode. *J Neurosci.* **19**, 599-609.

Bevan MD., Booth PA., Eaton SA., & Bolam JP. 1998. Selective innervation of neostriatal interneurons by a subclass of neuron in the globus pallidus of the rat. *J Neurosci.* **18**, 9438-52.

Bevan MD., Francis CM., & Bolam JP. 1995. The glutamate-enriched cortical and thalamic input to neurons in the subthalamic nucleus of the rat: convergence with GABA-positive terminals. *J Comp Neurol.* **361**, 491-511.

Bevan MD., Magill PJ., Hallworth NE., Bolam JP., & Wilson CJ. 2002. Regulation of the timing and pattern of action potential generation in rat subthalamic neurons *in vitro* by GABA-A IPSPs. *J Neurophysiol.* **87**, 1348-62.

Bevan MD., Magill PJ., Terman D., Bolam JP., & Wilson CJ. 2003. Move to the rhythm: oscillations in the subthalamic nucleus-external globus pallidus network. *Trends Neurosci.* **25**, 525-31.

Bevan MD., & Wilson CJ. 1999. Mechanisms underlying spontaneous oscillation and rhythmic firing in rat subthalamic neurons. *J Neurosci.* **19**, 7617-28.

Bevan MD., Wilson C J., Bolam JP., & Magill, PJ. 2000. Equilibrium potential of $GABA_A$ current and implications for rebound burst firing in rat subthalamic neurons *in vitro*. *J Neurophysiol.* **83**, 3169-72.

Bezard E., Boraud T., Bioulac B., & Gross CE. 1999. Involvement of the subthalamic nucleus in glutamatergic compensatory mechanisms. *Eur J Neurosci.* **11**, 2167-70.

Bezard E., Boraud T., Bioulac B., & Gross CE. 1997. Compensatory effects of glutamatergic inputs to the substantia nigra pars compacta in experimental parkinsonism. *Neurosci.* **81**, 399-404.

Bezard E., Boraud T., Chalon S., Brotchie JM., Guilloteau D., & Gross CE. 2001. Pallidal border cells: an anatomical and electrophysiological study in the 1-methyl-4-phenyl-1,2,3,6-tetrahydropyridine-treated monkey. *Neurosci.* **103**, 117-23.

Billings LM., & Marshall JF. 2004. Glutamic acid decarboxylase 67 mRNA regulation in two globus pallidus neuron populations by dopamine and the subthalamic nucleus. *J Neurosci.* **24**, 3094-103.

Bibbiani F., Oh JD., & Chase TN. 2001. Serotonin 5-HT_{1A} agonist improves motor complications in rodent and primate parkinsonian models. *Neurology.* **57**, 1829-34.

Blanchet PJ., Metman LV., & Chase TN. 2003. Renaissance of amantadine in the treatment of Parkinson's disease. *Adv Neurol.* **91**, 251-7.

Blandini F., Nappi G., Tassorelli C., & Martigoni E. 2000. Functional changes of the basal ganglia circuitry in Parkinson's disease. *Progress in Neurobiol.* **62**, 63-88.

Bolam JP., & Smith Y. 1990. The GABA and substance P input to dopaminergic neurones in the substantia nigra of the rat. *Brain Res.* **529**, 57-78.

Bolam JP., & Smith Y. 1992. The striatum and the globus pallidus send convergent synaptic inputs onto single cells in the entopeduncular nucleus of the rat: a double anterograde labelling study combined with postembedding immunocytochemistry for GABA. *J Comp Neurol.* **321**, 456-76.

Bolam JP., Smith Y., Ingham CA., von Krosigk M., & Smith AD. 1993. Convergence of synaptic terminals from the striatum and the globus pallidus onto single neurones in the substantia nigra and the entopeduncular nucleus. *Prog Brain Res.* **99**, 73-88.

Boraud T., Bezard E., Bioulac B., & Gross C. 1996. High frequency stimulation of the internal Globus Pallidus (GPi) simultaneously improves parkinsonian symptoms and reduces the firing frequency of GPi neurons in the MPTP-treated monkey. *Neurosci Lett.* **215**, 17-20.

Boraud T., Bezard E., Bioulac B., & Gross CE. 2000. Ratio of inhibited-to-activated pallidal neurons decreases dramatically during passive limb movement in the MPTP-treated monkey. *J Neurophysiol.* **83**, 1760-3.

Boraud T., Bezard E., Bioulac B., & Gross CE. 2001. Dopamine agonist-induced dyskinesias are correlated to both firing pattern and frequency alterations of pallidal neurones in the MPTP-treated monkey. *Brain.* **124**, 546-57.

Boraud T., Bezard E., Bioulac B., & Gross CE. 2002. From single extracellular unit recording in experimental and human Parkinsonism to the development of a functional concept of the role played by the basal ganglia in motor control. *Prog Neurobiol.* **66**, 265-83.

Boraud T., Bezard E., Guehl D., Bioulac B., & Gross C. 1998. Effects of L-DOPA on neuronal activity of the globus pallidus externalis (GPe) and globus pallidus internalis (GPi) in the MPTP-treated monkey. *Brain Research.* **787**, 157-60.

Boraud T., Bezard E., Stutzmann JM., Bioulac B., & Gross CE. 2000. Effects of riluzole on the electrophysiological activity of pallidal neurons in the 1-methyl-4-phenyl-1,2,3,6-tetrahydropyridine-treated monkey. *Neurosci Lett.* **281**, 75-8.

Bouthenet ML., Souil E., Martres MP., Sokoloff P., Giros B., & Schwartz JC. 1991. Localization of dopamine D3 receptor mRNA in the rat brain using in situ hybridization histochemistry: comparison with dopamine D2 receptor mRNA. *Brain Res.* **564**, 203-19.

Boyson SJ., McGonigle P., & Molinoff PB. 1986. Quantitative autoradiographic localization of the D1 and D2 subtypes of dopamine receptors in rat brain. *J Neurosci.* **6**, 3177-88

Brecht M., Singer W., & Engel AK. 1999. Patterns of synchronization in the superior colliculus of anesthetized cats. *J Neurosci.* **19**, 3567-79.

Breysse N., Amalric M., & Salin P. 2003. Metabotropic glutamate 5 receptor blockade alleviates akinesia by normalizing activity of selective basal-ganglia structures in parkinsonian rats. *J Neurosci.* **23**, 8302-9.

Brown P. 2003. Oscillatory nature of human basal ganglia activity: relationship to the pathophysiology of Parkinson's disease. *Mov Disord.* **18**, 357-63.

Brown P., & Marsden CD. 1998. What do the basal ganglia do? *Lancet.* **351**, 1801-4.

Brown P., & Marsden JF. 2001. Cortical network resonance and motor activity in humans. *Neuroscientist.* **7**, 518-27.

Brown P., Kupsch A., Magill PJ., Sharott A., Harnack D., & Meissner W. 2002. Oscillatory local field potentials recorded from the subthalamic nucleus of the alert rat. *Exp Neurol.* **177**, 581-5.

Brown P., Oliviero A., Mazzone P., Insola A., Tonali P., & Di Lazzaro V. 2001. Dopamine dependency of oscillations between subthalamic nucleus and pallidum in Parkinson's disease. *J Neurosci.* **21**, 1033-8.

Brown P., Mazzone P., Oliviero A., Altibrandi MG., Pilato F., Tonali PA., & Di Lazzaro V. 2004. Effects of stimulation of the subthalamic area on oscillatory pallidal activity in Parkinson's disease. *Exp Neurol.* **188**, 480-90.

Brown P., Salenius S., Rothwell JC., & Hari R. 1998. Cortical correlate of the Piper rhythm in humans. *J Neurophysiol.* **80**, 2911-7.

Campbell GA., Eckardt MJ., & Weight FF. 1985. Dopaminergic mechanisms in subthalamic nucleus of rat: analysis using horseradish peroxidase and microiontophoresis. *Brain Res.* **333**, 261-70.

Canteras NS., Shammah-Lagnado SJ., Silva BA., & Ricardo JA. 1990. Afferent connections of the subthalamic nucleus: a combined retrograde and anterograde horseradish peroxidase study in the rat. *Brain Res.* **513**, 43-59.

Carlson JH., Bergstrom DA., Demo SD., & Walters JR. 1990. Nigrostriatal lesion alters neurophysiological responses to selective and nonselective D-1 and D-2 dopamine agonists in rat globus pallidus. *Synapse.* **5**, 83-93.

Carpenter MB., Carleton SC., Keller JT., & Conte P. 1981. Connections of the subthalamic nucleus in the monkey. *Brain Res.* **224**, 1-29.

Carpenter MB., Fraser RA., & Shriver JE. 1968. The organization of pallidosubthalamic fibers in the monkey. *Brain Res.* **11**, 522-59.

Cassidy M., Mazzone P., Oliviero A., Insola A., Tonali P., Di Lazzaro V., & Brown P. 2002. Movement-related changes in synchronization in the human basal ganglia. *Brain.* **125**, 1235-46.

Carlson JH., Bergstrom DA., Demo SD., & Walters JR. 1990. Nigrostriatal lesion alters neurophysiological responses to selective and nonselective D-1 and D-2 dopamine agonists in rat globus pallidus. *Synapse.* **5**, 83-93.

Cepeda C., Walsh JP., Hull CD., Howard SG., Buchwald NA., & Levine MS. 1989. Dye-coupling in the neostriatum of the rat: I. Modulation by dopamine-depleting lesions. *Synapse.* **4**, 229-37.

Chan CS., Shigemoto R., Mercer JN., & Surmeier DJ. 2004. HCN2 and HCN1 channels govern the regularity of autonomous pacemaking and synaptic resetting in globus pallidus neurons. *J Neurosci.* **24**, 9921-32.

Chang HT., Wilson CJ., & Kitai ST. 1981. Single neostriatal efferent axons in the globus pallidus: a light and electron microscopic study. *Science.* **213**, 915-8.

Chen L., Savio Chan C., & Yung WH. 2004. Electrophysiological and behavioral effects of zolpidem in rat globus pallidus. *Exp Neurol.* **186**, 212-20.

Chergui K., Akaoka H., & Charlety PJ., Saunier CF., Buda M., & Chouvet G. 1994. Subthalamic nucleus modulates burst firing of nigral dopamine neurones via NMDA receptors. *Neuroreport.* **5**, 1185-8.

Chesselet MF., & Delfs JM. 1996. Basal ganglia and movement disorders: an update. *Trends Neurosci.* **19**, 417-22.

Courtemanche R., Fujii N., & Graybiel AM. 2003. Synchronous, focally modulated beta-band oscillations characterize local field potential activity in the striatum of awake behaving monkeys. *J Neurosci.* **23**, 11741-52.

Cooper AJ., & Stanford IM. 2000. Electrophysiological and morphological characteristics of three subtypes of rat globus pallidus neurone *in vitro*. *J.Physiol.* **527**, 291-304.

Cooper AJ., & Stanford IM. 2001. Dopamine D2 receptor mediated presynaptic inhibition of striatopallidal GABA(A) IPSCs in vitro. *Neuropharm.* **41**, 62-71.

Cooper AJ., & Stanford I M. 2002. Calbindin D28-k positive projection neurones and calretinin positive interneurones of the rat globus pallidus. *Brain Research.* **527**, 291-304.

Cornwall J., Cooper JD., & Phillipson OT. 1990. Projections to the rostral reticular thalamic nucleus in the rat. *Exp Brain Res.* **80**, 157-71.

Cossette M., Lecomte F., & Parent A. 2005. Morphology and distribution of dopaminergic neurons intrinsic to the human striatum. *J Chem Neuroanat.* **29**, 1-11.

Cossette M., Levesque M., & Parent A. 1999. Extrastriatal dopaminergic innervation of human basal ganglia. *Neurosci Res.* **34**, 51-4.

Cragg SJ., Baufreton J., Xue Y., Bolam JP., & Bevan MD. 2004. Synaptic release of dopamine in the subthalamic nucleus. *Eur J Neurosci.* **20**, 1788-802.

Delong MR. 1971. Activity of pallidal neurons during movement. *J Neurophysiol.* **34**, 414-27.

DeLong MR. 1990. Primate models of movement disorders of basal ganglia origin. *Trends Neurosci.* **13**, 281-5.

DeLong MR., Crutcher MD., & Georgopoulos AP. 1985. Primate globus pallidus and subthalamic nucleus: functional organization. *J Neurophysiol.* **53**, 530-43.

Demchyshyn LL., McConkey F., & Niznik HB. 2000. Dopamine D5 receptor agonist high affinity and constitutive activity profile conferred by carboxyl-terminal tail sequence. *J Biol Chem.* **275**, 23446-55.

Deschenes M., Bourassa J., Doan VD., & Parent A. 1996. A single-cell study of the axonal projections arising from the posterior intralaminar thalamic nuclei in the rat. *Eur J Neurosci.* **8**, 329-43.

Desmurget M., Grafton ST., Vindras P., Grea H., & Turner RS. 2004. The basal ganglia network mediates the planning of movement amplitude. *Eur J Neurosci.* **19**, 2871-80.

Dostrovsky JO., & Lozano AM. 2002. Mechanisms of deep brain stimulation. *Mov Disord.* **17**, S63-8.

Dostrovsky JO., Hutchison WD., & Lozano AM. 2002. The globus pallidus, deep brain stimulation, and Parkinson's disease. *Neuroscientist.* **8**, 284-90.

Doyle LM., Kuhn AA., Hariz M., Kupsch A., Schneider GH., & Brown P. 2005. Levodopa-induced modulation of subthalamic beta oscillations during self-paced movements in patients with Parkinson's disease. *Eur J Neurosci.* **21**, 1403-12.

Dragunow M., Robertson GS., Faull RL., Robertson HA., & Jansen K. 1990. D2 dopamine receptor antagonists induce fos and related proteins in rat striatal neurons. *Neurosci.* **37**, 287-94.

Drouot X., Oshino S., Jarraya B., Besret L., Kishima H., Remy P., Dauguet J., Lefaucheur JP., Dolle F., Conde F., Bottlaender M., Peschanski M., Keravel Y., Hantraye P., & Palfi S. 2004. Functional recovery in a primate model of Parkinson's disease following motor cortex stimulation. *Neuron.* **44**, 769-78.

El-Banoua F., Caraballo I., Flores JA., Galan-Rodriguez B., & Fernandez-Espejo E. 2004. Effects on turning of microinjections into basal ganglia of D(1) and D(2) dopamine receptors agonists and the cannabinoid CB(1) antagonist SR141716A in a rat Parkinson's model. *Neurobiol Dis.* **16**, 377-85.

Eberle-Wang K., Lucki I., & Chesselet MF. 1996. A role for the subthalamic nucleus in 5-HT_{2C}-induced oral dyskinesia. *Neurosci.* **72**,117-28.

Eberle-Wang K., Mikeladze Z., Uryu K., & Chesselet MF. 1997. Pattern of expression of the $serotonin_{2C}$ receptor messenger RNA in the basal ganglia of adult rats. *J Comp Neurol.* **384**, 233-47.

Engel AK., & Singer W. 2001. Temporal binding and the neural correlates of sensory awareness. *Trends Cogn Sci.* **5**, 16-25.

Engel AK., Fries P., & Singer W. 2001. Dynamic predictions: oscillations and synchrony in top-down processing. *Nat Rev Neurosci.* **2**, 704-16.

Feger J., Bevan M., & Crossman AR. 1994. The projections from the parafascicular thalamic nucleus to the subthalamic nucleus and the striatum arise from separate neuronal populations: a comparison with the corticostriatal and corticosubthalamic efferents in a retrograde fluorescent double-labelling study. *Neurosci.* **60**, 125-32.

Filion M., & Tremblay L. 1991. Abnormal spontaneous activity of globus pallidus neurons in monkeys with MPTP-induced parkinsonism. *Brain Res.* **547**, 142-51.

Flores G., Liang JJ., Sierra A., Martinez-Fong D., Quirion R., Aceves J., & Srivastava LK. 1999. Expression of dopamine receptors in the subthalamic nucleus of the rat: characterization using reverse transcriptase-polymerase chain reaction and autoradiography. *Neurosci.* **91**, 549-56.

Flores G., Rosales MG., Hernandez S., Sierra A., & Aceves J. 1995. 5-Hydroxytryptamine increases spontaneous activity of subthalamic neurons in the rat. *Neurosci Lett.* **192**, 17-20.

Floran B., Aceves J., Sierra A., & Martinez-Fong D. 1990. Activation of D1 dopamine receptors stimulates the release of GABA in the basal ganglia of the rat. *Neurosci Lett.* **116**, 136-40.

Floran B., Floran L., Erlij D., & Aceves J. 2004. Dopamine D4 receptors inhibit depolarisation-induced [3H]GABA relaease in the rat subthalamic nucleus. *Eur J Pharmacol.* **498**, 97-102.

Foffani G., Priori A., Egidi M., Rampini P., Tamma F., Caputo E., Moxon KA., Cerutti S., Barbieri S.. 2003. 300-Hz subthalamic oscillations in Parkinson's disease. *Brain.* **126**, 2153-63.

Fogelson N., Kuhn AA., Silberstein P., Limousin PD., Hariz M., Trottenberg T., Kupsch A., & Brown P. 2005. Frequency dependent effects of subthalamic nucleus stimulation in Parkinson's disease. *Neurosci Lett.* **382**, 5-9.

Francois C., Savy C., Jan C., Tande D., Hirsch EC., & Yelnik J. 2000. Dopaminergic innervation of the subthalamic nucleus in the normal state, in MPTP-treated monkeys, and in Parkinson's disease patients. *J Comp Neurol.* **425**,121-9.

Franklin KBJ., & Paxinos G. 1997. The Mouse Brain In Strereotaxic Coordianates. San Diego: Academic Press.

Fremeau RT Jr., Duncan GE., Fornaretto MG., Dearry A., Gingrich JA., Breese GR., & Caron MG. 1991. Localization of D1 dopamine receptor mRNA in brain supports a role in cognitive, affective, and neuroendocrine aspects of dopaminergic neurotransmission. *Proc Natl Acad Sci U S A.* **88**, 3772-6.

Fujimoto K., & Kita H. 1993. Response characteristics of subthalamic neurons to the stimulation of the sensorimotor cortex in the rat. *Brain Res.* **609**, 185-92.

Gandia JA, De Las Heras S, Garcia M, Gimenez-Amaya JM. 1993. Afferent projections to the reticular thalamic nucleus from the globus pallidus and the substantia nigra in the rat. *Brain Res Bull.* **32**, 351-8.

Garcia-Munoz M., Patino P., Wright AJ., & Arbuthnott GW. 1983. The anatomical substrate of the turning behaviour seen after lesions in the nigrostriatal dopamine system. *Neurosci.* **8**, 87-95.

Garcia L., D'Alessandro G., Bioulac B., & Hammond C. 2005. High-frequency stimulation in Parkinson's disease: more or less? *Trends Neurosci.* **28**, 209-16.

Garcia L., Audin J., D'Alessandro G., Bioulac B., & Hammond C. 2003. Dual effect of high-frequency stimulation on subthalamic neuron activity. *J Neurosci.* **23**, 8743-51.

Gauthier J., Parent M., Levesque M., & Parent A. 1999. The axonal arborization of single nigrostriatal neurons in rats. *Brain Res.* **834**, 228-32.

Gerfen CR., Engber TM., Mahan LC., Susel Z., Chase TN., Monsma FJ Jr., & Sibley DR. 1990. D1 and D2 dopamine receptor-regulated gene expression of striatonigral and striatopallidal neurons. *Science.* **250**, 1429-32.

Gerfen CR. 2000a. Dopamine-mediated gene regulation in models of Parkinson's disease. *Ann Neurol.* **47**,42-52.

Gerfen CR. 2000b. Molecular effects of dopamine on striatal-projection pathways. *Trends Neurosci.* **23**, S64-70.

Gerfen CR., Keefe KA., & Gauda EB. 1995. D1 and D2 dopamine receptor function in the striatum: coactivation of D1- and D2-dopamine receptors on separate populations of

neurons results in potentiated immediate early gene response in D1-containing neurons. *J Neurosci.* **15**, 8167-76.

Gerfen CR., Miyachi S., Paletzki R., & Brown P. 2002. D1 dopamine receptor supersensitivity in the dopamine-depleted striatum results from a switch in the regulation of ERK1/2/MAP kinase. *J Neurosci.* **22**, 5042-54.

Gerlach M., Gotz M., Dirr A., Kupsch A., Janetzky B., Oertel W., Sautter J., Schwarz J., Reichmann H., & Riederer P. 1996. Acute MPTP treatment produces no changes in mitochondrial complex activities and indices of oxidative damage in the common marmoset *ex vivo* one week after exposure to the toxin. *Neurochem Int.* **28**, 41-9.

Gillies AJ., & Willshaw DJ. 1998. A massively connected subthalamic nucleus leads to the generation of widespread pulses. *Proc Biol Sci.* **265**, 2101-9.

Giovanni A., Sieber BA., Heikkila RE., & Sonsalla PK. 1994. Studies on species sensitivity to the dopaminergic neurotoxin 1-methyl-4-phenyl-1,2,3,6-tetrahydropyridine. Part 1: Systemic administration. *J Pharmacol Exp Ther.* **270**, 1000-7.

Goldberg JA., Boraud T., Maraton S., Haber SN., Vaadia E., & Bergman H. 2002. Enhanced synchrony among primary motor cortex neurons in the 1-methyl-4-phenyl-1,2,3,6-tetrahydropyridine primate model of Parkinson's disease. *J Neurosci.* **22**, 4639-53.

Goldberg JA., Rokni U., Boraud T., Vaadia E., & Bergman H. 2004. Spike synchronization in the cortex/basal-ganglia networks of Parkinsonian primates reflects global dynamics of the local field potentials. *J Neurosci.* **24**, 6003-10.

Govindaiah G., & Cox CL. 2005. Excitatory actions of dopamine via D1-like receptors in the rat lateral geniculate nucleus. *J Neurophysiol.* **94**, 3708-18.

Grace AA., & Bunney BS. 1983. Intracellular and extracellular electrophysiology of nigral dopaminergic neurons. 1. Identification and characterization. *Neurosci.* **10**, 301-15.

Graybiel AM., Canales JJ., & Capper-Loup C. 2000. Levodopa-induced dyskinesias and dopamine-dependent stereotypies: a new hypothesis. *Trends Neurosci.* **23**, S71-7.

Grofova I., Deniau JM., & Kitai ST. 1982. Morphology of the substantia nigra pars reticulata projection neurons intracellularly labeled with HRP. *J Comp Neurol.* **208**, 352-68.

Gross CE., Boraud T., Guehl D., Bioulac B., & Bezard E. 1999. From experimentation to the surgical treatment of Parkinson's disease: prelude or suite in basal ganglia research? *Prog Neurobiol.* **59**, 509-32.

Guehl D., Pessiglione M., Francois C., Yelnik J., Hirsch EC., Feger J., & Tremblay L. 2003. Tremor-related activity of neurons in the 'motor' thalamus: changes in firing rate and pattern in the MPTP vervet model of parkinsonism. *Eur J Neurosci.* **17**, 2388-400.

Guerineau NC., Gahwiler BH., & Gerber U. 1994. Reduction of resting K+ current by metabotropic glutamate and muscarinic receptors in rat CA3 cells: mediation by G-proteins. *J Physiol.* **474**, 27-33.

Guerineau NC., Bossu JL., Gahwiler BH., & Gerber U. 1995. Activation of a nonselective cationic conductance by metabotropic glutamatergic and muscarinic agonists in CA3 pyramidal neurons of the rat hippocampus. *J Neurosci.* **15**, 4395-407.

Hallett PJ., Dunah AW., Ravenscroft P., Zhou S., Bezard E., Crossman AR., Brotchie JM., & Standaert DG. 2005. Alterations of striatal NMDA receptor subunits associated with the development of dyskinesia in the MPTP-lesioned primate model of Parkinson's disease. *Neuropharm.* **48**, 503-16.

Hallworth NE., Wilson CJ., & Bevan MD. 2003. Apamin-sensitive small conductance calcium-activated potassium channels, through their selective coupling to voltage-gated calcium channels, are critical determinants of the precision, pace, and pattern of action potential generation in rat subthalamic nucleus neurons in vitro. *J Neurosci.* **23**, 7525-42.

Hammond C., & Yelnik J. 1983. Intracellular labelling of rat subthalamic neurones with horseradish peroxidase: computer analysis of dendrites and characterization of axon arborization. *Neurosci.* **8**, 781-90.

Harris NC., & Constanti A. 1995. Mechanism of block by ZD 7288 of the hyperpolarization-activated inward rectifying current in guinea pig substantia nigra neurons in vitro. *J Neurophysiol.* **74**, 2366-78.

Hashimoto T., Elder CM., Okun MS., Patrick SK., & Vitek JL. 2003. Stimulation of the subthalamic nucleus changes the firing pattern of pallidal neurons. *J Neurosci.* **23**, 1916-23.

Hassani OK., & Feger J. 1999. Effects of intrasubthalamic injection of dopamine receptor agonists on subthalamic neurons in normal and 6-hydroxydopamine-lesioned rats: an electrophysiological and c-Fos study. *Neurosci.* **92**, 533-43.

Hassani OK., Mouroux M., & Feger J. 1996. Increased subthalamic neuronal activity after nigral dopaminergic lesion independent of disinhibition via the globus pallidus. *Neurosci.* **72**, 105-15.

Hassani OK., Francois C., Yelnik J., & Feger J. 1997. Evidence for a dopaminergic innervation of the subthalamic nucleus in the rat. *Brain Res.* **749**, 88-94.

Hauber W. 1998. Blockade of subthalamic dopamine D1 receptors elicits akinesia in rats. *Neuroreport.* **9**, 4115-8.

Hauber W., & Lutz S. 1999a. Dopamine D1 or D2 receptor blockade in the globus pallidus produces akinesia in the rat. *Behav Brain Res.* **106**, 143-50.

Hauber W., & Lutz S. 1999b. Blockade of dopamine D2, but not of D1 receptors in the rat globus pallidus induced Fos-like immunoreactivity in the caudate-putamen, substantia nigra and entopeduncular nucleus. *Neurosci Lett.* **271**:73-6.

Hazrati LN., Parent A., Mitchell S., & Haber SN. 1990. Evidence for interconnections between the two segments of the globus pallidus in primates: a PHA-L anterograde tracing study. *Brain Res.* **533**, 171-5.

Hedreen JC. 1999. Tyrosine hydroxylase-immunoreactive elements in the human globus pallidus and subthalamic nucleus. *J Comp Neurol.* **409**, 400-10.

Heidenreich BA., Mitrovic I., Battaglia G., & Napier TC. 2004. Limbic pallidal adaptations following long-term cessation of dopaminergic transmission: lack of upregulation of dopamine receptor function. *Exp Neurol.* **186**, 145-57.

Heimer G., Bar-Gad I., Goldberg JA., & Bergman H. 2002. Dopamine replacement therapy reverses abnormal synchronization of pallidal neurons in the 1-methyl-4-phenyl-1,2,3,6-tetrahydropyridine primate model of parkinsonism. *J Neurosci.* **22**, 7850-5.

Hemsley KM., Farrall EJ., & Crocker AD. 2002. Dopamine receptors in the subthalamic nucleus are involved in the regulation of muscle tone in the rat. *Neurosci Lett.* **317**,123-6.

Hersch SM., Ciliax BJ., Gutekunst CA., Rees HD., Heilman CJ., Yung KK., Bolam JP., Ince E., Yi H., & Levey AI. 1995. Electron microscopic analysis of D1 and D2 dopamine receptor proteins in the dorsal striatum and their synaptic relationships with motor corticostriatal afferents. *J Neurosci.* **15**, 5222-37.

Hontanilla B., Parent A., de las Heras S., & Gimenez-Amaya JM. 1998. Distribution of calbindin D-28k and parvalbumin neurons and fibers in the rat basal ganglia. *Brain Res Bull.* **47**, 107-16

Hoover BR., & Marshall JF. 2004. Molecular, chemical, and anatomical characterization of globus pallidus dopamine D2 receptor mRNA-containing neurons. *Synapse.* **52**, 100-13.

Hornykiewicz O. 1966. Dopamine (3-hydroxytyramine) and brain function. *Pharmacol Rev.* **18**, 925-64.

Hornykiewicz O. 1973. Dopamine in the basal ganglia. Its role and therapeutic implications (including the clinical use of L-DOPA). *Br Med Bull.* **29**, 72-8.

Huguenard JR., & McCormick DA. 1992. Simulation of the currents involved in rhythmic oscillations in thalamic relay neurons. *J Neurophysiol.* **68**, 1373-83.

Hutchison WD., Lozano AM., Tasker RR., Lang AE., & Dostrovsky JO. 1997. Identification and characterization of neurons with tremor-frequency activity in human globus pallidus. *Exp Brain Res.* **1997**, 557-63.

Hutchison WD., Allan RJ., Opitz H., Levy R., Dostrovsky JO., Lang AE., & Lozano AM. 1998. Neurophysiological identification of the subthalamic nucleus in surgery for Parkinson's disease. *Ann Neurol.* **44**, 622-8.

Hutchison WD., Dostrovsky JO., Walters JR., Courtemanche R., Boraud T., Goldberg J., & Brown P. 2004. Neuronal oscillations in the basal ganglia and movement disorders: evidence from whole animal and human recordings. *J Neurosci.* **24**, 40-3.

Hammond C., Rouzaire-Dubois B., Feger J., Jackson A., & Crossman AR. 1983. Anatomical and electrophysiological studies on the reciprocal projections between the subthalamic nucleus and nucleus tegmenti pedunculopontinus in the rat. *Neurosci.* **9**, 41-52.

Jenner P., Taquet H., Mauborgne A., Benoliel JT., Cesselin F., Rose S., Javoy-Agid F., Agid Y., & Marsden CD. 1986. Lack of change in basal ganglia neuropeptide content following subacute 1-methyl-4-phenyl-1,2,3,6-tetrahydropyridine treatment of the common marmoset. *J Neurochem.* **47**, 1548-51.

Jenner P. Pharmacology of dopamine agonists in the treatment of Parkinson's disease. 2002. *Neurology.* **58**, S1-8.

Jiang ZG., Pessia M., & North RA. 1993. Dopamine and baclofen inhibit the hyperpolarization-activated cation current in rat ventral tegmental neurones. *J Physiol.* **462**, 753-64.

Johnson AE., Coirini H., Kallstrom L., & Wiesel FA. 1994. Characterization of dopamine receptor binding sites in the subthalamic nucleus. *Neuroreport.* **5**, 1836-8

Johnson SW., & Seutin V. 1997. Bicuculline methiodide potentiates NMDA-dependent burst firing in rat dopamine neurons by blocking apamin-sensitive Ca^{2+}-activated K^{+} currents. *Neurosci Lett.* **231,** 13-6.

Johnson SW., & Wu YN. 2004. Multiple mechanisms underlie burst firing in rat midbrain dopamine neurons *in vitro*. *Brain Res.* **1019**, 293-6.

Johnson SW., Seutin V., & North RA. 1992. Burst firing in dopamine neurons induced by N-methyl-D-aspartate: role of electrogenic sodium pump. *Science.* **258**, 665-7.

Kaneoke Y., & Vitek JL. 1996. Burst and oscillation as disparate neuronal properties. *J Neurosci Methods.* **68**, 211-23.

Kawaguchi Y. 1997. Neostriatal cell subtypes and their functional roles. *Neurosci Res.* **27**, 1-8.

Kawaguchi Y., Wilson CJ., Augood SJ., & Emson PC. 1995. Striatal interneurones: chemical, physiological and morphological characterization. *Trends Neurosci.* **18**, 527-35.

Kawaguchi Y., Wilson CJ., & Emson PC. 1989. Intracellular recording of identified neostriatal patch and matrix spiny cells in a slice preparation preserving cortical inputs. *J Neurophysiol.* **62**, 1052-68.

Kawaguchi Y., Wilson CJ., Augood SJ., & Emson PC. 1997. Striatal interneurones: chemical, physiological and morphological characterization. *Trends Neurosci.* **18**, 527-35.

Kelland MD., Soltis RP., Anderson LA., Bergstrom DA., & Walters JR. 1995. *In vivo* characterization of two cell types in the rat globus pallidus which have opposite

responses to dopamine receptor stimulation: comparison of electrophysiological properties and responses to apomorphine, dizocilpine, and ketamine anesthesia. *Synapse*. **20**, 338-50.

Kincaid AE., Albin RL., Newman SW., Penney JB., & Young AB. 1992. 6-Hydroxydopamine lesions of the nigrostriatal pathway alter the expression of glutamate decarboxylase messenger RNA in rat globus pallidus projection neurons. *Neurosci.* **51**, 705-18.

Kincaid AE., Penney JB Jr., Young AB., & Newman SW. 1991. Evidence for a projection from the globus pallidus to the entopeduncular nucleus in the rat. *Neurosci Lett.* **128**, 121-5.

Kita H. 1994. Parvalbumin-immunopositive neurons in rat globus pallidus: a light and electron microscopic study. *Brain Res.* **657**, 31-41.

Kitai ST., & Deniau JM. 1981. Cortical inputs to the subthalamus: intracellular analysis. *Brain Res.* **214**, 411-5.

Kita H., & Kitai ST. 1987. Efferent projections of the subthalamic nucleus in the rat: light and electron microscopic analysis with the PHA-L method. *J Comp Neurol.* **260**, 435-52.

Kita H., & Kitai ST. 1991. Intracellular study of rat globus pallidus neurons: membrane properties and responses to neostriatal, subthalamic and nigral stimulation. *Brain Res.* **564**, 296-305.

Kita H., & Kitai ST. 1994. The morphology of globus pallidus projection neurons in the rat: an intracellular staining study. *Brain Res.* **636**, 308-19.

Kita H., Chang HT., & Kitai ST. 1983a. Pallidal inputs to subthalamus: intracellular analysis. *Brain Res.* **264**, 255-65.

Kita H., Chang HT., & Kitai ST. 1983b. The morphology of intracellularly labeled rat subthalamic neurons: a light microscopic analysis. *J Comp Neurol.* **215**, 245-57.

Kita H., Nambu A., Kaneda K., Tachibana Y., & Takada M. 2004. Role of ionotropic glutamatergic and GABAergic inputs on the firing activity of neurons in the external pallidum in awake monkeys. *J Neurophysiol.* **92**, 3069-84.

Kitai ST., Shepard PD., Callaway JC., & Scroggs R. 1999. Afferent modulation of dopamine neuron firing patterns. *Curr Opin Neurobiol.* **9**, 690-7.

Komendantov AO., Komendantova OG., Johnson SW., & Canavier CC. 2004. A modeling study suggests complementary roles for GABAA and NMDA receptors and the SK channel in regulating the firing pattern in midbrain dopamine neurons. *J Neurophysiol.* **91**, 346-57.

Koos T., & Tepper JM. 1999. Inhibitory control of neostriatal projection neurons by GABAergic interneurons. *Nat Neurosci.* **2**, 467-72.

Kornhuber J., Kim JS., Kornhuber ME., & Kornhuber HH. 1984. The cortico-nigral projection: reduced glutamate content in the substantia nigra following frontal cortex ablation in the rat. *Brain Res.* **322**, 124-6.

Koyano K., Velimirovic BM., Grigg JJ., Nakajima S., & Nakajima Y. 1993. Two signal transduction mechanisms of substance P-induced depolarization in locus coeruleus neurons. *Eur J Neurosci.* **5**, 1189-97.

Krack P., Pollak P., Limousin P., Hoffmann D., Xie J., Benazzouz A., & Benabid AL. 1998. Subthalamic nucleus or internal pallidal stimulation in young onset Parkinson's disease. *Brain*. **121**, 451-7.

Krack P., Hamel W., Mehdorn HM., & Deuschl G. 1999. Surgical treatment of Parkinson's disease. *Curr Opin Neurol*. **12**, 417-25.

Kreiss DS., Anderson LA., & Walters JR. 1996. Apomorphine and dopamine D(1) receptor agonists increase the firing rates of subthalamic nucleus neurons. *Neurosci*. **72**, 863-76.

Kreiss DS., Mastropietro CW., Rawji SS., & Walters JR. 1997. The response of subthalamic nucleus neurons to dopamine receptor stimulation in a rodent model of Parkinson's disease. *J Neurosci*. **17**, 6807-19.

Kuhn AA., Williams D., Kupsch A., Limousin P., Hariz M., Schneider GH., Yarrow K., & Brown P. 2004. Event-related beta desynchronization in human subthalamic nucleus correlates with motor performance. *Brain*. **127**, 735-46.

Kuwajima M., Hall RA., Aiba A., & Smith Y. 2004. Subcellular and subsynaptic localization of group I metabotropic glutamate receptors in the monkey subthalamic nucleus. *J Comp Neurol*. **474**, 589-602.

Lacey MG., Mercuri NB., & North RA. 1989. Two cell types in rat substantia nigra zona compacta distinguished by membrane properties and the actions of dopamine and opioids. *J Neurosci*. **9**, 1233-41.

Langston JW., Ballard P., Tetrud JW., & Irwin I. 1983. Chronic Parkinsonism in humans due to a product of meperidine-analog synthesis. *Science*. **219**, 979-80.

Larkman PM., & Kelly JS. 1992. Ionic mechanisms mediating 5-hydroxytryptamine- and noradrenaline-evoked depolarization of adult rat facial motoneurones. *J Physiol.* **456**, 473-90.

Lavoie B., & Parent A. 1990. Immunohistochemical study of the serotoninergic innervation of the basal ganglia in the squirrel monkey. *J Comp Neurol.* **299**, 1-16.

Lavoie B., & Parent A. 1994. Pedunculopontine nucleus in the squirrel monkey: projections to the basal ganglia as revealed by anterograde tract-tracing methods. *J Comp Neurol.* **344**, 210-31.

Lavoie B., Smith Y., & Parent A. 1989. Dopaminergic innervation of the basal ganglia in the squirrel monkey as revealed by tyrosine hydroxylase immunohistochemistry. *J Comp Neurol.* **289**, 36-52.

Le W., & Appel SH. 2004. Mutant genes responsible for Parkinson's disease. *Curr Opin Pharmacol.* **4**, 79-84.

Lee CR., Abercrombie ED., & Tepper JM. 2004. Pallidal control of substantia nigra dopaminergic neuron firing pattern and its relation to extracellular neostriatal dopamine levels. *Neurosci.* **129**, 481-9.

Lee KM., Ahn TB., Jeon BS., & Kim DG. 2004. Change in phase synchronization of local field potentials in anesthetized rats after chronic dopamine depletion. *Neurosci Res.* **49**, 179-84.

Legrand JC., Darbon P., & Streit J. 2004. Contributions of NMDA receptors to network recruitment and rhythm generation in spinal cord cultures. *Eur J Neurosci.* **19**, 521-32.

Le Moine C., Tison F., & Bloch B. 1990. D2 dopamine receptor gene expression by cholinergic neurons in the rat striatum. *Neurosci Lett.* **117**, 248-52.

Levant B. 1997. The D3 dopamine receptor: neurobiology and potential clinical relevance. *Pharmacol Rev.* **49**, 231-52.

Levy R., Ashby P., Hutchison WD., Lang AE., Lozano AM., & Dostrovsky JO. 2002a. Dependence of subthalamic nucleus oscillations on movement and dopamine in Parkinson's disease. *Brain.* **25**, 1196-209.

Levy R., Hazrati LN., Herrero MT., Vila M., Hassani OK., Mouroux M., Ruberg M., Asensi H., Agid Y., Feger J., Obeso JA., Parent A., & Hirsch EC. 1997. Re-evaluation of the functional anatomy of the basal ganglia in normal and Parkinsonian states. *Neurosci.* **76**, 335-43.

Levy R., Hutchison WD., Lozano AM., & Dostrovsky JO. 2000. High-frequency synchronization of neuronal activity in the subthalamic nucleus of parkinsonian patients with limb tremor. *J Neurosci.* **20**,7766-75.

Levy R., Dostrovsky JO., Lang AE., Sime E., Hutchison WD., & Lozano AM. 2001. Effects of apomorphine on subthalamic nucleus and globus pallidus internus neurons in patients with Parkinson's disease. *J Neurophysiol.* **86**, 249-60.

Levy R., Hutchison WD., Lozano AM., & Dostrovsky JO. 2002b. Synchronized neuronal discharge in the basal ganglia of parkinsonian patients is limited to oscillatory activity. *J Neurosci.* **22**, 2855-61.

Limousin P., Pollak P., Benazzouz A., Hoffmann D., Broussolle E., Perret JE., & Benabid AL. 1995. Bilateral subthalamic nucleus stimulation for severe Parkinson's disease. *Mov Disord.* **10**, 672-4.

Lindvall O., & Bjorklund A. 1979. Dopaminergic innervation of the globus pallidus by collaterals from the nigrostriatal pathway. *Brain Res.* **172**, 169-73.

Lisman JE. 1997. Bursts as a unit of neural information: making unreliable synapses reliable. *Trends Neurosci.* **20**, 38-43.

Loucif KC., Wilson CL., Lacey MG., & Stanford IM. 2005. Functional connectivity between the globus pallidus and subthalamic nucleus in a mouse brain slice preparation. *J Physiol.* **567**, 977-87.

Lokwan SJ., Overton PG., Berry MS., & Clark D. 1999. Stimulation of the pedunculopontine tegmental nucleus in the rat produces burst firing in A9 dopaminergic neurons. *Neurosci.* **92**, 245-54.

Lozano AM., Lang AE., Levy R., Hutchison W., & Dostrovsky J. 2000. Neuronal recordings in Parkinson's disease patients with dyskinesias induced by apomorphine. *Ann Neurol.* **47**, S141-6.

Magee JC.1998. Dendritic hyperpolarization-activated currents modify the integrative properties of hippocampal CA1 pyramidal neurons. *J Neurosci.* **18**, 7613-24.

Magill PJ., Bolam JP., & Bevan MD. 2000. Relationship of activity in the subthalamic nucleus-globus pallidus network to cortical electroencephalogram. *J Neurosci.* **20**, 820-33.

Magill PJ., Bolam JP., & Bevan MD. 2001. Dopamine regulates the impact of the cerebral cortex on the subthalamic nucleus-globus pallidus network. Relationship of activity in the subthalamic nucleus-globus pallidus network to cortical electroencephalogram. *J Neurosci.* **106**, 313-30.

Magill PJ., Sharott A., Bevan MD., Brown P., & Bolam JP. 2004. Synchronous unit activity and local field potentials evoked in the subthalamic nucleus by cortical stimulation. *J Neurophysiol.* **92**, 700-14.

Magill PJ., Sharott A., Harnack D., Kupsch A., Meissner W., & Brown P. 2005. Coherent spike-wave oscillations in the cortex and subthalamic nucleus of the freely moving rat. *Neurosci.* **132**, 659-64.

Magnin M., Morel A., & Jeanmonod D. 2000. Single-unit analysis of the pallidum, thalamus and subthalamic nucleus in parkinsonian patients. *Neurosci.* **96**, 549-64.

Mansour A., Meador-Woodruff JH., Zhou QY., Civelli O., Akil H., & Watson SJ. 1991. A comparison of D1 receptor binding and mRNA in rat brain using receptor autoradiographic and in situ hybridization techniques. *Neurosci.* **45**, 359-71.

Marino MJ., Awad-Granko H., Ciombor KJ., & Conn PJ. 2002. Haloperidol-induced alteration in the physiological actions of group I mGluRs in the subthalamic nucleus and the substantia nigra pars reticulata. *Neuropharm.* **43**, 147-59.

Marsden CD., & Obeso JA. 1994. The functions of the basal ganglia and the paradox of stereotaxic surgery in Parkinson's disease. *Brain.* **117** , 877-97.

Marsden JF., Limousin-Dowsey P., Ashby P., Pollak P., & Brown P. 2001. Subthalamic nucleus, sensorimotor cortex and muscle interrelationships in Parkinson's disease. *Brain.* **124**, 378-88.

Marsden CD. 1990. Parkinson's disease. *Lancet.* **335**, 948-52.

Martin LP., & Waszczak BL. 1996. Dopamine D2, receptor-mediated modulation of the GABAergic inhibition of substantia nigra pars reticulata neurons. *Brain Res.* **729**, 156-69.

Matsumura M., Kojima J., Gardiner TW., & Hikosaka O. 1992. Visual and oculomotor functions of monkey subthalamic nucleus. *J Neurophysiol.* **67**, 1615-32.

Matsumura M., Tremblay L., Richard H., & Filion M. 1995. Activity of pallidal neurons in the monkey during dyskinesia induced by injection of bicuculline in the external pallidum. *Neurosci.* **65**, 59-70.

Maurice N., Deniau JM., Glowinski J., & Thierry AM. 1998. Relationships between the prefrontal cortex and the basal ganglia in the rat: physiology of the corticosubthalamic circuits. *J Neurosci.* **18**, 9539-46.

Maurice N., Deniau JM., Glowinski J., & Thierry AM. 1999. Relationships between the prefrontal cortex and the basal ganglia in the rat: physiology of the cortico-nigral circuits. *J Neurosci.* **19**, 4674-81.

McCormick DA., & Huguenard JR. 1992. A model of the electrophysiological properties of thalamocortical relay neurons. *J Neurophysiol.* **68**, 1384-400.

McCormick DA., & Pape HC. 1990a. Properties of a hyperpolarization-activated cation current and its role in rhythmic oscillation in thalamic relay neurones. *J Physiol.* **431**, 291-318.

McCormick DA., & Pape HC. 1990b. Noradrenergic and serotonergic modulation of a hyperpolarization-activated cation current in thalamic relay neurones. *J Physiol.* 431, 319-42.

McRitchie DA., Hardman CD., & Halliday GM. 1996. Cytoarchitectural distribution of calcium binding proteins in midbrain dopaminergic regions of rats and humans. *J Comp Neurol.* **364**, 121-50.

Mehta A., Thermos K., & Chesselet MF. 2000. Increased behavioral response to dopaminergic stimulation of the subthalamic nucleus after nigrostriatal lesions. *Synapse.* **37**, 298-307.

Mehta A., Eberle-Wang K., & Chesselet MF. 2001. Increased m-CPP-induced oral dyskinesia after lesion of serotonergic neurons. *Pharmacol Biochem Behav.* **68**, 347-53.

Mehta A., Menalled L., & Chesselet M-F. 2005. Behavioral responses to injections muscimol into the subthalamic nucleus: temporal changes after nigrostriatal lesions. *Neurosci.* **131**, 769-78.

Miller DW., & Abercrombie ED. 1996. Effects of MK-801 on spontaneous and amphetamine-stimulated dopamine release in striatum measured with in vivo microdialysis in awake rats. *Brain Res Bull.* **40**, 57-62.

Millhouse OE. 1986. Pallidal neurons in the rat. *J Comp Neurol.* **254**, 209-27.

Mintz I., Hammond C., & Feger J. 1986. Excitatory effect of iontophoretically applied dopamine on identified neurons of the rat subthalamic nucleus. *Brain Res.* **375**, 172-5.

Mitchell IJ., Cross AJ., Sambrook MA., & Crossman AR. 1986. Neural mechanisms mediating 1-methyl-4-phenyl-1,2,3, 6-tetrahydropyridine-induced parkinsonism in the monkey: relative contributions of the striatopallidal and striatonigral pathways as suggested by 2-deoxyglucose uptake. *Neurosci Lett* . **63**, 61-5.

Mitchell IJ., Clarke CE., Boyce S., Robertson RG., Peggs D., Sambrook MA., & Crossman AR. 1989. Neural mechanisms underlying parkinsonian symptoms based upon regional uptake of 2-deoxyglucose in monkeys exposed to 1-methyl-4-phenyl-1,2,3,6,-tetrahydropyridine. *Neurosci.* **32**, 213-26.

Miwa H., Nishi K., Fuwa T., & Mizuno Y. 1998. Globus pallidus lesions inhibit the induction of c-Fos by haloperidol in the basal ganglia output nuclei in rats. *Neurosci Lett.* **250**, 29-32.

Miwa H., Nishi K., Fuwa T., & Mizuno Y. 2000. Effects of blockade of metabotropic glutamate receptors in the subthalamic nucleus on haloperidol-induced Parkinsonism in rats. *Neurosci Lett.* **282**, 21-4.

Moore RY., Bhatnagar RK., & Heller A. 1971. Anatomical and chemical studies of a nigro-neostriatal projection in the cat. *Brain Res.* **30**, 119-35.

Moro E., Lang AE., Strafella AP., Poon YY., Arango PM., Dagher A., Hutchison WD., & Lozano AM. 2004. Bilateral globus pallidus stimulation for Huntington's disease. *Ann Neurol.* **56**, 290-4.

Mori S., Takino T., Yamada H., & Sano Y. 1985. Immunohistochemical demonstration of serotonin nerve fibers in the subthalamic nucleus of the rat, cat and monkey. *Neurosci Lett.* **62**, 305-9.

Moro E., Esselink RJ., Xie J., Hommel M., Benabid AL., & Pollak P. 2002. The impact on Parkinson's disease of electrical parameter settings in STN stimulation. *Neurology.* **59**, 706-13.

Mouroux M., Hassani OK., & Feger J. 1995. Electrophysiological study of the excitatory parafascicular projection to the subthalamic nucleus and evidence for ipsi- and contralateral controls. *Neurosci.* **67**, 399-407.

Murase S., Grenhoff J., Chouvet G., Gonon FG., & Svensson TH. 1993. Prefrontal cortex regulates burst firing and transmitter release in rat mesolimbic dopamine neurons studied in vivo. *Neurosci Lett.* **157**, 53-6.

Murer MG., Riquelme LA., Tseng KY., & Pazo JH. 1997. Substantia nigra pars reticulata single unit activity in normal and 6-OHDA-lesioned rats: effects of intrastriatal apomorphine and subthalamic lesions. *Synapse.* **27**, 278-93.

Murer MG., Dziewczapolski G., Salin P., Vila M., Tseng KY., Ruberg M., Rubinstein M., Kelly MA., Grandy DK., Low MJ., Hirsch E., Raisman-Vozari R., & Gershanik O. 2000. The indirect basal ganglia pathway in dopamine D2 receptor-deficient mice. *Neurosci.* **99**, 643-50.

Murthy VN., & Fetz EE. 1992. Coherent 25- to 35-Hz oscillations in the sensorimotor cortex of awake behaving monkeys. *Proc Natl Acad Sci.* **89**, 5670-4.

Nakanishi H., Hori N., & Kastuda N. 1985. Neostriatal evoked inhibition and effects of dopamine on globus pallidal neurons in rat slice preparations. *Brain Res.* **358**, 282-6.

Nakanishi H., Kita H., & Kitai ST. 1987a. Intracellular study of rat substantia nigra pars reticulata neurons in an in vitro slice preparation: electrical membrane properties and response characteristics to subthalamic stimulation. *Brain Res.* **437**, 45-55.

Nakanishi H., Kita H., & Kitai ST. 1987b. Electrical membrane properties of rat subthalamic neurons in an *in vitro* slice preparation. *Brain Res.* **437**, 35-44.

Nakanishi H., Kita H., & Kitai ST. 1990. Intracellular study of rat entopeduncular nucleus neurons in an in vitro slice preparation: electrical membrane properties. *Brain Res.* **527**, 81-8.

Nambu A., & Llinás R. 1994. Electrophysiology of globus pallidus neurons *in vitro*. *J Neurophysiol.* **72**, 1127-1139.

Nambu A., & Llinas, R. 1997. Morphology of globus pallidus neurons: Its correlation with electrophysiology in guinea pig brain slices. *Journal of Comparative Neurology.* **377**, 85-94.

Nambu A., Tokuno H., Hamada I., Kita H., Imanishi M., Akazawa T., Ikeuchi Y., & Hasegawa N. 2000. Excitatory cortical inputs to pallidal neurons via the subthalamic nucleus in the monkey. *J Neurophysiol.* **84**, 289-300.

Nambu A., Tokuno H., & Takada M. 2002. Functional significance of the cortico-subthalamo-pallidal 'hyperdirect' pathway. *Neurosci Res.* **43**, 111-7.

Napier TC., Simson PE., & Givens BS. 1991. Dopamine electrophysiology of ventral pallidal/substantia innominata neurons: comparison with the dorsal globus pallidus. *J Pharmacol Exp Ther.* **258**, 249-62.

Nauta HJ., & Cole M. 1978. Efferent projections of the subthalamic nucleus: an autoradiographic study in monkey and cat. *J Comp Neurol.* **180**, 1-16.

Nedergaard S., Flatman JA., & Engberg I. 1993. Nifedipine- and omega-conotoxin-sensitive Ca^{2+} conductances in guinea-pig substantia nigra pars compacta neurones. *J Physiol.* **466**, 727-47.

Neuenschwander S., Castelo-Branco M., & Singer W. 1999. Synchronous oscillations in the cat retina. *Vision Res.* **39**, 2485-97.

Neuenschwander S., Castelo-Branco M., Baron J., & Singer W. 2002. Feed-forward synchronization: propagation of temporal patterns along the retinothalamocortical pathway. *Philos Trans R Soc Lond B Biol Sci.* **357**, 1869-76.

Neuper C., & Pfurtscheller G. 2001. Evidence for distinct beta resonance frequencies in human EEG related to specific sensorimotor cortical areas. *Clin Neurophysiol.* **112**, 2084-97.

Neve KA., Seamans JK., & Trantham-Davidson H. 2004. Dopamine receptor signaling. *J Recept Signal Transduct Res.* **24**,165-205.

Niktarash AH., & Shahidi GA. 2004. Effects of the activity of the internal globus pallidus-pedunculopontine loop on the transmission of the subthalamic nucleus-external globus pallidus-pacemaker oscillatory activities to the cortex. *Comput Neurosci.* **16**, 113-27.

Ni Z., Bouali-Benazzouz R., Gao D., Benabid AL., & Benazzouz A. 2000. Changes in the firing pattern of globus pallidus neurons after the degeneration of nigrostriatal pathway are mediated by the subthalamic nucleus in the rat. *Eur J Neurosci.* **12**, 4338-44.

Ni Z., Bouali-Benazzouz R., Gao D., Benabid AL., & Benazzouz A. 2001a. Intrasubthalamic injection of 6-hydroxydopamine induces changes in the firing rate and pattern of subthalamic nucleus neurons in the rat. *Synapse.* **40**, 145-53.

Ni Z., Gao D., Bouali-Benazzouz R., Benabid AL., & Benazzouz A. 2001b. Effect of microiontophoretic application of dopamine on subthalamic nucleus neuronal activity in

normal rats and in rats with unilateral lesion of the nigrostriatal pathway. *Eur J Neurosci.* **14**, 373-81.

Nicholson SL., & Brotchie JM. 2002. 5-hydroxytryptamine (5-HT, serotonin) and Parkinson's disease - opportunities for novel therapeutics to reduce the problems of levodopa therapy. *Eur J Neurol.* **9**, 1-6.

Nini A., Feingold A., Slovin H., & Bergman H. 1995. Neurons in the globus pallidus do not show correlated activity in the normal monkey, but phase-locked oscillations appear in the MPTP model of parkinsonism. *J Neurophysiol.* **74**, 1800-5.

Nixon PD., McDonald KR., Gough PM., Alexander IH., & Passingham RE. 2004. Cortico-basal ganglia pathways are essential for the recall of well-established visuomotor associations. *Eur J Neurosci.* **20**, 3165-78.

Nomura S., Mizuno N., & Sugimoto T. 1980. Direct projections from the pedunculopontine tegmental nucleus to the subthalamic nucleus in the cat. *Brain Res.* **196**, 223-7.

Nutt JG., Obeso JA., & Stocchi F. 2000. Continuous dopamine-receptor stimulation in advanced Parkinson's disease. *Trends Neurosci.* **23**, S109-15.

Obeso JA., Rodriguez-Oroz MC., Rodriguez M., Lanciego JL., Artieda J., Gonzalo N., & Olanow CW. 2000. Pathophysiology of the basal ganglia in Parkinson's disease. *Trends Neurosci.* **23**, S8-19.

Obeso JA., Rodriguez-Oroz M., Marin C., Alonso F., Zamarbide I., Lanciego JL., & Rodriguez-Diaz M. 2004. The origin of motor fluctuations in Parkinson's disease: importance of dopaminergic innervation and basal ganglia circuits. *Neurology.* **62**, 17-30.

Olds ME., Jacques DB., & Kopyov O. 1998. Globus pallidus lesions depress the excitatory responses to apomorphine but not amphetamine in the subthalamic nucleus of the behaving rat with a 6-OHDA nigra lesion. *Brain Res.* **812**, 50-64.

Olds ME., Jacques DB., & Kopyov O. 1999. Subthalamic responses to amphetamine and apomorphine in the behaving rat with a unilateral 6-OHDA lesion in the substantia nigra. *Synapse.* **34**, 228-40.

Onn SP., & Grace AA. 1994. Dye coupling between rat striatal neurons recorded in vivo: compartmental organization and modulation by dopamine. *J Neurophysiol.* **71**, 1917-34.

Oorschot DE. 1996. Total number of neurons in the neostriatal, pallidal, subthalamic, and substantia nigral nuclei of the rat basal ganglia: a stereological study using the cavalieri and optical disector methods. *J Comp Neurol.* **366**, 580-99.

Orieux G., Francois C., Feger J., Hirsch EC. 2002. Consequences of dopaminergic denervation on the metabolic activity of the cortical neurons projecting to the subthalamic nucleus in the rat. *J Neurosci.* **22**, 8762-70.

Otsuka T., Murakami F., & Song WJ. 2001. Excitatory postsynaptic potentials trigger a plateau potential in rat subthalamic neurons at hyperpolarized states. *J Neurophysiol.* **86**; 1816-25.

Overton P., & Clark D. 1992. Iontophoretically administered drugs acting at the N-methyl-D-aspartate receptor modulate burst firing in A9 dopamine neurons in the rat. *Synapse.* **10**, 131-40.

Pagni CA., Altibrandi MG., Bentivoglio A., Caruso G., Cioni B., Fiorella C., Insola A., Lavano A., Maina R., Mazzone P., Signorelli CD., Sturiale C., Valzania F., Zeme S., &

Zenga F. 2005. Extradural motor cortex stimulation (EMCS) for Parkinson's disease. History and first results by the study group of the Italian neurosurgical society. *Acta Neurochir Suppl.* **93**,113-9.

Paladini CA., Iribe Y., & Tepper JM. 1999. GABAA receptor stimulation blocks NMDA-induced bursting of dopaminergic neurons in vitro by decreasing input resistance. *Brain Res.* **832**, 145-51.

Parent A., & Hazrati LN. 1995a. Functional anatomy of the basal ganglia. I. The cortico-basal ganglia-thalamo-cortical loop. *Brain Res Rev.* **20**, 91-127.

Parent A., & Hazrati LN. 1995b. Functional anatomy of the basal ganglia. II. The place of subthalamic nucleus and external pallidum in basal ganglia circuitry. *Brain Res Rev.* **20**, 128-54.

Parent M., & Parent A. 2004 The pallidofugal motor fiber system in primates. *Parkinsonism Relat Disord.* **10**, 203-11.

Parent A., & Smith Y. 1987. Differential dopaminergic innervation of the two pallidal segments in the squirrel monkey (Saimiri sciureus). *Brain Res.* **426**, 397-400.

Parent A., Charara A., & Pinault D. 1995. Single striatofugal axons arborizing in both pallidal segments and in the substantia nigra in primates. *Brain Res.* **698**, 280-4.

Parent A., Sato F., Wu Y., Gauthier J., Levesque M., & Parent M. 2000. Organization of the basal ganglia: the importance of axonal collateralization. *Trends Neurosci.* **23**, S20-7.

Parkinson J. 1817. The shaking palsy. London: Sherwood, Neely and Jones.

Parry TJ., Eberle-Wang K., Lucki I., & Chesselet MF. 1994. Dopaminergic stimulation of subthalamic nucleus elicits oral dyskinesia in rats. *Exp Neurol.* **128**, 181-90.

Paul K., Keith DJ., & Johnson SW. 2003. Modulation of calcium-activated potassium small conductance (SK) current in rat dopamine neurons of the ventral tegmental area. *Neurosci Lett.* **348**, 180-4.

Payoux P., Remy P., Damier P., Miloudi M., Loubinoux I., Pidoux B., Gaura V., Rascol O., Samson Y., & Agid Y. 2004. Subthalamic nucleus stimulation reduces abnormal motor cortical overactivity in Parkinson disease. *Arch Neurol.* **61**, 1307-13.

Pessiglione M., Guehl D., Rolland AS., Francois C., Hirsch EC., Feger J., & Tremblay L. 2005. Thalamic neuronal activity in dopamine-depleted primates: evidence for a loss of functional segregation within basal ganglia circuits. *J Neurosci.* **25**, 1523-31.

Pfurtscheller G., Neuper C., & Kalcher J. 1993. 40-Hz oscillations during motor behavior in man. *Neurosci Lett.* **164**, 179-82.

Pisani A., Bonsi P., Centonze D., Gubellini P., Bernardi G., & Calabresi P. 2003. Targeting striatal cholinergic interneurons in Parkinson's disease: focus on metabotropic glutamate receptors. *Neuropharm.* **45**, 45-56.

Plenz D., Herrera-Marschitz M., & Kitai ST. 1998. Morphological organization of the globus pallidus-subthalamic nucleus system studied in organotypic cultures. *J Comp Neurol.* **397**, 437-57.

Plenz D., & Kital ST. 1999. A basal ganglia pacemaker formed by the subthalamic nucleus and external globus pallidus. *Nature.* **400**, 677-82.

Pompeiano M., Palacios JM., & Mengod G. 1994. Distribution of the serotonin 5-HT_2 receptor family mRNAs: comparison between 5-HT_{2A} and 5-HT_{2C} receptors. *Mol Brain Res.* **23**, 163-78.

Prensa L., Cossette M., & Parent A. 2000. Dopaminergic innervation of human basal ganglia. *J Chem Neuroanat.* **20**, 207-13.

Priori A., Foffani G., Pesenti A., Bianchi A., Chiesa V., Baselli G., Caputo E., Tamma F., Rampini P., Egidi M., Locatelli M., Barbieri S., & Scarlato G. 2002. Movement-related modulation of neural activity in human basal ganglia and its L-DOPA dependency: recordings from deep brain stimulation electrodes in patients with Parkinson's disease. *Neurol Sci.* **23**, S101-2.

Priori A., Foffani G., Pesenti A., Tamma F., Bianchi AM., Pellegrini M., Locatelli M., Moxon KA., & Villani RM. 2004. Rhythm-specific pharmacological modulation of subthalamic activity in Parkinson's disease. *Exp Neurol.* **189**, 369-79.

Poisik OV., Mannaioni G., Traynelis S., Smith Y., & Conn PJ. 2003. Distinct functional roles of the metabotropic glutamate receptors 1 and 5 in the rat globus pallidus. *J Neurosci.* **23**, 122-30.

Rajakumar N., Rushlow W., Naus CC., Elisevich K., & Flumerfelt BA. 1994. Neurochemical compartmentalization of the globus pallidus in the rat: an immunocytochemical study of calcium-binding proteins. *J Comp Neurol.* **346**, 337-48.

Rajput AH., Fenton ME., Di Paolo T., Sitte H., Pifl C., & Hornykiewicz O. 2004. Human brain dopamine metabolism in levodopa-induced dyskinesia and wearing-off. *Parkinsonism Relat Disord.* **10**, 221-6.

Raz A., Feingold A., Zelanskaya V., Vaadia E., & Bergman H. 1996. Neuronal synchronization of tonically active neurons in the striatum of normal and parkinsonian primates. *J Neurophysiol.* **76**, 2083-8.

Raz A., Frechter-Mazar V., Feingold A., Abeles M., Vaadia E., & Bergman H. 2001. Activity of pallidal and striatal tonically active neurons is correlated in mptp-treated monkeys but not in normal monkeys. *J Neurosci.* **21**, RC128.

Raz A., Vaadia E., & Bergman H. 2000. Firing patterns and correlations of spontaneous discharge of pallidal neurons in the normal and the tremulous 1-methyl-4-phenyl-1,2,3,6-tetrahydropyridine vervet model of parkinsonism. *J Neurosci.* **20**, 8559-71.

Richards CD., Shiroyama T., & Kitai ST. 1997. Electrophysiological and immunocytochemical characterization of GABA and dopamine neurons in the substantia nigra of the rat. *Neurosci.* **80**, 545-57.

Robelet S., Melon C., Guillet B., Salin P., & Kerkerian-Le Goff L. 2004. Chronic L-DOPA treatment increases extracellular glutamate levels and GLT1 expression in the basal ganglia in a rat model of Parkinson's disease. *Eur J Neurosci.* **20**, 1255-66.

Robertson GS., Vincent SR., & Fibiger HC. 1990. Striatonigral projection neurons contain D1 dopamine receptor-activated c-Fos. *Brain Res.* **523**, 288-90.

Rohlfs A., Nikkhah G., Rosenthal C., Rundfeldt C., Brandis A., & Samii M, Loscher W. 1997. Hemispheric asymmetries in spontaneous firing characteristics of substantia nigra pars reticulata neurons following a unilateral 6-hydroxydopamine lesion of the rat nigrostriatal pathway. *Brain Res.* **761**, 352-6.

Rosenkranz JA., & Johnston D. 2006. Dopaminergic regulation of neuronal excitability through modulation of Ih in layer V entorhinal cortex. *J Neurosci.* **26**, 3229-44.

Rubin JE., & Terman D. 2004. High frequency stimulation of the subthalamic nucleus eliminates pathological thalamic rhythmicity in a computational model. *J Comput Neurosci.* **16**, 211-35.

Ruskin DN., Bergstrom DA., & Walters JR. 1999. Multisecond oscillations in firing rate in the globus pallidus: synergistic modulation by D1 and D2 dopamine receptors. *J Pharmacol Exp Ther.* **290**, 1493-501.

Ryan LJ., & Clark KB. 1991. The role of the subthalamic nucleus in the response of globus pallidus neurons to stimulation of the prelimbic and agranular frontal cortices in rats. *Exp Brain Res.* **86**, 641-51.

Sadek A-R. 2005. Microcircuits of the globus pallidus. Thesis submitted for the degree of Doctor of Philosophy at the University College of Oxford.

Sadikot AF., Parent A., & Francois C. 1992. Efferent connections of the centromedian and parafascicular thalamic nuclei in the squirrel monkey: a PHA-L study of subcortical projections. *J Comp Neurol.* **315**, 137-59.

Sanes JN., & Donoghue JP. 1993. Oscillations in local field potentials of the primate motor cortex during voluntary movement. *Proc Natl Acad Sci.* **90**, 4470-4.

Sato F., Lavallee P., Levesque M., & Parent A. 2000a. Single-axon tracing study of neurons of the external segment of the globus pallidus in primate. *J Comp Neurol.* **417**, 17-31.

Sato F., Parent M., Levesque M., & Parent A. 2000b. Axonal branching pattern of neurons of the subthalamic nucleus in primates. *J Comp Neurol.* **424**, 142-52.

Schneider JS., & DiStefano L. 1995. Enhanced restoration of striatal dopamine concentrations by combined GM1 ganglioside and neurotrophic factor treatments. *Brain Res.* **674**, 260-4.

Sedelis M., Schwarting RK., & Huston JP. 2001. Behavioral phenotyping of the MPTP mouse model of Parkinson's disease. *Behav Brain Res.* **125**, 109-25.

Seeman P., & Van Tol HH. 1993. Dopamine receptor pharmacology. *Curr Opin Neurol Neurosurg.* **6**, 602-8.

Seutin V., Johnson SW., & North RA. 1993. Apamin increases NMDA-induced burst-firing of rat mesencephalic dopamine neurons. *Brain Res.* **630**, 341-4.

Sharott A., Magill PJ., Bolam JP., & Brown P. 2005a. Directional analysis of coherent oscillatory field potentials in the cerebral cortex and basal ganglia of the rat. *J Physiol.* **562**, 951-63.

Sharott A., Magill PJ., Harnack D., Kupsch A., Meissner W., & Brown P. 2005b. Dopamine depletion increases the power and coherence of beta-oscillations in the cerebral cortex and subthalamic nucleus of the awake rat. *Eur J Neurosci.* 21, 1413-22.

Shen KZ., & Johnson SW. 2000. Presynaptic dopamine D2 and muscarine M3 receptors inhibit excitatory and inhibitory transmission to rat subthalamic neurones in vitro. *J Physiol.* **525**, 331-41.

Shen K-Z., & Johnson SW. 2003. Group II metabotropic glutamate receptor modulation of excitatory transmission in rat subthalamic nucleus. *J Physiol.* **553**, 489-96.

Shen KZ., & North RA. 1992a. Substance P opens cation channels and closes potassium channels in rat locus coeruleus neurons. *Neurosci.* **50**, 345-53.

Shen KZ., & North RA. 1992b. Muscarine increases cation conductance and decreases potassium conductance in rat locus coeruleus neurones. *J Physiol.* **455**, 471-85.

Shen KZ., Zhu ZT., Munhall A., & Johnson SW. 2003. Dopamine receptor supersensitivity in rat subthalamus after 6-hydroxydopamine lesions. *Eur J Neurosci.* **18**, 2967-74.

Shi WX., Zheng P., Liang XF., & Bunney BS. 1997. Characterization of dopamine-induced depolarization of prefrontal cortical neurons. *Synapse.* **26**, 415-22.

Shimohama S., Sawada H., Kitamura Y., & Tanihuchi. 2003. *Trends in Molecular Medicine.* **9**, 360-5

Shink E., Bevan MD., Bolam JP., & Smith Y. 1996. The subthalamic nucleus and the external pallidum: two tightly interconnected structures that control the output of the basal ganglia in the monkey. *Neurosci.* **73**, 335-57.

Shink E., & Smith Y. 1995. Differential synaptic innervation of neurons in the internal and external segments of the globus pallidus by the GABA- and glutamate-containing terminals in the squirrel monkey. *J Comp Neurol.* **358**, 119-41.

Silberstein P., Kuhn AA., Kupsch A., Trottenberg T., Krauss JK., Wohrle JC., Mazzone P., Insola A., Di Lazzaro V., Oliviero A., Aziz T., & Brown P. 2003. Patterning of globus pallidus local field potentials differs between Parkinson's disease and dystonia. *Brain.* **126**, 2597-608.

Silverdale MA., Nicholson SL., Ravenscroft P., Crossman AR., Millan MJ., & Brotchie JM. 2004. Selective blockade of D(3) dopamine receptors enhances the anti-parkinsonian properties of ropinirole and levodopa in the MPTP-lesioned primate. *Exp Neurol.* **188**, 128-38.

Smith Y., & Bolam JP. 1989. Neurons of the substantia nigra reticulata receive a dense GABA-containing input from the globus pallidus in the rat. *Brain Res.* **493**,160-7.

Smith Y., & Bolam JP. 1990. The output neurones and the dopaminergic neurones of the substantia nigra receive a GABA-containing input from the globus pallidus in the rat. *J Comp Neurol.* **296**, 47-64.

Smith Y., & Kieval JZ. 2000. Anatomy of the dopamine system in the basal ganglia. *Trends Neurosci.* **23**, S28-33.

Smith Y., Lavoie B., Dumas J., & Parent A. 1989. Evidence for a distinct nigropallidal dopaminergic projection in the squirrel monkey. *Brain Res.* **482**, 381-6.

Smith Y., Bennett BD., Bolam JP., Parent A., & Sadikot AF. 1994a. Synaptic relationships between dopaminergic afferents and cortical or thalamic input in the sensorimotor territory of the striatum in monkey. *J Comp Neurol.* **344**, 1-19.

Smith Y., Hazrati LN., & Parent A. 1990. Efferent projections of the subthalamic nucleus in the squirrel monkey as studied by the PHA-L anterograde tracing method. *J Comp Neurol.* **294**, 306-23.

Smith Y., Wichmann T., & DeLong MR. 1994b. Synaptic innervation of neurones in the internal pallidal segment by the subthalamic nucleus and the external pallidum in monkeys. *J Comp Neurol.* **343**, 297-318.

Smith Y., Bevan M. D., Shink E., & Bolam J. P. 1998. Microcircuitry of the direct and indirect pathways of the basal ganglia. *Neurosci.* **86**, 353-387.

Sochurkova D., & Rektor I. 2003. Event-related desynchronization/synchronization in the putamen. An SEEG case study. *Exp Brain Res.* **149**, 401-4.

Soghomonian JJ., Pedneault S., Audet G., & Parent A. 1994. Increased glutamate decarboxylase mRNA levels in the striatum and pallidum of MPTP-treated primates. *J Neurosci.* **14**, 6256-65.

Song WJ., Baba Y., Otsuka T., & Murakami F. 2000. Characterization of $Ca^{(2+)}$ channels in rat subthalamic nucleus neurons. *J Neurophysiol.* **84**, 2630-7.

Stanford IM. 2003. Independent neuronal oscillators of the rat globus pallidus. *J Neurophysiol.* **89**, 1713-7.

Stanford IM., Kantaria MA., Chahal HS., Loucif KC., & Wilson CL. 2005 .5-Hydroxytryptamine induced excitation and inhibition in the subthalamic nucleus: action at $5\text{-}HT_{2C}$, $5\text{-}HT_4$ and $5\text{-}HT_{1A}$ receptors. *Neuropharm.* **49**, 1228-34.

Stanford IM., & Lacey MG. 1996. Differential actions of serotonin, mediated by $5\text{-}HT_{1B}$ and $5\text{-}HT_{2C}$ receptors, on GABA-mediated synaptic input to rat substantia nigra pars reticulata neurons in vitro. *J Neurosci.* **16**, 7566-73.

Stefani A., Bassi A., Mazzone P., Pierantozzi M., Gattoni G., Altibrandi MG., Giacomini P., Peppe A., Bernardi G., & Stanzione P. Subdyskinetic apomorphine responses in globus pallidus and subthalamus of parkinsonian patients: lack of clear evidence for the 'indirect pathway'. *Clin Neurophysiol.* **113**, 91-100.

Sugimoto T., & Hattori T. 1983. Confirmation of thalamosubthalamic projections by electron microscopic autoradiography. *Brain Res.* **267**, 335-9.

Sugimoto T., Hattori T., Mizuno N., Itoh K., & Sato M. 1983. Direct projections from the centre median-parafascicular complex to the subthalamic nucleus in the cat and rat. *J Comp Neurol.* **214**, 209-16.

Surmeier DJ., Eberwine J., Wilson CJ., Cao Y., Stefani A., & Kitai ST. 1992. Dopamine receptor subtypes colocalize in rat striatonigral neurons. *Proc Natl Acad Sci.* **89**, 10178-82.

Tai CH., Boraud T., Bezard E., Bioulac B., Gross C., & Benazzouz A. 2003. Electrophysiological and metabolic evidence that high-frequency stimulation of the subthalamic nucleus bridles neuronal activity in the subthalamic nucleus and the substantia nigra reticulata. *Faseb J.* **17**, 1820-30.

Tepper JM., & Bolam JP. 2004. Functional diversity and specificity of neostriatal interneurons. *Curr Opin Neurobiol.* **14**, 685-92.

Tepper JM., Koos T., & Wilson CJ. 2004. GABAergic microcircuits in the neostriatum. *Trends Neurosci.* **27**, 662-9.

Terman D., Rubin JE., Yew AC., & Wilson C J. 2002. Activity patterns in a model for the subthalamopallidal network of the basal ganglia. *J Neurosci.* **22**, 2963-76.

Timmermann L., Wojtecki L., Gross J., Lehrke R., Voges J., Maarouf M., Treuer H., Sturm V., & Schnitzler A. 2004. Ten-Hertz stimulation of subthalamic nucleus deteriorates motor symptoms in Parkinson's disease. *Mov Disord.* **19**, 1328-33.

Tofighy A., Abbott A., Centonze D., Cooper AJ., Noor E., Pearce M., Puntis M., Stanford IM., Wigmore MA., & Lacey MG. 2003. Excitation by dopamine of rat subthalamic nucleus neurones *in vitro* -a direct action with unconventional pharmacology. *Neurosci.* **116**, 157-66.

Touchon JC., Moore C., Frederickson J., & Meshul CK. 2004. Lesion of subthalamic or motor thalamic nucleus in 6-hydroxydopamine-treated rats: effects on striatal glutamate and apomorphine-induced contralateral rotations. *Synapse.* **51**, 287-98.

Tsien RY. 1980. New calcium indicators and buffers with high selectivity against magnesium and protons: design, synthesis, and properties of prototype structures. *Biochemistry*. **19**, 2396-404.

Tseng KY., Kasanetz F., Karguieman L., Riquelme LA., & Murer MG. 2001a. Cortical slow ocilllatory activity is reflected in the membrane potential and spike trains of striatal neurons in rats with chronic nigrostriatal lesions. *J Neurosci*. **21**, 6430-9.

Tseng KY., Kasanetz F., Kargieman L., Pazo JH., Murer MG., & Riquelme LA. 2001b. Subthalamic nucleus lesions reduce low frequency oscillatory firing of substantia nigra pars reticulata neurons in a rat model of Parkinson's disease. *Brain Res*. **904**, 93-103.

Ungerstedt U. 1971. Postsynaptic supersensitivity after 6-hydroxy-dopamine induced degeneration of the nigro-striatal dopamine system. *Acta Physiol Scand*. **367**, 69-93.

Ungerstedt U., & Arbuthnott GW. 1970. Quantitative recording of rotational behavior in rats after 6-hydroxy-dopamine lesions of the nigrostriatal dopamine system. *Brain Res*. **24**, 485-93.

Urbain N., Gervasoni D., Souliere F., Lobo L., Rentero N., Windels F., Astier B., Savasta M., Fort P., Renaud B., Luppi PH., & Chouvet G. 2000. Unrelated course of subthalamic nucleus and globus pallidus neuronal activities across vigilance states in the rat. *Eur J Neurosci*. **12**, 3361-74.

Urbain N., Gervasoni D., Souliere F., Lobo L., Rentero N., Windels F., Astier B., Savasta M., Fort P., Renaud B., Luppi PH., & Chouvet G. 2002a. Unrelated course of subthalamic nucleus and globus pallidus neuronal activities across vigilance states in the rat. *Eur J Neurosci*. **12**, 3361-74.

Urbain N., Rentero N., Gervasoni D., Renaud B., & Chouvet G. 2002b. The switch of subthalamic neurons from an irregular to a bursting pattern does not solely depend on their GABAergic inputs in the anesthetic-free rat. *J Neurosci.* **22**, 8665-75.

Van Der Kooy D., & Hattori T. 1980. Single subthalamic nucleus neurons project to both the globus pallidus and substantia nigra in rat. *J Comp Neurol.* **192**, 751-68.

Venance L., Glowinski J., & Giaume C. 2004. Electrical and chemical transmission between striatal GABAergic output neurones in rat brain slices. *J Physiol.* **559**, 215-30.

Vila M, Levy R, Herrero MT, Faucheux B, Obeso JA, Agid Y, Hirsch EC. 1996. Metabolic activity of the basal ganglia in parkinsonian syndromes in human and non-human primates: a cytochrome oxidase histochemistry study. *Neurosci.* **71**, 903-12.

Vila M., Levy R., Herrero MT., Ruberg M., Faucheux B., Obeso JA., Agid Y., & Hirsch EC. 1997. Consequences of nigrostriatal denervation on the functioning of the basal ganglia in human and nonhuman primates: an in situ hybridization study of cytochrome oxidase subunit I mRNA. *J Neurosci.* **17**, 765-73.

Vila M., Marin C., Ruberg M., Jimenez A., Raisman-Vozari R., Agid Y., Tolosa E., & Hirsch EC. 1999. Systemic administration of NMDA and AMPA receptor antagonists reverses the neurochemical changes induced by nigrostriatal denervation in basal ganglia. *J Neurochem.* **73**, 344-52.

Vila M., Perier C., Feger J., Yelnik J., Faucheux B., Ruberg M., Raisman-Vozari R., Agid Y., & Hirsch EC. 2000. Evolution of changes in neuronal activity in the subthalamic nucleus of rats with unilateral lesion of the substantia nigra assessed by metabolic and electrophysiological measurements. *Eur J Neurosci.* **12**, 337-44.

von Krosigk M., Bal T., & McCormick DA. 1993. Cellular mechanisms of a synchronized oscillation in the thalamus. *Science.* **261**, 361-4.

Vorobyov VV., Schibaev NV., Morelli M., & Carta AR. 2003. EEG modifications in the cortex and striatum after dopaminergic priming in the 6-hydroxydopamine rat model of Parkinson's disease. *Brain Res.* **972**, 177-85.

Walters JR., Bergstrom DA., Carlson JH., Chase TN., & Braun AR. 1987. D1 dopamine receptor activation required for postsynaptic expression of D2 agonist effects. *Science.* **236**, 719-22.

Waszczak BL., Martin L., Boucher N., Zahr N., Sikes RW., & Stellar JR. 2001. Electrophysiological and behavioral output of the rat basal ganglia after intrastriatal infusion of d-amphetamine: lack of support for the basal ganglia model. *Brain Res.* **920**, 170-82.

Welter ML., Houeto JL., Bonnet AM., Bejjani PB., Mesnage V., Dormont D., Navarro S., Cornu P., Agid Y., & Pidoux B. 2004. Effects of high-frequency stimulation on subthalamic neuronal activity in parkinsonian patients. *Arch Neurol.* **61**, 89-96.

Werner P., Hussy N., Buell G., Jones KA., & North RA. 1996. D2, D3, and D4 dopamine receptors couple to G protein-regulated potassium channels in Xenopus oocytes. *Mol Pharmacol.* **49**, 656-61.

Wichmann T., & Delong MR. 1999. Neurobiology - Oscillations in the basal ganglia. *Nature.* **400**, 621-22.

Wichmann T., & DeLong MR. 2003. Pathophysiology of Parkinson's disease: the MPTP primate model of the human disorder. *Ann N Y Acad Sci.* **991**, 199-213.

Wichmann T., Bergman H., & DeLong MR. 1994a. The primate subthalamic nucleus. III. Changes in motor behavior and neuronal activity in the internal pallidum induced by subthalamic inactivation in the MPTP model of parkinsonism. *J Neurophysiol.* **72**, 521-30.

Wichmann T., Bergman H., & DeLong MR. 1994b. The primate subthalamic nucleus. I. Functional properties in intact animals. *J Neurophysiol.* **72**, 494-50.

Wichmann T., Bergman H., Starr PA., Subramanian T., Watts RL., & DeLong MR. 1999. Comparison of MPTP-induced changes in spontaneous neuronal discharge in the internal pallidal segment and in the substantia nigra *pars* reticulata in primates. *Exp Brain Res.* **25**, 397-409.

Wichmann T., Kliem MA., & Soares J. 2002. Slow oscillatory discharge in the primate basal ganglia. *J Neurophysiol.* **87**, 1145-8.

Wiesendanger E., Clarke S., Kraftsik R., & Tardif E. 2004. Topography of cortico-striatal connections in man: anatomical evidence for parallel organization. *Eur J Neurosci.* **20**, 1915-22.

Williams D., Tijssen M., Van Bruggen G., Bosch A., Insola A., Di Lazzaro V., Mazzone P., Oliviero A., Quartarone A., Speelman H., & Brown P. 2002. Dopamine-dependent changes in the functional connectivity between basal ganglia and cerebral cortex in humans. *Brain.* **125**, 1558-69.

Williams D., Kuhn A., Kupsch A., Tijssen M., van Bruggen G., Speelman H., Hotton G., Yarrow K., & Brown P. 2003. Behavioural cues are associated with modulations of synchronous oscillations in the human subthalamic nucleus. *Brain.* **126**, 1975-85.

Williams D., Kuhn A., Kupsch A., Tijssen M., van Bruggen G., Speelman H., Hotton G., Loukas C., & Brown P. 2005. The relationship between oscillatory activity and motor reaction time in the parkinsonian subthalamic nucleus. *Eur J Neurosci.* **21**, 249-58.

Wilson CJ., & Kawaguchi Y. 1996. The origins of two-state spontaneous membrane potential fluctuations of neostriatal spiny neurons. *J Neurosci.* **16**, 2397-410.

Wilson CL., Cash D., Loucif KC., Lacey MG., & Stanford IM. 2005. Dopamine regularises firing in subthalamic nucleus neurones from 1-methyl-4-phenyl-1,2,3,6-tetrahydropyridine lesioned mice *in vitro*. *J.Physiol.* **567P,** PC192.

Wilson CL., Puntis M., & Lacey MG. 2003. Overwhelmingly asynchronous firing of rat subthalamic nucleus neurones in brain slices provides little evidence for intrinsic interconnectivity. *Neurosci.* **123**, 187-200.

Wilson CJ., Weyrick A., Terman D., Hallworth NE., & Bevan MD. 2004. A model of reverse spike frequency adaptation and repetitive firing of subthalamic nucleus neurons. *J Neurophysiol.* **91**, 1963-80.

Wu J., & Hablitz JJ. 2005. Cooperative activation of D1 and D2 dopamine receptors enhances a hyperpolarization-activated inward current in layer I interneurons. *J Neurosci.* 25, 6322-8.

Wu Y., Richard S., & Parent A. 2000. The organization of the striatal output system: a single-cell juxtacellular labeling study in the rat. *Neurosci Res.* **38**, 49-62.

Xiang Z., Wang L., & Kitai ST. 2005. Modulation of spontaneous firing in rat subthalamic neurons by 5-HT receptor subtypes. *J Neurophysiol.* **93**,1145-57.

Yan Z, Song WJ, Surmeier J. 1997. D2 dopamine receptors reduce N-type Ca2+ currents in rat neostriatal cholinergic interneurons through a membrane-delimited, protein-kinase-C-insensitive pathway. *J Neurophysiol.* 77, 1003-15.

Zheng F., & Johnson SW. 2002. Group I metabotropic glutamate receptor-mediated enhancement of dopamine cell burst firing in rat ventral tegmental area in vitro. *Brain Res.* **948**, 171-4.

Zhu Z., Bartol M., Shen K., & Johnson SW. 2002a. Excitatory effects of dopamine on subthalamic nucleus neurons: in vitro study of rats pretreated with 6-hydroxydopamine and levodopa. *Brain Res.* **945**, 31-40.

Zhu ZT., Munhall A., Shen KZ., & Johnson SW. 2004. Calcium-dependent subthreshold oscillations determine bursting activity induced by N-methyl-D-aspartate in rat subthalamic neurons *in vitro*. *Eur J Neurosci.* **19**, 1296-304.

Zhu ZT., Munhall A., Shen KZ., & Johnson SW. 2005. NMDA enhances a depolarization-activated inward current in subthalamic neurons. *Neuropharm.* **49**, 317-27.

Zhu ZT., Shen KZ., & Johnson SW. 2002b. Pharmacological identification of inward current evoked by dopamine in rat subthalamic neurons in vitro. *Neuropharm.* **42**, 772-81.